

1 Dear Editors,

2 Please find enclosed the marked-up revised manuscript (**Ref. Manuscript ID:essd-2019-122**)  
3 entitled **“Temporal inventory of glaciers in the Suru sub-basin, western Himalaya:  
4 Impacts of the regional climate variability”**. On behalf of all the authors, I would like to  
5 convey my sincere thanks to the topical editor, the editorial and administrative team of the  
6 Earth System Science Data for timely processing of the manuscript and suggesting  
7 constructive comments for improving the original manuscript substantially. In line with the  
8 suggested corrections (mainly grammatical errors) we have edited the text and revised the  
9 manuscript accordingly.

10 Thanks for your consideration.

11 Yours Sincerely,

12 Aparna Shukla.

13

14

15

16

17

18

19

20

21

22

23

24

25

26 **Temporal inventory of glaciers in the Suru sub-basin, western**  
27 **Himalaya: Impacts of the regional climate variability**

28

29 Aparna Shukla<sup>1,2\*</sup>, Siddhi Garg<sup>1</sup>, Manish Mehta<sup>1</sup>, Vinit Kumar<sup>1</sup>, Uma Kant Shukla<sup>3</sup>

30

31 <sup>1</sup>Wadia Institute of Himalayan Geology, 33, GMS Road, Dehradun-248001, India32 <sup>2</sup>Ministry of Earth Sciences, New Delhi- 110003, India33 <sup>3</sup>Department of Geology, Banaras Hindu University, Varanasi -221005, India

34

35 \*Correspondence to: Aparna Shukla (aparna.shukla22@gmail.com)

36

37

38

39

40

41

42

43

44

45

46

47

48

49

50

51

52

53

54

55

56

57

58

59

60

61

62

63

64

65

66

## 67 Abstract

68 Updated knowledge about the glacier extent and characteristics in the Himalaya cannot be overemphasised.  
 69 Availability of precise glacier inventories in the latitudinally diverse western Himalayan region is particularly  
 70 crucial. In this study we have created an inventory of the Suru sub-basin, western Himalaya for year 2017 using  
 71 Landsat OLI data. Changes in glacier parameters have also been monitored from 1971 to 2017 using temporal  
 72 satellite remote sensing data and limited field observations. Inventory data show that the sub-basin has 252  
 73 glaciers covering 11% of the basin, having an average slope of  $25 \pm 6^\circ$  and dominantly north orientation. The  
 74 average snow line altitude (SLA) of the basin is  $5011 \pm 54$  masl with smaller (47%) and cleaner (43%) glaciers  
 75 occupying the bulk area. Longterm climate data (1901-2017) show an increase in the mean annual temperature  
 76 ( $T_{\max}$  &  $T_{\min}$ ) by  $0.77^\circ\text{C}$  ( $0.25$  &  $1.3^\circ\text{C}$ ) in the sub-basin, driving the overall glacier variability in the region.  
 77 Temporal analysis reveals a glacier shrinkage of  $-6 \pm 0.02\%$ , an average retreat rate of  $4.3 \pm 1.02 \text{ ma}^{-1}$ , debris  
 78 increase of 62% and  $22 \pm 60$  m SLA rise in past 46 years. This confirms their transitional response between the  
 79 Karakoram and the Greater Himalayan Range (GHR) glaciers. Besides, glaciers in the sub-basin occupy two  
 80 major ranges, i.e., GHR and Ladakh range (LR) and experience local climate variability, with the GHR glaciers  
 81 exhibiting a warmer and wetter climate as compared to the LR glaciers. This variability manifestes itself in the  
 82 varied response of GHR and LR glaciers. While the GHR glaciers exhibit an overall rise in SLA (GHR:  $49 \pm 69$   
 83 m; LR: decrease by  $18 \pm 50$  m), the LR glaciers have deglaciated more (LR: 7%; GHR: 6%) with an enhanced  
 84 accumulation of debris cover (LR: 73%; GHR: 59%). Inferences from this study reveal prevalence of glacier  
 85 disintegration and overall degeneration, transition of clean ice to partially debris covered glaciers, local climate  
 86 variability and non-climatic (topographic and morphometric) factor induced heterogeinty in glacier response as  
 87 the major processes operatives in this region. The dataset Shukla et al., (2019) is accessible at  
 88 <https://doi.pangaea.de/10.1594/PANGAEA.904131>

Deleted: s

Deleted: s

89  
 90 **Key words:** Suru sub basin, western Himalaya, glacier inventory, climate change

91  
 92 **Location of the dataset:** <https://doi.pangaea.de/10.1594/PANGAEA.904131>

## 94 1 Introduction

95 State of the Himalayan cryosphere has a bearing on multiple aspects of hydrology, climatology, environment  
 96 and sustenance of living organisms at large (Immerzeel et al., 2010; Miller et al., 2012). Being sensitive to the  
 97 ongoing climate fluctutations, glaciers keep adjusting themselves and these adaptations record the changing  
 98 patterns in the global climate (Bolch et al., 2012). Any alteration in the glacier parameters would ultimately  
 99 affect the hydrology of the region, thereby influencing the downstream communities (Kaser et al., 2010;  
 100 Pritchard, 2017). Owing to these reasons, quantifying the mass loss over different Himalayan regions in the past  
 101 years, ascertaining present status of the cryosphere and how these changes are likely to affect the freshwater  
 102 accessibility in the region are at the forefront of contemporary cryospheric research (Brun et al. 2017; Sakai and  
 103 Fujita, 2017). This aptly triggered several regional (Kaab et al., 2012; Gardelle et al., 2013; Brun et al. 2017;  
 104 Zhou et al., 2018; Maurer et al., 2019), local (Bhushan et al., 2018; Vijay and Braun, 2018) and glacier specific  
 105 studies (Dobhal et al., 2013; Bhattacharya et al., 2016; Azam et al., 2018) in the region. These studies at varying

108 scales contribute towards solving the jigsaw puzzle of the Himalayan cryosphere. The regional scale studies  
109 operate on small scale for bringing out more comprehensive, holistic and synoptic spatio-temporal patterns of  
110 glacier response, the local scale studies monitor glaciers at basin level or groups and offer more details on  
111 heterogenous behaviour and plausible reasons thereof. However, the glacier specific studies whether based on  
112 field or satellite or integrative information are magnified versions of the local scale studies and hold the  
113 potential to provide valuable insights into various morphological, topographic and local-climate induced  
114 controls on glacier evolution. Despite these efforts, data on the glacier variability and response remain  
115 incomplete, knowledge of the governing processes still preliminary and the future viability pathways of the  
116 Himalayan cryospheric components are uncertain.

Deleted: s

117 Though the literature suggests a generalised mass loss scenario (except for the Karakoram region) over the  
118 Himalayan glaciers, disparities in rates and pace of shrinkage remain. Maurer et al. (2019) report the average  
119 mass wastage of  $-0.32 \text{ m w.e.a}^{-1}$  for the Himalayan glaciers during 1975-2016. They suggest that the glaciers in  
120 the eastern Himalaya ( $-0.46 \text{ m w.e.a}^{-1}$ ) have experienced slightly higher mass loss as compared to the western ( $-$   
121  $0.45 \text{ m w.e.a}^{-1}$ ), followed by the central ( $-0.38 \text{ m w.e.a}^{-1}$ ). However, considerable variability in the glacier  
122 behaviour exists within the western Himalayas (Scherler et al., 2011; Kaab et al., 2012; Vijay and Braun, 2017;  
123 Bhushan et al., 2018; Mölg et al., 2018). Studies suggest that largely the glaciers in the Karakoram Himalayas  
124 have either remained stable or gained mass in the last few decades (Kääb et al., 2015; Cogley, 2016), while a  
125 contrasting behaviour is observed for the GHR glaciers experiencing large scale degeneration, with more than  
126 65% glaciers retreating during 2000-2008 (Scherler et al., 2011). However, there are two views pertaining to the  
127 glaciers in the Trans Himalayan range, with one suggesting their intermediate response between the Karakoram  
128 Himalaya and GHR (Chudley et al., 2017) and the other emphasizing upon their affinity either towards the GHR  
129 or the Karakoram Himalayan glaciers (Schmidt and Nusser, 2017). Therefore, in order to add more data and  
130 build a complete understanding of the glacier response, particularly in the western Himalaya, more local scale  
131 studies are necessary.

132 Complete and precise glacier inventories form the basic prerequisites not only for comprehensive glacier  
133 assessment but also for various hydrological and climate modelling related applications (Vaughan et al., 2013).  
134 Information on spatial coverage of glaciers in any region is a much valued dataset and holds paramount  
135 importance in the future assessment of glaciers. Errors in the glacier outlines may propagate and introduce  
136 higher uncertainties in the modelled outputs (Paul et al., 2017). Besides, results from modelling studies  
137 conducted over same region but using different sources of glacier boundaries are rendered uncomparable,  
138 constraining the evaluation of models and thus their future development. On the other hand, quality, accuracy  
139 and precision associated with glacier mapping and outline delineation requires dedicated efforts. Several past  
140 studies discuss the methods for, challenges in achieving an accurate glacier inventory and resolutions for the  
141 same (Paul et al., 2013; 2015; 2017). Thorough knowledge of glaciology and committed manual endeavour are  
142 two vital requirements in this regard. Realisation of above facts did result in several devoted attempts to prepare  
143 detailed glacier inventories at global scale, such as Randolph glacier inventory (RGI), Global land ice  
144 measurements from space (GLIMS) and recently Chinese glacier inventory (CGI) and Glacier area mapping for  
145 discharge from the Asian mountains (GAMDAM) (Raup et al., 2007; Pfeffer et al., 2014; Shiyin et al., 2014;  
146 Nuimura et al., 2015). However, several issues related to gap areas, differences in mapping methods and skills  
147 of the analysts involved act as limitations and need further attention.

149 Considering the above, present work studies the glaciers in the Suru Sub-basin (SSB), western Himalaya,  
 150 Jammu and Kashmir. Primary objectives of this study include: 1) presenting the inventory of recent glacier data  
 151 [area, length, debris cover, SLA, elevation (min & max), slope and aspect] in the SSB; 2) assessing the temporal  
 152 changes for four epochs in past 46 years; and 3) analysing the observed glacier response in relation to the  
 153 regional climate trends, local climate variability and other factors (regional hypsometry, topographic  
 154 characteristics, debris cover and geomorphic features). Several remote sensing and field based studies of  
 155 regional (Vijay and Braun, 2018) , local (Bhushan et al., 2018, Kamp et al., 2011; Pandey et al., 2011; Shukla  
 156 and Qadir, 2016, Rashid et al 2017, Murtaza and Romshoo, 2015) and glacier-specific nature (Garg et al., 2018;  
 157 2019; Shukla et al., 2018) have been conducted for monitoring the response of the glaciers to the climate  
 158 change. Glaciological studies carried out in or adjacent to the SSB suggest increased shrinkage, slowdown and  
 159 downwasting of the studied glaciers at variable rates (Kamp et al., 2011; Pandey et al., 2011; Shukla and Qadir,  
 160 2016; Bhushan et al., 2018). These studies also hint towards the possible role of topographic & morphometric  
 161 factors as well as debris cover in glacier evolution, though confined to their own specific regions. Previous  
 162 studies have also estimated the glacier statistics of SSB and reported the total number of glaciers and the  
 163 glacierized area to be 284 and 718.86 km<sup>2</sup> (Sangewar and Shukla, 2009) and 110 and 156.61 km<sup>2</sup> (SAC report,  
 164 2016), respectively. While the RGI reports varying results by two groups of analysts (number of glaciers: 514 &  
 165 304 covering an area of 550 & 606 km<sup>2</sup>, respectively) for 2000 itself.  
 166 Previous findings suggesting progressive degeneration of glaciers, apparent variation and discrepancies in  
 167 inventory estimates and also the fact that the currently available glacier details for the sub-basin are nearly 20  
 168 years old, mandate the recent and accurate assessment of the glaciers in the SSB and drive the present study.

Deleted: Prime

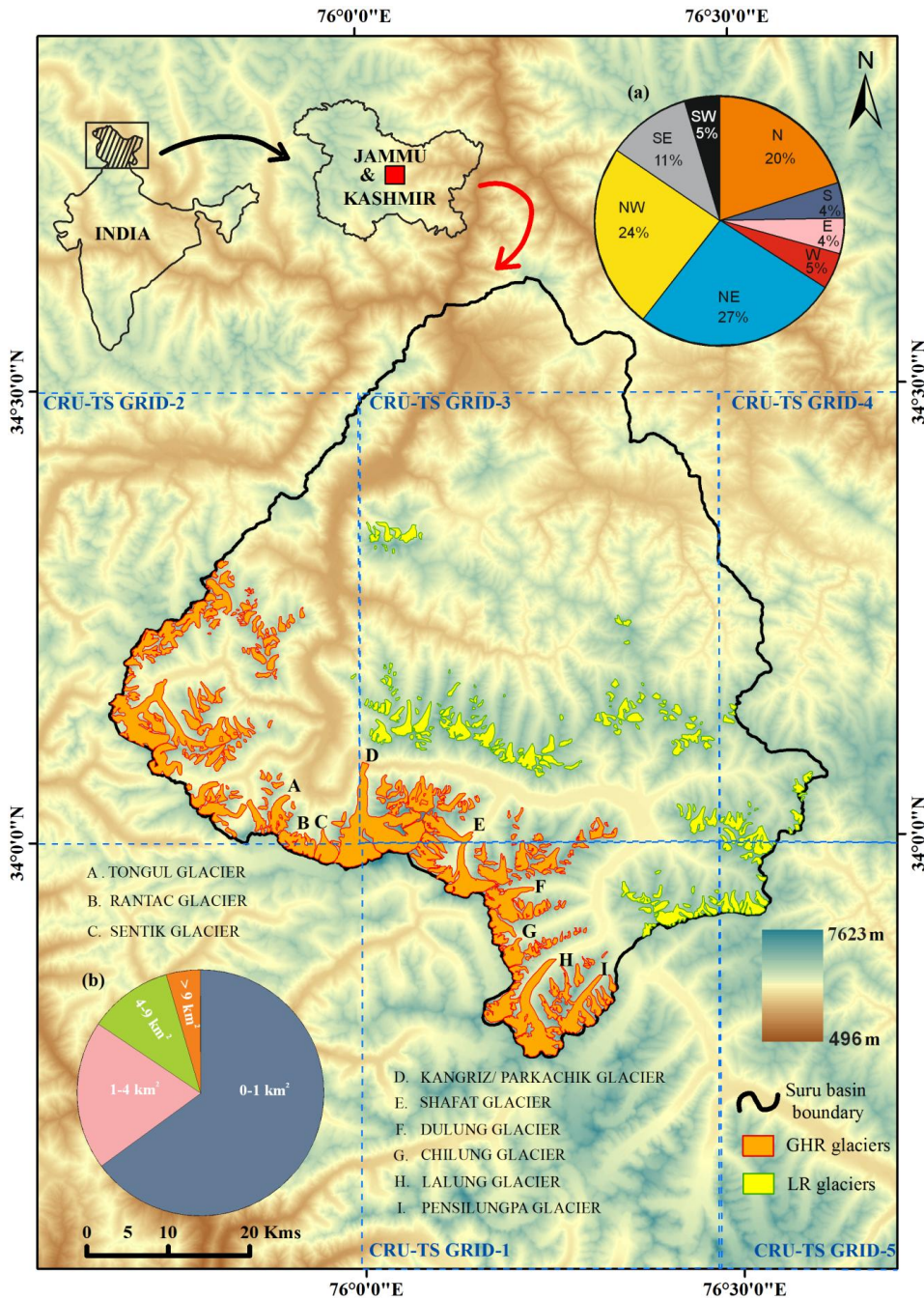
Deleted: .

169

## 170 2 Study area

171 The present study focuses on the glaciers of the SSB situated in the state of Jammu and Kashmir, western  
 172 Himalaya (Fig. 1). The geographic extent of the study area lies within latitude and longitude of 33° 50' to 34°  
 173 40' N to 75° 40'to 76° 30' E.

174 Geographically, the sub-basin covers part of two major ranges, i.e., GHR and LR and shows the presence of the  
 175 highest peaks of Nun (7135 masl) and Kun (7077 masl) in the GHR (Vittoz, 1954). The glaciers in these ranges  
 176 have distinct morphology, with the larger ones located in the GHR and comparatively smaller towards the LR  
 177 (Fig. 1).

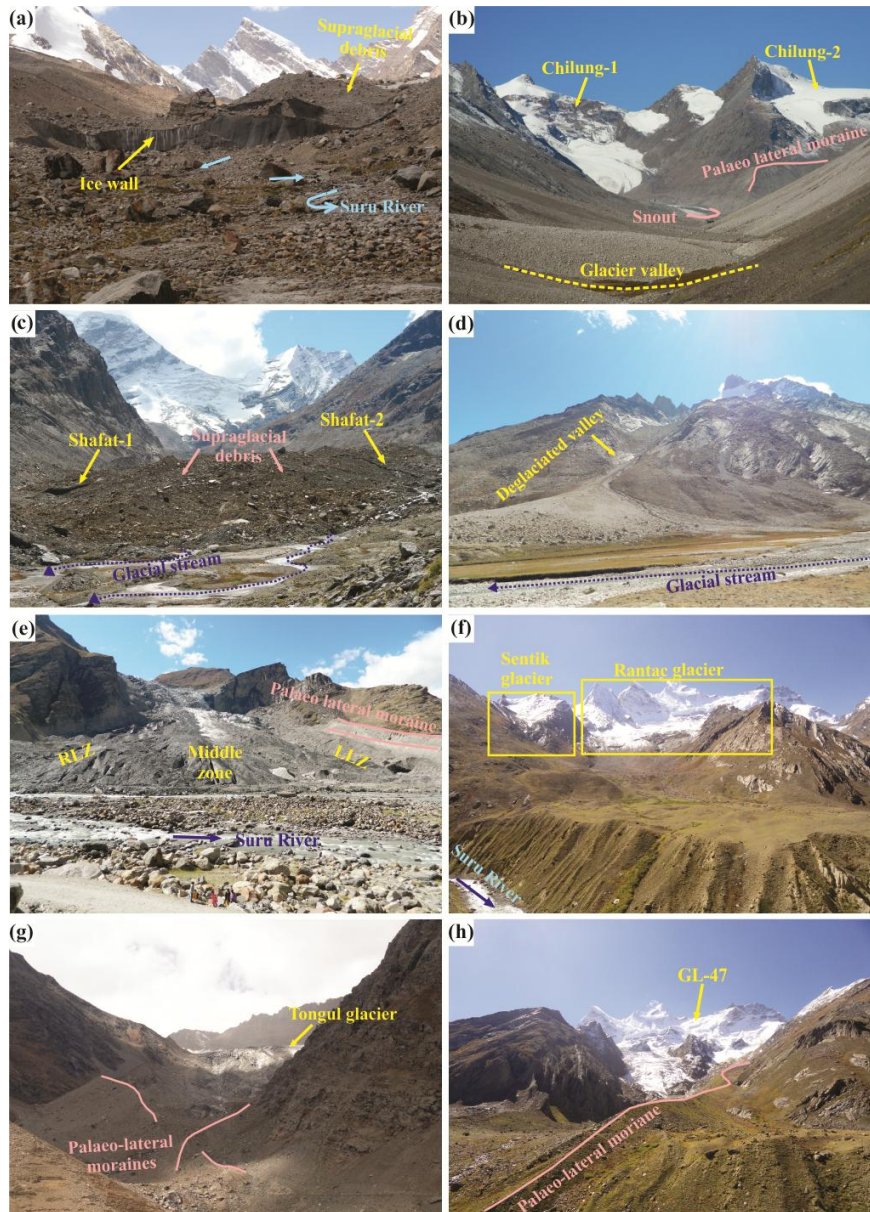


180  
 181 Figure 1: Location map of the study area. The glaciers in the Suru Sub-basin (black outline) are studied for their  
 182 response towards the climatic conditions during the period 1971-2017. Blue rectangles with dashed outlines  
 183 (GRID-1, 2, 3, 4 and 5) are the Climate Research Unit (CRU)-Time Series (TS) 4.02 grids of dimension  $0.5^\circ \times$   
 184  $0.5^\circ$ . (a) Pie-chart inset showing orientation-wise percentage distribution of glaciers in the sub-basin. North (N),  
 185 north-east (NE), north-west (NW), south (S), south-east (SE), south-west (SW), east (E) and west (W)

186 represents the direction of the glaciers. (b) Pie chart inset showing size-distribution of glaciers in the SSB. The  
187 glacier boundaries [GHR (orange) and LR (yellow)] are overlain on the Advanced Land Observing Satellite  
188 (ALOS) Digital Surface Model (DSM).

189  
190 The meltwater from these glaciers feeds the Suru River (tributary of Indus River), which emerges from the  
191 Pensilungpa glacier (Fig. 2a) at an altitude of ~4675 m asl. The river further flows north for a distance of ~24  
192 kms and takes a westward turn from Rangdum (~4200 m asl). While flowing through this path, the Suru River is  
193 fed by some of the major glaciers of the GHR namely Lalung, Dulung (Fig. 1), Chilung (Fig. 2b), Shafat (Fig.  
194 2c; d), Kangriz/ Parkachik (Fig. 2e), Sentik, Rantac (Fig.2f), Tongul (Fig. 2g) and Glacier no.47 (Fig. 2h).  
195 Amongst these major glaciers, Kangriz forms the largest glacier in the SSB, covering an area of ~53 km<sup>2</sup> and  
196 descends down from the peaks of Nun and Kun (Garg et al., 2018). The Suru River continues to flow for a  
197 distance of nearly 54 kms and after crossing a mountain spur and the townships of Tongul, Panikhar and  
198 Sankoo, the river further flows north until it finally merges with River Indus at Nurla (~3028 m asl).





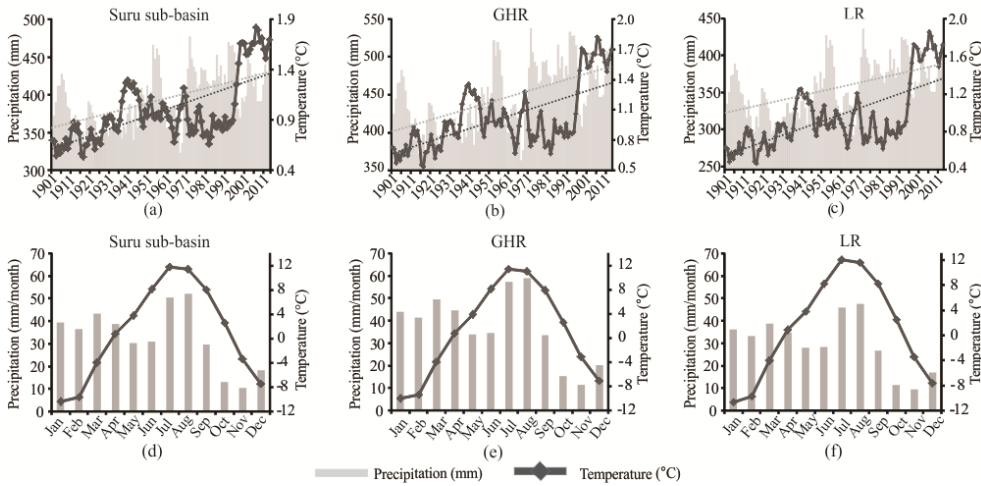
199  
 200 Figure 2: Field photographs of some of the investigated glaciers in the study area captured during the field visits  
 201 in September, 2016 and 2017. (a), (b), (c), (e), (f), (g), (h) Snouts of Pensilungpa, Chilung, Shafat, Kangriz,  
 202 Sentik & Rantac, Tongul glaciers and Glacier no.47, respectively. (d) Deglaciaded valley near the Shafat glacier.  
 203

204 The westerlies are an important source of moisture in this region (Dimri, 2013) with wide range of fluctuations  
 205 in snowfall during winters. In the Padum valley, annual mean precipitation (Snowfall) and temperature amounts  
 206 to nearly 2050 to 6840 mm and 4.3 °C, respectively (Raina and Kaul, 2011; <http://en.climate-data.org>). The  
 207 longterm average annual temperature and precipitation have varied from 5.5 °C/ 588.77 mm (Kargil) to -2.04

Deleted: has



209 °C/ 278.65 mm in Leh during the period 1901-2002 (IMD, 2015). However, in order to understand the long term  
 210 variability of climatic conditions in the SSB, we have utilized the Climate Research Unit (CRU)-Time Series  
 211 (TS) 4.02 data during the period 1901-2017 (Fig. 3; Harris and Jones, 2018). Derived from this data, the annual  
 212 mean temperature and precipitation of the SSB for the period 1901-2017 has been  $0.99 \pm 0.45$  °C and  $393 \pm 76$   
 213 mm, respectively. (Standard deviations associated with the mean temperature and precipitation have been  
 214 italicized throughout the text).



215  
 216 Figure 3: Annual and seasonal variability in the climate data for the period 1901-2017. (a), (b) and (c) 5 year  
 217 moving average of the mean annual precipitation (mm) and temperature (°C) recorded for 5 grids covering the  
 218 glaciers in the entire SSB, GHR and LR (sub-regions), respectively during the period 1901-2017. The light grey  
 219 colored dashed lines depict the respective trend lines for precipitation and temperature conditions during the period  
 220 1901-2017. (d), (e) and (f) Monthly mean precipitation and temperature data for the entire  
 221 SSB, GHR and LR (sub-regions), respectively for the time period 1901-2017.  
 222

## 223 3 Datasets and Methods

### 224 3.1 Datasets used

225 The study uses multi-sensor and multi-temporal satellite remote sensing data for extracting the glacier  
 226 parameters for four time periods, i.e., 1971/1977, 1994, 2000 and 2017, details of which are mentioned in Table  
 227 1. It involves 6 Landsat level 1 terrain corrected (L1T), 3 strips of declassified Corona KH-4B and 1 Sentinel  
 228 multispectral scenes, downloaded from USGS Earth Explorer (<https://earthexplorer.usgs.gov/>). Besides, a global  
 229 digital surface model (DSM) dataset utilizing the data acquired by the Panchromatic remote-sensing Instrument  
 230 for Stereo Mapping (PRISM) onboard the Advanced Land Observing Satellite (ALOS) have also been  
 231 incorporated (<https://www.eorc.jaxa.jp/ALOS/en/aw3d30/>). ALOS World 3D comprises of a fine resolution  
 232 DSM (approx 5m vertical accuracy). It is primarily used for delineating the basin boundary, extraction of SLA,  
 233 elevation range, regional hypsometry and slope.

Deleted: has

234  
 235 Table 1: Detailed specifications of the satellite data utilised in the present study. GB= glacier boundaries,  
 236 DC=debris cover

S. no	Satellite sensors(Date of acquisition)	Remarks on quality	Scene Id	RMSE error	Registration accuracy (m)	Purpose
1.	Corona KH-4B (28 Sep 1971)	Cloud free	DS1115-2282DA056/ DS1115-2282DA055/ DS1115-2282DA054	0.1	0.3	Delineation of GB
2.	LandsatMSS (19 Aug 1977/ 1 Aug 1977)	Cloud free/ peak ablation (17 Aug)	LM02_L1TP_159036_19770819_20180422_01_T2/ LM02_L1TP_159036_19770801_20180422_01_T2	0.12	10	Delineation of GB, SLA&DC
3.	LandsatTM (27 Aug 1994)	Partially cloud covered/ peak ablation	LT05_L1TP_148036_19940827_20170113_01_T1/ LT05_L1GS_148037_19940827_20170113_01_T2	0.22	6	Delineation of GB, SLA&DC
4.	LandsatTM (26 July 1994)	Seasonal snow cover	LT05_L1TP_148036_19940726_20170113_01_T1	0.2	6	Delineation of GB
5.	LandsatET M <sup>+</sup> (4 Sep 2000)	Cloud free/ peak ablation	LE71480362000248S GS00	Base image		Delineation of GB, SLA& DC
6.	LandsatOLI (25 July 2017)	Partially cloud covered/ peak ablation	LC08_L1TP_148036_20170810_01_T1	0.15	4.5	Delineation of GB & DC, estimation of SLA
7.	Sentinel MSI (20 Sep 2017)	Cloud free	S2A_MSIL1C_20170920T053641_N0205_R005_T43SET_20170920T053854	0.12	1.2	Delineation of GB & DC
8.	LISS IV (27 Aug 2017)	Cloud free	183599611	0.2	1.16	Accuracy assessment

239 The aforementioned satellite images were acquired keeping into consideration certain necessary pre-requisites,  
 240 such as, peak ablation months (July/ August/ September), regional coverage, minimal snow and cloud cover for  
 241 the accurate identification and demarcation of the glaciers. Only three Corona KH-4B strips were available for  
 242 period 1971, which covered the SSB partially, i.e., 40% of the GHR and 57% of the LR glaciers. Therefore, rest  
 243 of the glaciers were delineated using the Landsat MSS image of the year 1977 (Table 1). Similarly, some of the  
 244 glaciers could not be mapped using the Landsat TM image of 27 Aug 1994 as the image was partially covered  
 245 with clouds. Therefore, 26 July 1994 image of the same sensor was used in order to delineate the boundaries of  
 246 the cloud covered glaciers.

247 Besides, long term climate data have been obtained from CRU-TS 4.02, which is a high resolution gridded  
 248 climate dataset obtained from the monthly meteorological observations collected at different weather stations of  
 249 the World. In order to generate this long term data, station anomalies from 1961-1990 are interpolated into 0.5°  
 250 latitude and longitude grid cells (Harris and Jones, 2018). This dataset includes six independent climate  
 251 variables (mean temperature, diurnal temperature range, precipitation, wet-day frequency, vapour pressure and  
 252 cloud cover). However, in this study monthly mean, minimum and maximum temperature and precipitation data  
 253 are taken into consideration.

Deleted: has

254

### 255 3.2 Methodology adopted

256 The following section mentions the methods adopted for data extraction, analysis and uncertainty estimation.

257

#### 258 3.2.1 Glacier mapping and estimation of glacier parameters

259 Initially, the satellite images were co-registered by projective transformation at sub-pixel accuracy with the  
 260 Root Mean Square Error (RMSE) of less than 1m (Table 1), taking the Landsat ETM<sup>+</sup> image and ALOS DSM  
 261 as reference. However, the Corona image was co-registered following a two step approach: (1) projective  
 262 transformation was performed using nearly 160-250 GCPs (2) spline adjustment of the image strips (Bhambri et  
 263 al., 2012). The glaciers were mapped using a hybrid approach, i.e., normalized difference snow index (NDSI)  
 264 for delineating snow-ice boundaries and manual digitization of the debris cover. Considering that not many  
 265 changes would have occurred in the accumulation region, major modifications have been done in the boundaries  
 266 below the equilibrium line altitude (ELA) (Paul et al., 2017). The glacierets/ tributary glaciers contributing to  
 267 the main trunk are considered as single glacier entity. NDSI was applied on a reference image of Landsat ETM<sup>+</sup>  
 268 using an area threshold range of 0.55-0.6. A median filter of kernel size 3\*3 was used to remove the noise and  
 269 very small pixels. In this manner, glaciers covering a minimum area of 0.01 km<sup>2</sup> have been mapped. However,  
 270 some pixels of frozen water, shadowed regions were manually corrected. Thereafter, the debris covered part of  
 271 the glaciers was mapped manually by taking help from slope and thermal characteristics of the glaciers. Besides,  
 272 high resolution imageries from the Google Earth<sup>TM</sup> were also referred for the accurate demarcation of the  
 273 glaciers. Identification of the glacier terminus was done based on the presence of certain characteristic features  
 274 at the snout such as ice wall, proglacial lakes and emergence of streams. Length of the glacier was measured  
 275 along the central flow line (CFL) drawn from the bergschrund to the snout. Fluctuations in the snout position  
 276 (i.e., retreat) of an individual glacier was estimated using the parallel line method, in which parallel strips of 50  
 277 m spacing are taken on both sides of the CFL. Thereafter, the average values of these strips intersecting the  
 278 glacier boundaries were used to determine the frontal retreat of the glaciers (Shukla and Qadir, 2016; Garg et al.,

280 2017a;b). Mean SLA estimated at the end of the ablation season can be effectively used as a reliable proxy for  
 281 mass balance estimation for a hydrological year (Guo et al., 2014). The maximum spectral contrast between  
 282 snow and ice in the SWIR and NIR bands helps in delineation of the snow line separating the two facies. The  
 283 same principle was used in this study to yield the snow line. Further, a 15 m sized buffer was created on both  
 284 sides of the snow line to obtain the mean SLA. Other factors such as elevation (max & min), regional  
 285 hypsometry and slope were extracted utilising the ALOS DSM.

### 287 3.2.2 Analysis of climate variables

288 To ascertain the long term climate trends in the sub-basin, mean annual temperature (min & max) and  
 289 precipitation ~~are~~ derived by averaging the mean monthly data of the respective years. Besides, seasonal trends  
 290 ~~are~~ also analysed for winter (November-March) and summer (April-October) months. Moreover, the climate  
 291 variables ~~are~~ assessed separately for the ~46 year period (1971-2017), which is the study period of present  
 292 research.

~~Deleted:~~ have been

~~Deleted:~~ have

~~Deleted:~~ been

~~Deleted:~~ have also been

293 Further, the climate dataset was statistically analysed for five grids using Mann-Kendall test to obtain the  
 294 magnitude and significance of the trends (Supplementary table S2). The magnitude of trends in time series data  
 295 was determined using Sen's slope estimator (Sen, 1968). Quantitatively, the temperature and precipitation trends  
 296 have been assessed here in absolute terms (determined from Sen's slope). The change in climate parameters  
 297 (temperature and precipitation) was determined using following formula:

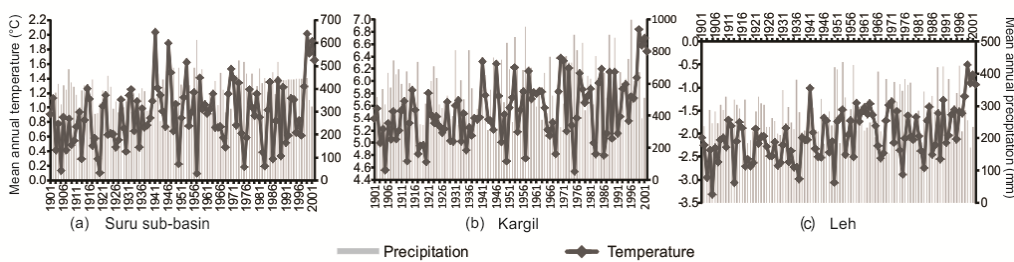
$$\text{Change} = (\beta * L) / M \quad (1)$$

299 where  $\beta$  is Sen's slope estimator,  $L$  is length of period and  $M$  is the long term mean.

300 These tests were performed at confidence level,  $S= 0.1(90\%)$ ,  $0.05(95\%)$  and  $0.01(99\%)$ , which differed for  
 301 both the variables (Supplementary table S2). Spatial interpolation of climate data was achieved using the Inverse  
 302 Distance Weighted (IDW) algorithm. For this purpose, a total number of 15 CRU TS grids (in vicinity of our  
 303 study area) were taken so as to have an ample number of data points in order to achieve the accurate results.

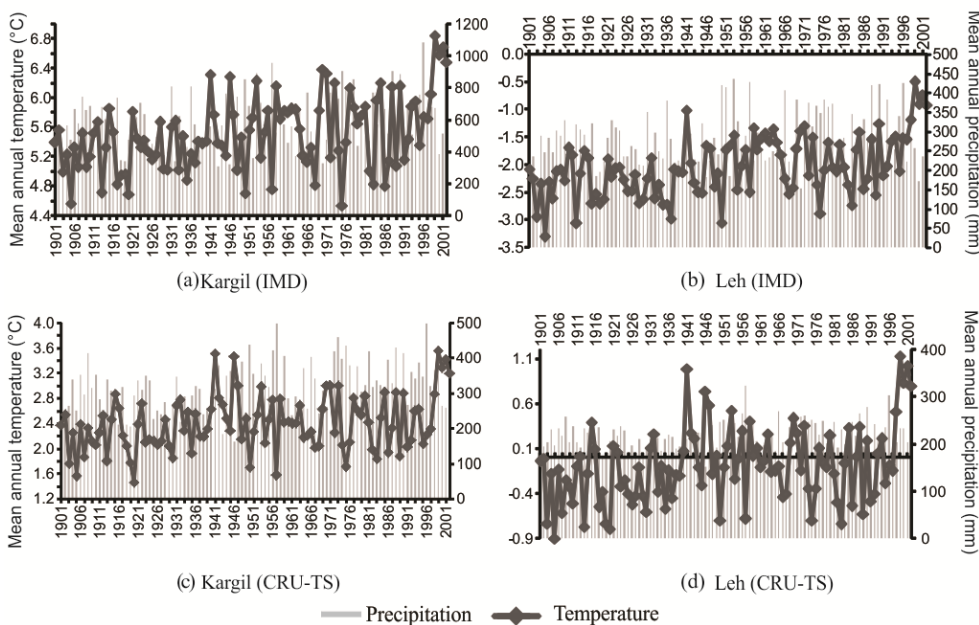
304 Further, in order to check data consistency, we have taken instrument data from nearest stations of Kargil and  
 305 Leh (due to the unavailability of meteorological stations in the Suru sub-basin) and compared with the CRU-TS  
 306 derived data for the entire Suru sub-basin during 1901-2002 period (Fig. 4).

~~Deleted:~~ up



307  
 308 Figure 4: Mean annual temperature and precipitation patterns of CRU-TS derived gridded data in (a) Suru sub-  
 309 basin and IMD recorded station at (b) Kargil and (c) Leh.

315 The mean annual temperature pattern of Suru sub-basin shows a near negative trend till 1937, with an increase  
 316 thereafter. Similar trends have been observed for Kargil and Leh, despite their distant location from the Suru  
 317 sub-basin (areal distance of Kargil and Leh is ~63 and 126 km, respectively from the centre of Suru sub-basin).  
 318 However, it is noteworthy to mention that all the locations had attained maximum mean annual temperature in  
 319 1999 (Suru: 2.02°C; Kargil: 6.84°C; Leh: -0.5°C). We observe an almost similar trend in all the cases (Fig. 4),  
 320 with an accelerated warming post 1995/96. However, the magnitude varies, with longterm mean annual  
 321 temperature of 0.9, 5.5 and -2.04°C observed in Suru sub-basin, Kargil and Leh, respectively (Fig. 4). The  
 322 possible reason for this difference in their magnitudes could possibly be attributed to their distinct geographical  
 323 locations and difference in their nature, with former being point, while latter being the interpolated gridded data.  
 324 Also, we have used the station data, obtained from nearest available IMD sites, i.e., Kargil and Leh and  
 325 compared with their respective CRU-TS data (mean annual temperature and precipitation).



326  
 327 Figure 5: Analysis of meteorological (mean annual temperature and precipitation) datasets derived from Indian  
 328 Meteorological Department (IMD) stations at (a) Kargil & (b) Leh and the respective [(c) Kargil and (d) Leh]  
 329 gridded data obtained from climate research unit (CRU)-time series (TS).

330 Though varying in magnitude, the climate data obtained from IMD as well as CRU-TS suggest almost similar  
 331 trends of temperature and precipitation during the period 1901-2002 for both Kargil and Leh (Fig. 5). The  
 332 annual mean temperature/ precipitation amounted to 5.5°C/589 mm (IMD) and 2.4°C/315 mm (CRU-TS) in  
 333 Kargil, while -2.04/279 mm (IMD) and -0.09/ 216 mm (CRU-TS) in Leh during the period 1901-2002 (Fig.  
 334 5). We observed that climatic variables show lower magnitude in case of CRU-TS as compared to the station  
 335 data from IMD (except CRU-TS derived temperature data recorded for Leh). The possible reason for this  
 336 difference between CRU-TS and station data can primarily be attributed to the difference in their nature, with  
 337 former being point, while latter being a gridded data (0.5° latitude and longitude grid cells). This analysis aptly

Deleted: have

339 brings out the bias in the CRU TS gridded data. Majorly the comparison shows that though the gridded data  
 340 correctly bring out the temporal trends in meteorological data, but differ with station data in magnitude (being  
 341 on lower side than the station estimates). This helps us better appreciate the climate variations in the Suru sub-  
 342 basin as well, since we learn that the reported temperature and precipitation changes are probably on the lower  
 343 side of the actual variations.

### 344 3.2.3 Uncertainty assessment

345 This study involves extraction of various glacial parameters utilizing satellite data with variable characteristics,  
 346 hence, susceptible to uncertainties, which may arise from various sources. These sources may be locational  
 347 (LE), interpretational (IE), classification (CE) or processing (PE) errors (Racoviteanu et al., 2009; Shukla and  
 348 Qadir, 2016). In our study, the LE and PE may have resulted on account of miss-registration of the satellite  
 349 images and inaccurate mapping, respectively. While IE and CE would have introduced due to the miss-  
 350 interpretation of glacier features during mapping. The former can be rectified by co-registration of the images  
 351 and estimation of sub-pixel co-registration RMSE (Table 1) and using standard statistical measures. However,  
 352 the latter can be visually identified and corrected but difficult for exact quantification owing to lack of reliable  
 353 reference data (field data) in most cases. As a standard procedure for uncertainty estimation, glacier outlines are  
 354 compared directly with the ground truth data as acquired using a Differential Global Positioning System (DGPS)  
 355 (Racoviteanu et al., 2008a). In this study, DGPS survey was conducted on the Pensilungpa and Kangriz glaciers  
 356 at an error of less than 1cm. Therefore, by comparing the snout position of Pensilungpa (2017) and Kangriz  
 357 (2018) glaciers derived from DGPS and OLI image, an accuracy of  $\pm 23$  and  $\pm 1.4$  m, respectively was obtained.  
 358 Also, the frontal retreat estimated for the Kangriz glacier using DGPS and OLI image is found to be  $38.63 \pm 47.8$   
 359 and  $39.98 \pm 56.6$  m, respectively during the period 2017-18. In this study, high resolution Linear imaging self-  
 360 scanning system (LISS)-IV imagery (spatial resolution of 5.8 m) is also used for validating the glacier mapping  
 361 results for the year 2017 (Table 1). Glaciers of varying dimensions and distribution of debris cover were  
 362 selected for this purpose. The area and length mapping accuracy for these selected glacier boundaries (G-1, G-2,  
 363 G-3, G-13, G-41, G-209, G-215, G-216, G-220, G-233) was found to be 3% and 0.5%, respectively.  
 364 The multi-temporal datasets were assessed for glacier length and area change uncertainty as per the methods  
 365 given by Hall et al. (2003) and Granshaw and Fountain (2006). Following formulations (Hall et al., 2003) were  
 366 used for estimation of the said parameters:

$$367 \text{Terminus uncertainty } (U_T) = \sqrt{a^2 + b^2} + \sigma \quad (2)$$

368 where, 'a' and 'b' are the pixel resolution of image 1 and 2, respectively and ' $\sigma$ ' is the registration error. The  
 369 terminus and areal uncertainty estimated are given in Table 2.

$$370 \text{Area change uncertainty } (U_A) = 2 * U_T * x \quad (3)$$

371 where, 'x' is the spatial resolution of the sensor.

372 Table 2. Terminus and Area change uncertainty associated with satellite dataset as defined by Hall et al. (2003).  
 373  $U_T$ = terminus uncertainty,  $U_A$ = area change uncertainty,  $x$ = spatial resolution,  $\sigma$  = registration accuracy.

Serial no.	Satellite sensor	Terminus uncertainty $U_T$ $= \sqrt{a^2 + b^2} + \sigma$	Area change uncertainty $U_A = 2 U_T * x$
------------	------------------	---	--

Deleted: been



1.	Corona KH-4B	3.12 m	0.00007 km <sup>2</sup>
2.	Landsat MSS	123.13 m	0.03km <sup>2</sup>
3.	Landsat TM	41.42 m	0.003 km <sup>2</sup>
4.	Landsat ETM <sup>+</sup>	48.42 m	0.003km <sup>2</sup>
5.	Landsat OLI	46.92 m	0.003km <sup>2</sup>

377  
378  
379  
380  
381  
382  
383  
384  
385  
386  
387  
388  
389  
390

Area mapping uncertainty ~~was~~ estimated using the buffer method, in which, a buffer size equal the registration error of the satellite image ~~was~~ taken into consideration (Bolch et al., 2012; Garg et al., 2017a,b). Error estimated using this method is found to be 0.48, 27.2, 9.6 and 3.41 km<sup>2</sup> for the 1971 (Corona), 1977 (MSS), 1994 (TM) and 2017 (OLI) image, respectively. Since the debris extents were delineated within the respective glacier boundaries, the proportionate errors are likely to have propagated in debris cover estimations which were estimated accordingly (Garg et al., 2017b).

**Deleted:** has also been

**Deleted:** is

Uncertainty in SLA estimation needs to be reported in the X, Y and Z directions. In this context, error in X and Y directions should be equal to the distance taken for creating the buffer on either side of the snow line demarcating the snow and ice facies. Since, the buffer size taken in this study was 15 m, therefore, error in X and Y direction was considered as  $\pm 15$  m. However, uncertainty in Z direction would be similar to the ALOS DSM, i.e.,  $\pm 5$  m.

391  
392  
393  
394  
395  
396  
397

## 4 Results

The present study involved creation of glacier inventory for the year 2017 and estimation of glacier (area, length, debris cover and SLA) parameters for four different time periods. For detailed insight, the variability of the glacier parameters have also been evaluated on decadal scale, in which the total time period has been sub-divided into three time frames, i.e., 1971-1994 (23 years), 1994-2000 (6 years) and 2000-2017 (17 years).

398  
399  
400  
401  
402  
403  
404  
405  
406  
407  
408  
409  
410  
411

### 4.1 Basin statistics

The SSB covers an area of  $\sim 4429$  km<sup>2</sup>. In 1971, the sub-basin had around 240 glaciers, with 126 glaciers located in the GHR and 114 in the LR, which remained the same till 2000. However, a major disintegration of glaciers took place during the period 2000-2017, which resulted into the breakdown of about 12 glaciers into smaller glacierets. The recent (2017) distribution of the glaciers in the GHR and LR is 130 and 122, respectively (Supplementary table S1). The overall glacierized area is  $\sim 11\%$ , with the size and length of the glaciers varying from 0.01 to 53.1 km<sup>2</sup> and 0.15 to 16.34 km, respectively.

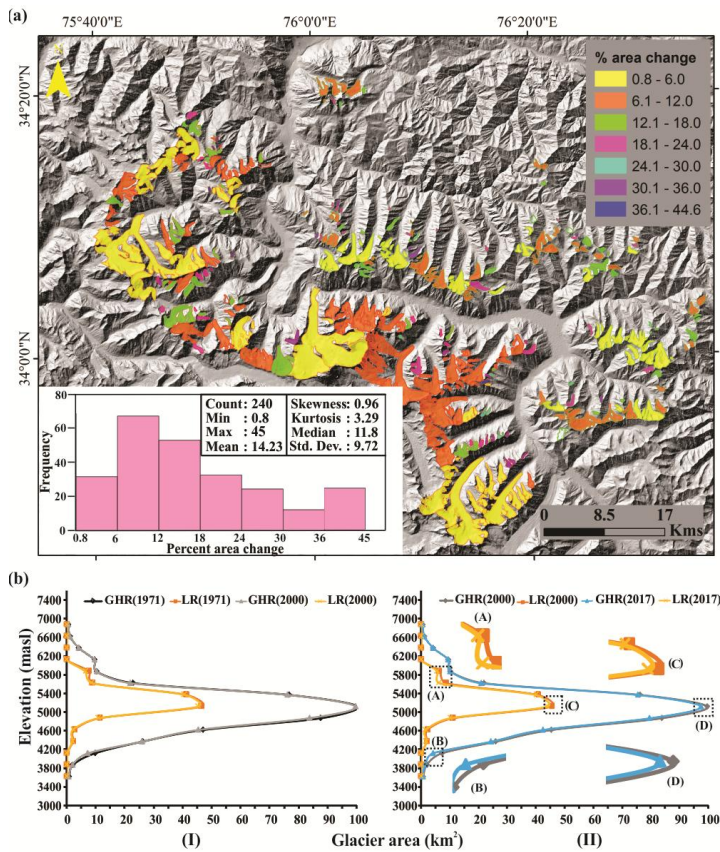
Within the sub-basin, the size range of glaciers in the GHR and LR vary from 0.01 (G-115) to 53.1 km<sup>2</sup> (G-50) and 0.03 (G-155/165) to 6.73 km<sup>2</sup> (G-209), respectively. Considering this, glaciers have been categorized into small (0-7 km<sup>2</sup>/ 0-2 km), medium (7-15 km<sup>2</sup>/ 2-7 km) and large (>15 km<sup>2</sup>/ >7 km). Based on size distribution, small (comprising all the LR and some GHR glaciers), medium and large glaciers occupy 47%, 15% and 38% of the glacierized sub-basin. Depending upon the percentage area occupied by the supraglacial debris out of the total glacier area, the glaciers have been categorized into clean (CG: 0-25%), partially debris-covered (PDG: 25-50%) and heavily debris-covered (HDG: >50%). Categorization of the glaciers based on this criteria shows their proportion in the glacierized basin as: CG (43%), PDG (40%) and HDG (17%). Majority of the glaciers in the

414 sub-basin are north facing (N/ NW/NE: 71%), followed by south (S/ SW/ SE: 20%), with very few oriented in  
 415 other (E/ W: 9%) directions (Fig. 1a). The mean elevation of the glaciers in the SSB is  $5134.8 \pm 225$  masl, with  
 416 an average elevation of  $5020 \pm 146$  and  $5260 \pm 117$  masl in the GHR and LR, respectively. Mean slope of the  
 417 glaciers is  $24.8 \pm 5.8^\circ$  and varies from  $24 \pm 6^\circ$  to  $25 \pm 6^\circ$  in the GHR and LR, respectively. While, percentage  
 418 distribution of glaciers shows that nearly 80% of the LR glaciers have steeper slope (20-40°) as compared to the  
 419 GHR glaciers (57%).

420

#### 421 4.2 Area changes

422 The glaciated area reduced from  $513 \pm 14$  km<sup>2</sup> (1971) to  $481 \pm 3.4$  km<sup>2</sup> (2017), exhibiting an overall deglaciation  
 423 of  $32 \pm 9$  km<sup>2</sup> ( $6 \pm 0.02\%$ ) during the period 1971-2017. Percentage area loss of the individual glaciers ranges  
 424 between 0.8 (G-50; Parkachik glacier) - 45 (G-81) %, with majority of the glaciers undergoing an area loss in  
 425 the range 6-12% during the period 1971-2017 (Fig.6a).



426

427 Figure 6: (a) Percent area loss of the glaciers in the SSB during the period 1971-2017. Frequency distribution  
 428 histogram depicting that majority of the glaciers have undergone an area loss in the range 6-12%. (b)  
 429 Hypsometric distribution of glacier area in the GHR and LR regions during the period (I) 1971-2000 and (II)  
 430 2000-2017. (A), (B), (C) and (D) insets in (II) shows the significant change in area at different elevation range  
 431 of the GHR and LR glaciers.

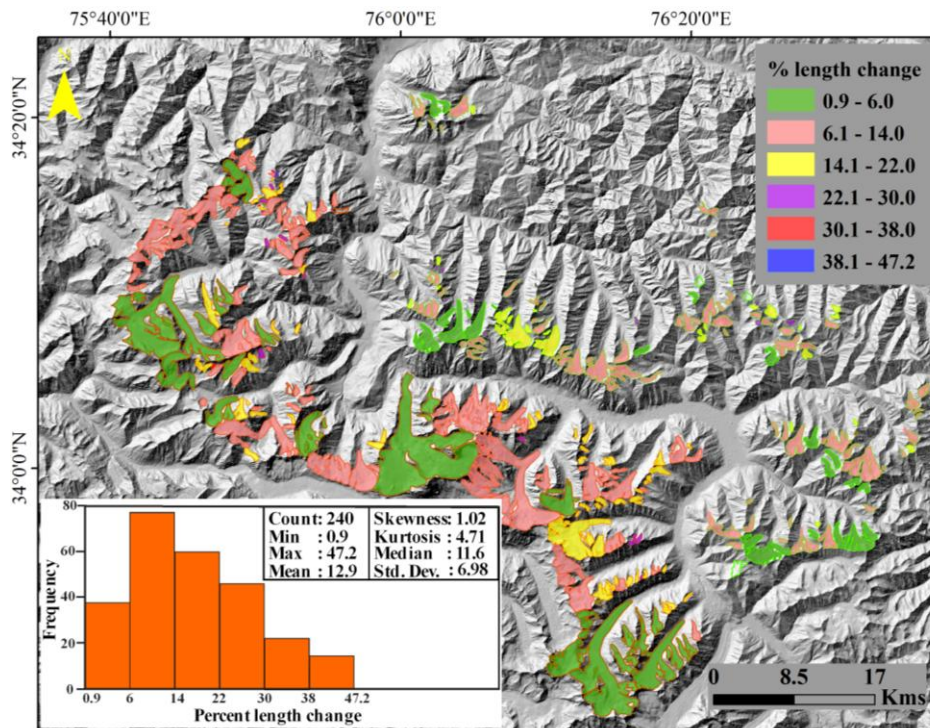
432

433 Results show that the highest pace of deglaciation is observed during 1994-2000 ( $0.95 \pm 0.005 \text{ km}^2\text{a}^{-1}$ ) and 2000-  
 434 2017 ( $0.86 \pm 0.0002 \text{ km}^2\text{a}^{-1}$ ) followed by 1971-1994 ( $0.5 \pm 0.001 \text{ km}^2\text{a}^{-1}$ ) (Supplementary figure S1a). Within the  
 435 SSB, glaciers in the LR exhibit higher deglaciation ( $7 \pm 7.2\%$ ) as compared to GHR ( $6 \pm 2\%$ ) during the period  
 436 1971-2017. Apart from deglaciation, G-50 also showed increment in glacier area during the period 1994-2000,  
 437 however, insignificantly.

438

### 439 4.3 Length changes

440 Fluctuations in the glacier snout have been estimated during the period 1971-2017 and it is observed that nearly  
 441 all the glaciers have retreated during the said period, however the retreat rates vary considerably. The overall  
 442 average retreat rate of the glaciers is observed to be  $4.3 \pm 1.02 \text{ ma}^{-1}$  during the period 1971-2017. Percentage  
 443 length change of the glaciers ranges between 0.9 to 47%, with majority of the glaciers retreating in the range 6-  
 444 14% during the period 1971-2017 (Fig.7).



445  
 446 Figure 7: Percent length change of the glaciers in the SSB during the period 1971-2017. Frequency distribution  
 447 histogram showing that majority of the glaciers have undergone length change of in the range 6-14%.  
 448

449 Decadal observations reveal the highest rate of retreat during 1994-2000 ( $7.37 \pm 8.6 \text{ ma}^{-1}$ ) followed by 2000-  
 450 2017 ( $4.66 \pm 1.04 \text{ ma}^{-1}$ ) and lowest during 1971-1994 ( $3.22 \pm 2.3 \text{ ma}^{-1}$ ) (Supplementary figure S 1b). Also, the  
 451 average retreat rate in the GHR and LR glaciers was observed to be  $5.4 \pm 1.04 \text{ ma}^{-1}$  and  $3.3 \pm 1.04 \text{ ma}^{-1}$ ,  
 452 respectively, during the period 1971-2017. The retreat rate of individual glaciers varied from  $0.72 \pm 1.02 \text{ ma}^{-1}$

453 (G-114) to  $28.92 \pm 1.02 \text{ ma}^{-1}$  (G-7, i.e., Dulung glacier) during the period 1971-2017. Besides, the Kangriz  
 454 glacier (G-50) also showed advancement during the period 1994-2000 by  $5.23 \pm 8.6 \text{ ma}^{-1}$ .

455

#### 456 **4.4 Debris-cover changes**

457 Results show an overall increase in debris-cover extent by 62% ( $\sim 37 \pm 0.002 \text{ km}^2$ ) in the SSB glaciers during the  
 458 period 1971-2017. Decadal variations exhibit the maximum increase in the debris-cover by approximately 19  
 459  $\pm 0.00004 \text{ km}^2$  (24%) during 2000-2017 followed by an increase of  $13 \pm 0.0001 \text{ km}^2$  (20%) and  $5 \pm 0.0001 \text{ km}^2$   
 460 (9%) during 1994-2000 and 1971-1994, respectively (Supplementary figure S1c). However, GHR and LR  
 461 glaciers show an overall increase of debris cover extent by 59% and 73%, respectively during the entire study  
 462 period, i.e., 1971-2017.

463

#### 464 **4.5 SLA variations**

465 The mean SLA shows an average increase of  $22 \pm 60 \text{ m}$  during the period 1977-2017. On the decadal scale, SLA  
 466 variations showed the highest increase ( $161 \pm 59 \text{ m}$ ) during 1994-2000 with a considerably lower increase ( $8 \pm 59$   
 467  $\text{ m}$ ) during 1977-1994 and decrease ( $150 \pm 60 \text{ m}$ ) during 2000-2017. Amongst the four time periods (1977, 1994,  
 468 2000 & 2017) used for mean SLA estimation, the highest SLA is noted during 2000 ( $5158 \pm 65 \text{ masl}$ ) and  
 469 minimum during 1977 ( $4988 \pm 65 \text{ masl}$ ) (Supplementary figure S1d).

470 During the period 1977-2017, the average SLA of the LR glaciers is observed to be relatively higher ( $5155 \pm 7$   
 471  $\text{ masl}$ ) as compared to the GHR glaciers ( $4962 \pm 9 \text{ masl}$ ). In contrast, an overall rise in mean SLA was noted in  
 472 GHR ( $49 \pm 69 \text{ m}$ ), while a decrease in LR glaciers ( $18 \pm 45 \text{ m}$ ) during the time frame of 1977-2017.

473

### 474 **5 Discussion**

475 The present study reports detailed temporal inventory data of the glaciers in the SSB considering multiple  
 476 glacier parameters, evaluates the ensuing changes for ascertaining the status of glaciers and relates them to  
 477 climate variability and other inherent terrain characteristics. The results suggest an overall degeneration of the  
 478 glaciers with pronounced spatial and temporal heterogeneity in response.

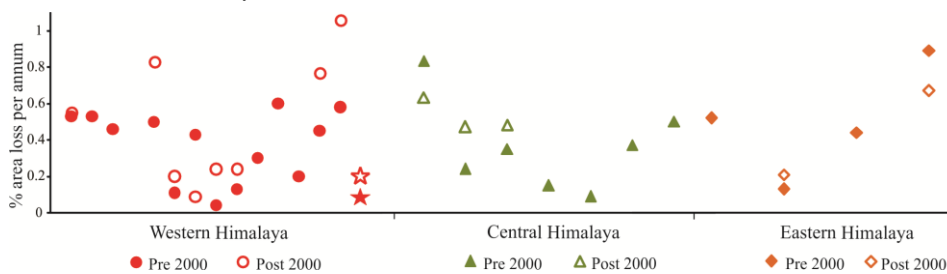
479

#### 480 **5.1 Glacier variability in Suru sub-basin: A comparative evaluation**

481 Basin statistics reveal that in the year 2000, the SSB comprised of 240 glaciers covering an area of  
 482 approximately  $496 \text{ km}^2$ . However, these figures differ considerably from the previously reported studies in this  
 483 particular sub-basin, with the total number of glaciers and the glacierized area varying from 284/  $718.86 \text{ km}^2$   
 484 (Sangewar and Shukla, 2009) to 110/  $156.61 \text{ km}^2$  (SAC report, 2016), respectively. In contrast, the glacierized  
 485 area is found to be less, however comparable with the RGI boundaries ( $550.88 \text{ km}^2$ ). Besides, debris cover  
 486 distribution of the glaciers during 2000 is observed to be  $\sim 16\%$  in the present study, which is almost half of that  
 487 reported in RGI (30%). Variability in these figures is possibly due to the differences in the mapping techniques,  
 488 thereby increasing the risk of systematic error. Moreover, due to the involvement of different analysts in the  
 489 latter, the results may more likely suffer with random errors.

490 Results from this study reveal an overall deglaciation of the glaciers in the SSB at an annual rate of  $\sim 0.1$   
 491  $\pm 0.0004\%$  during the period 1971-2017. This quantum of area loss is comparatively less to the average annual

492 rate of 0.4% reported in the western Himalaya (Supplementary table S3). However, our results are comparable  
 493 with Birajdar et al. (2014), Chand and Sharma (2015) and Patel et al. (2018) and differ considerably with other  
 494 studies in the western Himalayas (Supplementary table S3). Period wise deglaciation varied from  $0.1 \pm 0.0007$  to  
 495  $0.2 \pm 0.005\% \text{ a}^{-1}$  during 1971-2000 and 2000-2017, respectively. This result is in line with the recent findings by  
 496 Maurer et al. (2019), who suggest a higher average mass loss post 2000 ( $-0.43 \text{ m w.e.a}^{-1}$ ), which is almost  
 497 double the rate reported during 1975-2000 ( $-0.22 \text{ m w.e.a}^{-1}$ ) for the entire Himalaya.  
 498 Comparing the deglaciation rates of the glaciers within the western Himalayan region reveals considerable  
 499 heterogeneity therein (Supplementary table S3). It is observed that the Karakoram Himalayan glaciers, in  
 500 particular had been losing area till 2000 at an average rate of  $0.09\% \text{ a}^{-1}$ , with an increase in area thereafter by  
 501  $\sim 0.05\% \text{ a}^{-1}$  (Liu et al., 2006; Minora et al., 2013; Bhambri et al., 2013). However, glaciers in the GHR and Trans  
 502 Himalayan range have been deglaciating with higher average annual rate of 0.4 and  $0.6\% \text{ a}^{-1}$ , respectively during  
 503 the period 1962-2016 (Kulkarni et al., 2007; Kulkarni et al., 2011; Rai et al., 2013; Chand and Sharma, 2015;  
 504 Mir et al., 2017; Schmidt and Nusser, 2017; Chudley et al., 2017; Patel et al., 2018; Das and Sharma, 2018). In  
 505 contrast to these studies, deglaciation rates in SSB, which comprises of glaciers in GHR as well as LR have  
 506 varied from  $0.1\% \text{ a}^{-1}$  (GHR) to  $0.2\% \text{ a}^{-1}$  (LR) (present study). These results evidently depict that the response of  
 507 the SSB glaciers is transitional between the Karakoram Himalayan and GHR glaciers. Period wise area loss of  
 508 the glaciers in the Himalayan region suggest maximum average deglaciation of eastern ( $0.49\%/\text{yr}$ ), followed by  
 509 central ( $0.36\%/\text{yr}$ ) and western ( $0.35\%/\text{yr}$ ) Himalayan glaciers before 2000. Contrarily, after 2000, the central  
 510 Himalayan glaciers deglaciated at the maximum rate ( $0.52\%/\text{yr}$ ) followed by western ( $0.46\%/\text{yr}$ ) and eastern  
 511 ( $0.44\%/\text{yr}$ ) Himalayan glaciers (Fig.8). Though these rates reflect the possible trend of deglaciation in the  
 512 Himalayan terrain, however, any conclusion drawn would be biased due to insufficient data, particularly in  
 513 eastern and central Himalaya.



514  
 515 Figure 8: Annual rate of percentage area loss of glaciers in three major sections of Himalaya before and after  
 516 2000. Details of the same have been mentioned in Table S3 of Supplementary sheet. Results from the present  
 517 study have been star marked in the western Himalaya.  
 518

519 In this study, we found an overall average retreat rate of  $4.3 \pm 1.02 \text{ ma}^{-1}$  during the period 1971-2017. However,  
 520 the average retreat rates of seven glaciers in the SSB, reported by Kamp et al., (2011) is found to be nearly twice  
 521 ( $24 \text{ ma}^{-1}$ ) of that found in this study ( $10 \text{ ma}^{-1}$ ). The comparatively higher retreat rates in the former might be due  
 522 to the consideration of different time frames. The average retreat rates in other basins of the western Himalaya is  
 523 also found to be higher ( $7.8 \text{ ma}^{-1}$ ) in the Doda valley (Shukla and Qadir, 2016),  $8.4 \text{ ma}^{-1}$  in Liddar valley  
 524 (Murtaza and Romshoo, 2015),  $15.5 \text{ ma}^{-1}$  in the Chandra-Bhaga basin (Pandey and Venkataraman, 2013) and 19



525  $\text{ma}^{-1}$  in the Baspa basin (Mir et al., 2017). These results show lower average retreat rate of the glaciers in the  
 526 SSB as compared to the other studies in the western Himalaya.  
 527 The observed average retreat rates during 2000-2017 ( $4.6 \pm 1.02 \text{ ma}^{-1}$ ) is found to be nearly twice of that, noted  
 528 during 1971-2000 ( $2 \pm 1.7 \text{ ma}^{-1}$ ). Similar higher retreat rates post 2000 have been reported in the Tista basin  
 529 (Raina, 2009), Doda valley (Shukla and Qadir, 2016), Chandra Bhaga basin (Pandey and Venkataraman, 2013)  
 530 and Zaskar basin (Pandey et al., 2011). However, these studies may not sufficiently draw a generalized picture  
 531 of glacier recession in the Himalayan region.

532

## 533 5.2 Spatio-temporal variability in the climate data

534 Climatic fluctuations play a crucial role in understanding glacier variability. In this regard, CRU-TS 4.02 dataset  
 535 helped in delineating the long term fluctuations in the temperature and precipitation records.

### 536 5.2.1 Basin-wide climate variability

537 During an entire duration of 116 years, i.e. from 1901-2017, maximum mean annual temperature is observed in  
 538 2016 ( $3.23 \text{ }^\circ\text{C}$ ) and minimum during 1957 ( $-0.51 \text{ }^\circ\text{C}$ ). Mean annual temperature shows an almost uniform trend  
 539 till 1996, with a pronounced rise thereafter till 2005/06 period (Fig. 3a;b;c). The globally averaged combined  
 540 land and ocean surface temperature data of 1983-2012 period **are** considered as the warmest 30-year period in  
 541 the last 1400 years (IPCC, 2013). This unprecedented rate of warming **is** primarily attributed to the rapid scale of  
 542 industrialization, increase in regional population and anthropogenic activities prevalent during this time period  
 543 (Bajracharya et al., 2008; IPCC, 2013). Thus, one of the probable reason for this sudden **increase** in temperature  
 544 pattern is possibly due to the greenhouse effect from enhanced emission of black carbon in this region (by 61%)  
 545 from 1991-2001. Evidences of incessant increase in temperature during 1990s **has** also been observed (through  
 546 chronology of Himalayan Pine) from the contemporaneous surge in tree growth rate (Singh and Yadav 2000). In  
 547 fact, 50% of the years since 1970 have experienced considerably high solar irradiance and warm phases of  
 548 ENSO, which is possibly one of the reasons for the considerable rise in temperature throughout the Himalaya  
 549 (Shekhar et al., 2017). Maximum mean annual precipitation is noted during 2015 (615 mm) and minimum  
 550 during 1946 (244 mm). However, the mean annual precipitation followed a similar trend till 1946 with an  
 551 increasing thereafter (Fig. 3a;b;c). Besides these general trends in temperature and precipitation, an overall  
 552 absolute increase in the mean annual temperature ( $T_{\text{max}}$  &  $T_{\text{min}}$ ) and precipitation data have been noted as  $0.77$   
 553  $^\circ\text{C}$  ( $0.25 \text{ }^\circ\text{C}$  &  $1.3 \text{ }^\circ\text{C}$ ) and 158 mm, respectively during the period 1901-2017. These observations suggest an  
 554 enhanced increase in  $T_{\text{min}}$  by nearly 5 times as compared to the  $T_{\text{max}}$  alongwith a simultaneous increase in the  
 555 precipitation during the period 1901-2017.

556 Seasonal variations reveal monthly mean temperature and precipitation of  $6.7 \text{ }^\circ\text{C}$  and 1071 mm during summer  
 557 (Apr-Oct) and  $-6.9 \text{ }^\circ\text{C}$  and 890 mm during winter (Nov-Mar) recorded during 1901-2017 period. Maximum  
 558 monthly mean temperature and precipitation have been observed in July ( $11.8 \text{ }^\circ\text{C}/ 50.4 \text{ mm}$ ) and August ( $11.4$   
 559  $^\circ\text{C}/ 52 \text{ mm}$ ) during the period 1901-2017, suggesting them to be the warmest and wettest months. While,  
 560 January is noted to be the coldest ( $-10.4 \text{ }^\circ\text{C}$ ) and November (10.3 mm) to be the driest months in the duration of  
 561 116 years (Fig. 3d;e;f). Summer/ winter mean annual temperature and precipitation have increased significantly  
 562 by an average  $0.74/ 1.28 \text{ }^\circ\text{C}$  and  $85/ 72 \text{ mm}$ , respectively during the period 1901-2017. These values reveal a  
 563 relatively higher rise in winter average temperature in contrast to the summer. However, enhanced increase in  
 564  $T_{\text{min}}$  ( $1.8^\circ\text{C}$ ) during winter and  $T_{\text{max}}$  ( $0.78^\circ\text{C}$ ) during summer have also been observed during the 1901-2017 time

Deleted: is

Deleted: has been

Deleted: increment

Deleted: have

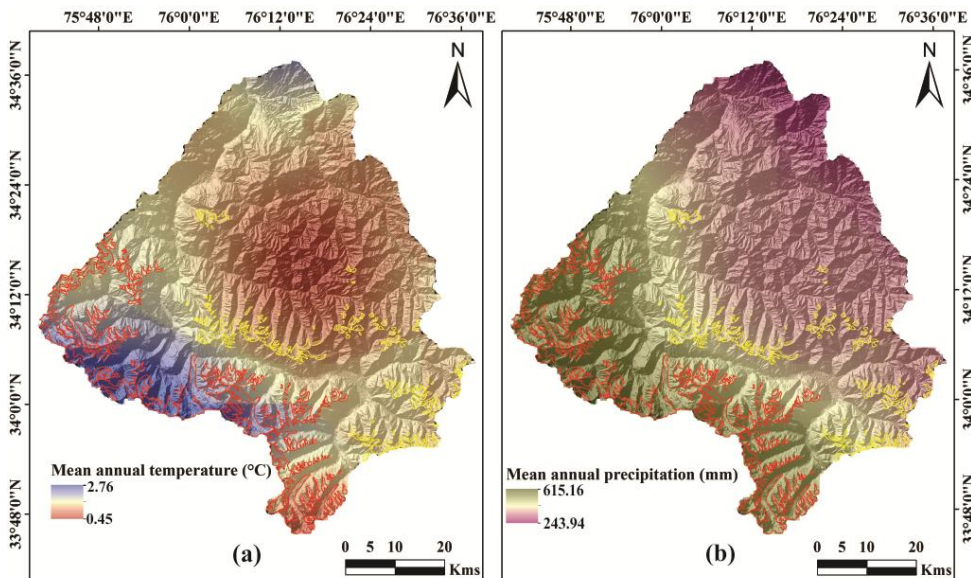


569 period. The relatively higher rise in the winter temperature (particularly  $T_{\min}$ ) and precipitation possibly suggest  
 570 that the form of precipitation might have changed from solid to liquid during this particular time span. Similar  
 571 increase in the winter temperature have also been reported from the NW Himalaya during the 20<sup>th</sup> century  
 572 (Bhutiyani et al., 2007).

573 In contrast to the long-term climate trends, we have also analyzed the climate data for the study period, i.e.,  
 574 1971-2017. An overall increase in the average temperature (0.3°C),  $T_{\max}$  (0.45°C)  $T_{\min}$  (1.02°C) and  
 575 precipitation by 213 mm is observed. Meanwhile, an enhanced increase in winter  $T_{\min}$  (1.7°C) and summer  $T_{\max}$   
 576 (0.45°C) are observed. These findings aptly indicate the important role of winter  $T_{\min}$  and summer  $T_{\max}$  in the  
 577 SSB.

### 578 5.2.2 Local climate variability

579 Apart from these generalized climatic variations, grid-wise analysis of the meteorological parameters reveal  
 580 existence of local climate variability within the sub-basin (Fig. 3; 9).



581  
 582 Figure 9: Spatial variation in meteorological data recorded for 15 grids in the SSB during the period 1901-2017.  
 583 Map showing the long term mean annual (a) temperature (°C) and (b) precipitation (mm) data within the sub-  
 584 basin suggesting the existence of significant local climate variability in the region. Glacier boundaries are shown  
 585 as: GHR (red) and LR (yellow).

586  
 587 Observations indicate that the glaciers covered in grid 4 have been experiencing a warmer climatic regimes with  
 588 the maximum annual mean temperature of 1.69 °C as compared to the other glaciers in the region (grid 2 = 1.4  
 589 °C, grid 5 = 0.74 °C, grid 1 = 0.65 °C and grid 3 = 0.45 °C). Spatial variability in annual mean precipitation data  
 590 reveal that grid 2 (448 mm) & grid 1 (442 mm) experienced wetter climate as compared to grid 4 (383 mm),  
 591 grid 3 (373 mm) and minimum in grid 5 (318 mm). These observations suggest that GHR glaciers have been  
 592 experiencing a warmer and wetter climate (1.03 °C/ 445 mm) as compared to the LR glaciers (0.96 °C/ 358 mm)

Deleted: s

Deleted: experiences

595 (Fig. 3e; f). These observations clearly show that local climate variability does exist in the basin for the entire  
 596 duration of 116 years (Fig. 9).

597

### 598 **5.3 Glacier changes: Impact of climatic and other plausible factors**

599 The alterations in the climatic conditions, discussed in Sect. 5.2, would in turn, influence the glacier parameters,  
 600 however varying with time. This section correlates the climatic and other factors (elevation range, regional  
 601 hypsometry, slope, aspect and proglacial lakes) with the variations in the glacier parameters.

602

#### 603 **5.3.1 Impact of climatic factors**

604 An overall degenerating pattern of the glaciers in the SSB is observed during the period 1971-2017, with  
 605 deglaciation of  $32 \pm 9 \text{ km}^2$  ( $6 \pm 0.02\%$ ). In the same duration, the glaciers have also retreated by an average  $199$   
 606  $\pm 46.9 \text{ m}$  (retreat rate:  $4.3 \pm 1.02 \text{ m a}^{-1}$ ) alongwith an increase in the debris cover by  $\sim 62\%$ . The observed overall  
 607 degeneration of the glaciers have possibly resulted due to the warming of climatic conditions during this  
 608 particular time frame. The conspicuous degeneration of these glaciers might have led to an increased melting of  
 609 the glacier surface, which in turn would have unveiled the englacial debris cover and increased its coverage in  
 610 the ablation zone (Shukla et al., 2009; Scherler et al., 2011). An enhanced degeneration of the glaciers have been  
 611 noted during 2000-2017 ( $0.85 \pm 0.005 \text{ km}^2 \text{ a}^{-1}$ ) than 1971-2000 ( $0.59 \pm 0.005 \text{ km}^2 \text{ a}^{-1}$ ). Also, nearly 12 glaciers  
 612 have shown disintegration into glacierets after 2000. These observations may be attributed to the relatively  
 613 higher annual mean temperature ( $1.68 \text{ }^\circ\text{C}$ ) during the former as compared to the period 1971-2000 ( $0.89 \text{ }^\circ\text{C}$ ).  
 614 Concomitant to the maximum glacier degeneration during the period 2000-2017, debris cover extent has also  
 615 increased more (24%) as compared to 1971-2000 (16%). The enhanced degeneration of the glaciers during  
 616 2000-2017 might have facilitated an increase in the distribution of supraglacial debris cover. A transition from  
 617 CGs to PDGs has also been noticed which resulted due to increase in the debris cover percentage over nearly 99  
 618 glaciers. The conversion from PDGs to HDGs (39) and from CGs to HDGs (2) has also occurred. Also, most of  
 619 these transitions have occurred during 2000-2017, which confirms the maximum degeneration of the glaciers  
 620 during this particular period.

621 It is observed in our study that smaller glaciers have deglaciated more (4.13%) than the medium (1.08%) and  
 622 larger (1.03%) sized glaciers during the period 1971-2017 (Supplementary figure S2). This result depicts an  
 623 enhanced sensitivity of the smaller glaciers towards the climate change (Bhambri et al., 2011; Basnett et al.,  
 624 2013; Ali et al., 2017). A similar pattern of glacier degeneration is noted during 1971-2000, with smaller  
 625 glaciers deglaciating more (5%) as compared to the medium sized (3%) and larger (1%) ones. However during  
 626 2000-2017, medium glaciers showed slightly greater degeneration (3.9%) as compared to the smaller (3.7%)  
 627 followed by larger ones (1.5%). We have also observed maximum length change for smaller glaciers (8%) in  
 628 comparison to medium (5%) and large glaciers (3%). These results indicate that the snout retreats are commonly  
 629 associated with small and medium sized glaciers (Mayewski et al., 1980).

630 Temporal and spatial variations in SLAs are an indicator of ELAs, which in turn provide direct evidences  
 631 related to the change in climatic conditions (Hanshaw and Bookhagen, 2014). SLAs are amongst the dynamic  
 632 glacier parameters that alters seasonally and annually, indicating their direct dependency towards the climatic  
 633 factors such as temperature and precipitation. In the present study, the mean SLA has gone up by an average  $22$   
 634  $\pm 60 \text{ m}$  during the period 1977-2017. This rise in SLA is synchronous with the increase in mean annual

635 temperature by 0.43°C. Moreover, the maximum rise in SLA during 1994-2000 is contemporaneous with the  
 636 rise of temperature by 0.64 °C during this time period.  
 637 Further, in order to understand the regional heterogeneity in glacier response within the sub-basin, parameters of  
 638 the GHR and LR glaciers are analyzed separately at four different time periods and correlated with the climatic  
 639 variables. It is found that the LR glaciers have deglaciated more (7.2%) as compared to the GHR glaciers  
 640 (5.9%). Similarly, more debris cover is found to have accumulated over the LR (73%) glaciers as compared to  
 641 the GHR (59%) glaciers during 1971-2017. This result shows that the relatively cleaner (LR) glaciers tend to  
 642 deglacierate more alongwith accumulation of more debris as compared to the debris and partially debris covered  
 643 glaciers (GHR glaciers) (Bolch et al., 2008; Scherler et al., 2011). Moreover, increase in mean annual  
 644 temperature in the LR (0.3°C) is slightly greater than in GHR (0.25°C) during the period 1971-2017, thus  
 645 exhibiting a positive correlation with deglaciation and debris cover distribution in these regions. We also  
 646 observed that the glacier area, length and debris cover extent of the LR glaciers show a good correlation with  
 647 winter  $T_{min}$  and average precipitation as compared to the GHR glaciers (Table 3). This shows that both  
 648 temperature as well as precipitation influence the degeneration of the glaciers and in turn affects the supraglacial  
 649 debris cover. It is believed that winter precipitation has a prime control on accumulation of snow on the glaciers,  
 650 hence acts as an essential determinant of glacier health (Mir et al., 2017). Also, the negative correlation of  
 651 glacier area with precipitation in this study possibly indicate the major role of increased winter temperature and  
 652 precipitation, which might have decreased the accumulation of snow, thereby decreasing the overall glacier area.  
 653 The average SLA for LR glaciers is observed to be higher as compared to the GHR glaciers. However, a  
 654 relatively higher rise in SLA is observed for GHR in contrast to the LR glaciers. Also, the mean SLA of the  
 655 GHR glaciers shows a good positive correlation with summer  $T_{max}$  as compared to the LR glaciers, while a  
 656 negative correlation with precipitation in the respective year (Table 3). Considering these observations, it  
 657 appears that a general rise in SLA can be attributed to regional climatic warming while that of individual SLA  
 658 variation in glaciers may be related to their unique topography (Shukla and Qadir, 2016).

659 From this analysis, it is quite evident that climatic factors directly influence the glacier response. Also, summer  
 660  $T_{max}$  have a stronger control over SLA, while glacier area,length and debris cover are predominantly controlled  
 661 by the winter  $T_{min}$  in the sub-basin.

662

663 Table 3: Coefficients of determination (r) between respective meteorological (temperature and precipitation)  
 664 data and observed glacier parameters in the Greater Himalayan Range (GHR) and Ladakh Range (LR) at 90%  
 665 confidence. Tavg, Tmin and Tmax are montly mean, monthly mean minimum, monthly mean maximum  
 666 temperatures and Pptismontly mean precipitation during different point in time (1971,1994, 2000 and 2017)

Major Mountain Ranges	Glacier Parameters	Climate Variables			
		Tavg	Tmin	Tmax	Ppt
GHR	Area	-0.826	<b>-0.897</b>	-0.347	-0.670
	Length	-0.908	<b>-0.926</b>	-0.345	-0.719
	Debris cover	0.842	<b>0.847</b>	0.434	0.593
	SLA	0.725	0.209	<b>0.725</b>	-0.315
LR	Area	-0.900	<b>-0.942</b>	-0.568	-0.779
	Length	-0.909	<b>-0.939</b>	-0.569	-0.778
	Debris cover	0.929	<b>0.907</b>	0.595	0.719
	SLA	0.658	0.395	<b>0.658</b>	-0.505

667

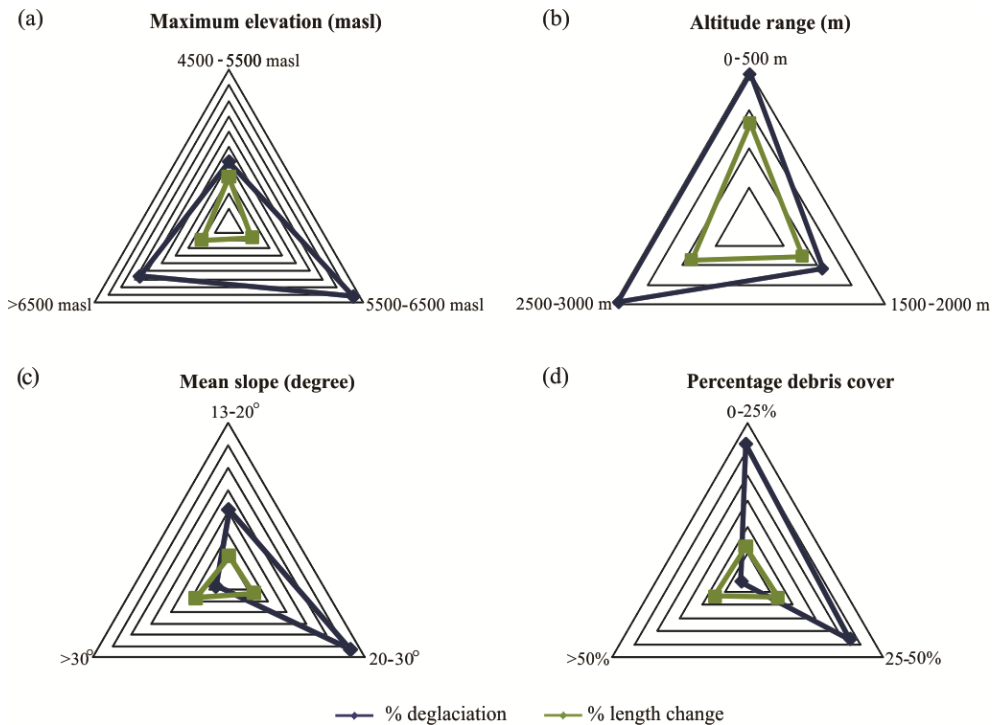
**668 5.3.2 Impact of other factors**

669 In addition to the climate variables, other factors such as hypsometry, maximum elevation, altitude range, slope,  
670 aspect and proglacial lakes also influence the response of individual glacier.

671 Glacier hypsometry is a measure of mass distribution over varying altitudes. It is affected by the mean SLA of  
672 the glaciers to a greater extent, as it is considered that if a large portion of the glacier has elevation equivalent to  
673 SLA, then even a slight alteration in SLA might significantly change the ablation and accumulation zones  
674 (Rivera et al., 2011; Garg et al., 2017b).

675 In this study, we observed that GHR and LR glaciers have nearly 45% and 10% of their area at an elevation  
676 similar to SLA. This suggests that GHR glaciers are more susceptible to retreat as compared to the LR glaciers,  
677 as a larger portion of the former belongs to the SLA. Moreover, the hypsometric distribution of glacier area in  
678 the GHR and LR of the SSB reveals maximum area change post 2000 (Fig.6b). In this regard, while GHR  
679 glaciers have undergone relatively higher area loss (21%) at lower elevation (3800-4200 masl), the LR glaciers  
680 lost maximum area (30%) at much higher elevation (5600-5900 masl) ranges (Fig.6b). Besides, a significant  
681 area loss has also been observed for both GHR (6%) and LR (7%) glaciers at their mean elevations post 2000  
682 (Fig.6b).

683 Elevation plays an important role in understanding the accumulation pattern at higher and ablation in the lower  
684 altitudes. The general perception is that the glaciers situated at relatively higher elevation are subjected to  
685 greater amount of precipitation and hence are susceptible to less deglaciation or even mass gain (Pandey and  
686 Venkataraman, 2013). Similarly, we have also noticed that the glaciers extending to comparatively higher  
687 maximum elevation experience minimum retreat (10%) and exhibit higher percentagedeglaciation (33%) as  
688 compared to the glaciers having lower maximum elevation (retreat:15% & deglaciation: 20%) (Fig.10a).



689  
 690 Figure 10: Differential degeneration of the glaciers during the period 1971-2017 with variability in non-climatic  
 691 factors. (a) Percentage deglaciation and length change of the glaciers at different ranges of maximum elevation,  
 692 (b) altitude range, (c) mean slope and (d) percentage debris cover.  
 693

694 Moreover, our study shows that the glaciers having lower altitude range have retreated and deglaciated more  
 695 (13% & 20%, respectively) as compared to the counterparts (Fig.10b). These observations indicate that glaciers  
 696 which possess higher maximum elevation and altitudinal range are subjected to less retreat and undergo greater  
 697 deglaciation.

698 Slope is another important factor which has a major role in the sustenance of the glacier as accumulation of ice  
 699 is facilitated by a gentler bedrock topography (DeBeer and Sharp, 2009; Patel et al., 2018). It is observed that  
 700 glaciers having steep slopes (30-40°) have retreated more (17%), however with minimum deglaciation (7%)  
 701 during the period 1971-2017 (Fig.10c). Similar results with steeper glaciers exhibiting minimum deglaciation  
 702 have been reported in the Parbati, Chandra and Miyar basins (Venkatesh et al., 2012; Patel et al., 2018).  
 703 However, it differs with Pandey and Venkataraman (2013) and Garg et al., (2017b), likely due to the differing  
 704 average size:  $25 \pm 33.78$  and  $17 \pm 33.2$  km<sup>2</sup> (present study:  $2 \pm 5.7$  km<sup>2</sup>) and slope: 5-20° and 12-26° (present  
 705 study: 13-41°), respectively, of glaciers used in these studies.

706 Presence of supraglacial debris cover influences the glacier processes. Depending on thickness, debris cover  
 707 may either enhance or retard the ablation process (Scherler et al., 2011). In this study, we observed that clean  
 708 glaciers have undergone maximum deglaciation (52%) as compared to the partially (46%) and heavily debris  
 709 covered glaciers (2%). However, they all have retreated almost similarly (12 to 14%), with slightly higher  
 710 retreat of partially debris covered glaciers (Fig.10d). Aspect/ orientation of glaciers provide information

711 regarding the duration for which they are exposed to the incoming solar radiation. Since, the south facing  
 712 glaciers are subjected to longer duration of exposure to the solar radiations as compared to the north facing  
 713 glaciers, therefore, are prone to greater deglaciation and retreat (Deota et al., 2011). Here, it is observed that the  
 714 glaciers having northerly aspect (north, north-east, north-west) have undergone maximum deglaciation as  
 715 compared to the counterparts. However, majority (71%) of the glaciers have northerly aspect, so any inferences  
 716 drawn in this respect would be biased. It is worthwhile to state that most of the south facing slopes in the basin  
 717 are devoid of glaciers but show presence of relict glacier valleys which would have been glaciated in the past.  
 718 At present only 48 south facing glaciers (south, south-east, south-west) with an average size of  $1 \pm 1.9 \text{ km}^2$  exist  
 719 in the SSB.

720 Similarly, the glacier changes are also influenced by the presence of certain features such as glacial (proglacial  
 721 or supraglacial) lakes or differential distribution of supraglacial debris cover. The presence of a proglacial or  
 722 supraglacial lakes significantly enhances the rate of glacier degeneration by increasing the melting processes  
 723 (Sakai, 2012; Basnett et al., 2013). As per our results, highest average retreat rate ( $\sim 31 \text{ ma}^{-1}$ ) is observed for  
 724 glaciers G-4 (Dulung glacier). Although, it is a debris free glacier, shows the highest retreat rates. Also, a  
 725 moraine-dammed lake is observed at the snout of this glacier and has continuously increased its size from  $0.15$   
 726  $\text{km}^2$  in 1977 to  $0.56 \text{ km}^2$  in 2017. This significant increase in the size of moraine-dammed lake has possibly  
 727 influenced the enhanced retreat rate of the glacier.

## 728 **6 Dataset availability**

729 Temporal inventory data for glaciers of Suru sub-basin, western Himalaya is available at  
 730 <https://doi.pangaea.de/10.1594/PANGAEA.904131> (Shukla et al., 2019).

731

## 732 **7 Conclusions**

733 The major inferences drawn from the study include:

734 1. The sub-basin comprised of 252 glaciers, covering an area of  $481.32 \pm 3.41 \text{ km}^2$  (11% of the glacierized area)  
 735 in 2017. Major disintegration of the glaciers occurred after 2000, with breakdown of 12 glaciers into glacierets.  
 736 Small (47%) and clean (43%) glaciers cover maximum glacierized area of the sub-basin. Topographic  
 737 parameters reveal that majority of the glaciers are north facing and the mean elevation and slope of the glaciers  
 738 are  $5134.8 \pm 225 \text{ masl}$  and  $24.8 \pm 5.8^\circ$ , respectively.

739

740 2. Variability in glacier parameters reveal an overall degeneration of the glaciers during the period 1971-2017,  
 741 with deglaciation of approximately  $0.13 \pm 0.0004\% \text{ a}^{-1}$  alongwith an increase in the debris cover by  $37 \pm 0.002$   
 742  $\text{km}^2$  ( $\sim 62\%$ ). Meanwhile, the glaciers have shown an average retreat rate of nearly  $4.3 \pm 1.02 \text{ ma}^{-1}$  with SLA  
 743 exhibiting an overall rise by an average  $22 \pm 60 \text{ m}$ .

744 3. Long-term meteorological records during the period 1901-2017 exhibit an overall increase in the temperature  
 745 ( $T_{\min}$ :  $1.3^\circ\text{C}$ ,  $T_{\max}$ :  $0.25^\circ\text{C}$ ,  $T_{\text{avg}}$ :  $0.77^\circ\text{C}$ ) and precipitation ( $158 \text{ mm}$ ) trends. Both temperature and precipitation  
 746 gradients influence the changes in glacier parameters, however, winter  $T_{\min}$  strongly influencing the glacier area,  
 747 length and debris cover while summer  $T_{\max}$  controlling the SLA. Spatial patterns in change of climate



748 parameters reveal existence of local climate variability in the sub-basin, with progressively warmer (1.03°C) and  
749 wetter (445 mm) climatic regime for glaciers hosted in the GHR as compared to the LR (0.96°C/ 358 mm).

750 4. The inherent local climate variability in the sub-basin has influenced the behavior of the glaciers in the GHR  
751 and LR. It has been observed that LR glaciers have been shrinking faster (area loss: 7%) and accumulating more  
752 debris cover (debris increase: 73%) as compared to the GHR glaciers (6% and 59%) during the period 1971-  
753 2017. The GHR glaciers have, however, experienced greater rise in SLA ( $220 \pm 121$  m) in comparison to the LR  
754 ones ( $91 \pm 56$  m) during the period 1977-2000, with a decrease thereafter.

755  
756 Results presented here show the transitional response of the glaciers in the SSB between the Karakoram  
757 Himalayan and GHR glaciers. The study also confirm the possible influence of factors other than climate such  
758 as glacier size, regional hypsometry, elevation range, slope, aspect and presence of proglacial lakes in the  
759 observed heterogenous response of the glaciers. Therefore, these factors need to be accounted for in more details  
760 in future for complete understanding of the observed glacier changes and response.

761

#### 762 **Team list**

- 763 1. Aparna Shukla
- 764 2. Siddhi Garg
- 765 3. Manish Mehta
- 766 4. Vinit Kumar
- 767 5. Uma Kant Shukla

768

#### 769 **Author contribution**

770 A.S. and S.G. conceived the idea and led the writing of manuscript. A.S. structured the study. S.G. performed  
771 the temporal analysis of the data. M.M. and V.K. helped in the field investigation of the glaciers. All the authors  
772 helped in interpretation of results and contributed towards the final form of the manuscript.

773

#### 774 **Competing interests**

775 The authors declare that they have no conflict of interest.

776

#### 777 **Acknowledgements**

778 Authors are grateful to the Director, Wadia Institute of Himalayan Geology, Dehradun for providing all the  
779 research facilities and support for successful completion of this work. We wish to convey our sincere thanks to  
780 the anonymous reviewers for detailed reviews and constructive comments, which greatly helped to improve the  
781 previous version of the manuscript. We are thankful to Prasad Gogineni (Handling Topical Editor) and Jens  
782 Klump (Handling Chief Editor) for their thoughtful suggestions on the manuscript. Also, we appreciate the  
783 efforts of the entire Editorial team of Earth System Science Data (ESSD) for timely processing of the article.  
784 Aparna Shukla acknowledges the Secretary, Ministry of Earth Science (MoES), New Delhi, India, for providing  
785 requisite support.

786

#### 787 **References**

- 788 Ali, I., Shukla, A. and Romshoo, S. A.: Assessing linkages between spatial facies changes and dimensional  
789 variations of glaciers in the upper Indus Basin, western Himalaya, *Geomorphology*, 284, 115-129,  
790 <https://doi.org/10.1016/j.geomorph.2017.01.005>, 2017.
- 791 ALOS Global Digital Surface Model "ALOS World 3D - 30m" (AW3D30).  
792 <http://www.eorc.jaxa.jp/ALOS/en/aw3d30/> (accessed on 1 August 2017).
- 793 Azam, M. F., Wagnon, P., Berthier, E., Vincent, C., Fujita, K. and Kargel, J. F.: Review of the status and mass  
794 changes of Himalayan-Karakoram glaciers, *Journal of Glaciology*, 64, 61-74,  
795 <https://doi.org/10.1017/jog.2017.86>, 2018.
- 796 Bajracharya, S. R., Maharjan, S. B., and Shrestha, F.: The status and decadal change of glaciers in Bhutan from  
797 1980's to 2010 based on the satellite data, *Annals of Glaciology*, 55, 159-166,  
798 <https://doi.org/10.3189/2014AoG66A125>, 2014.
- 799 Bajracharya, S. R., Mool, P. K., Shrestha, B. R.: Global climate change and melting of Himalayan glaciers.  
800 Melting glaciers and rising sea levels: Impacts and implications, Prabha Shastri Ranade (ed), The  
801 Icfai's University Press, India, 28-46, 2008.
- 802 Basnett, S., Kulkarni, A.V. and Bolch, T.: The influence of debris cover and glacial lakes on the recession of  
803 glaciers in Sikkim Himalaya, India, *Journal of Glaciology*, 59, 1035-1046,  
804 <https://doi.org/10.3189/2013JoG12J184>, 2013.
- 805 Bhabri, R., Bolch, T., Chaujar, R. K., and Kulshreshtha, S. C.: Glacier changes in the Garhwal Himalaya,  
806 India, from 1968 to 2006 based on remote sensing, *Journal of Glaciology*, 57, 543-556,  
807 <https://doi.org/10.3189/002214311796905604>, 2011.
- 808 Bhabri, R., Bolch, T. and Chaujar, R. K.: Frontal recession of Gangotri Glacier, Garhwal Himalayas, from  
809 1965 to 2006, measured through high-resolution remote sensing data, *Current Science*, 102, 489-494,  
810 2012.
- 811 Bhabri, R., Bolch, T., Kawishwar, P., Dobhal, D. P., Srivastava, D. and Pratap, B.: Heterogeneity in Glacier  
812 Response in the Upper Shyok Valley, Northeast Karakoram, *The Cryosphere*, 7, 1385-1398.  
813 <https://doi.org/10.5194/tc-7-1385-2013>, 2013.
- 814 Bhattacharya, A., Bolch, Mukherjee, K., Pieczonka, T., Kropacek, J. and Buchroithner, M.: Overall recession  
815 and mass budget of Gangotri Glacier, Garhwal Himalayas, from 1965 to 2015 using remote sensing  
816 data, *Journal of Glaciology*, 62, 1115-1133, <https://doi.org/10.1017/jog.2016.96>, 2016.
- 817 Bhushan, S., Syed, T. H., Arendt, A. A., Kulkarni, A. V. and Sinha, D.: Assessing controls on mass budget and  
818 surface velocity variations of glaciers in Western Himalaya, *Scientific Reports*, 8, 8885,  
819 <https://doi.org/10.1038/s41598-018-27014-y>, 2018.
- 820 Bhutiyan, M. R., Kale, V. S. and Pawar, N. J.: Long term trends in maximum, minimum and mean annual air  
821 temperature across the Northwestern Himalaya during the twentieth century, *Climate change*, 85, 159-  
822 177, <https://doi.org/10.1007/s10584-006-9196-1>, 2007.
- 823 Birajdar, F., Venkataraman, G., Bahuguna, I. and Samant, H.: A revised glacier inventory of Bhaga Basin  
824 Himachal Pradesh, India: current status and recent glacier variations, *ISPRS Annals of*  
825 *Photogrammetry, Remote Sensing and Spatial Information Sciences*, II-8, 37-43, <https://doi.org/10.5194/isprannals-s-ii-8-37-2014>, 2014.
- 827 Bolch, T., Buchroithner, M., Pieczonka, T. and Kunert, A.: Planimetric and Volumetric Glacier Changes in the  
828 Khumbu Himal, Nepal, Since 1962 Using Corona, Landsat TM and ASTER Data, *Journal of*  
829 *Glaciology*, 54, 592-600, <https://doi.org/10.3189/002214308786570782>, 2008.
- 830 Bolch, T., Kulkarni, A., Käab, A., Huggel, C., Paul, F., Cogley, J. G., Frey, H., Kargel, J. S., Fujita, K., Scheel,  
831 M., Bajracharya, S., and Stoffel, M.: The State and Fate of Himalayan Glaciers, *Science*, 336, 310-314,  
832 <https://doi.org/10.1126/science.1215828>, 2012.
- 833 Brun, F., Berthier, E., Wagnon, P., Käab, A. and Treichler, D.: A spatially resolved estimate of High Mountain  
834 Asia glacier mass balances from 2000 to 2006, *Nature Geoscience*, 10, 668-673, [10.1038/NGEO2999](https://doi.org/10.1038/NGEO2999),  
835 2017.

- 836 Chand, P. and Sharma, M. C.: Glacier changes in Ravi basin, North-Western Himalaya (India) during the last  
837 four decades (1971-2010/13), *Global and Planetary change*, 135, 133-  
838 147, <https://doi.org/10.1016/j.gloplacha.2015.10.013>, 2015.
- 839 Chevuturi, A., Dimri, A. P. and Thayyen, R. J.: Climate change over Leh, Ladakh (India), *Theoretical and*  
840 *Applied Climatology*, 131, 531-545, <https://doi.org/10.1007/s0070401619891>, 2018.
- 841 Chudley, T. R., Miles, E. S. and Willis, I. C.: Glacier characteristics and retreat between 1991 and 2014 in the  
842 Ladakh Range, Jammu and Kashmir, *Remote Sensing Letters*, 8, 518-527,  
843 <https://doi.org/10.1080/2150704X.2017.1295480>, 2017.
- 844 Cogley, J. G.: Glacier shrinkage across High Mountain Asia, *Annals of Glaciology*, 57, 41-49,  
845 <https://doi.org/10.3189/2016AoG71A040>, 2016.
- 846 Das, S. and Sharma, M. C.: Glacier changes between 1971 and 2016 in the Jankar Chhu Watershed, Lahaul  
847 Himalaya, India, *Journal of glaciology*, 1-16, <https://doi.org/10.1017/jog.2018.77>, 2018.
- 848 DeBeer, C. M. and Sharp, M. J.: Topographic influences on recent changes of very small glaciers in the  
849 Monashee mountains, British Columbia, Canada, *Journal of Glaciology*, 55, 691-700,  
850 <https://doi.org/10.3189/002214309789470851>, 2009.
- 851 Deota, B. S., Trivedi, Y. N., Kulkarni, A. V., Bahuguna, I. M. and Rathore, B. P.: RS and GIS in mapping of  
852 geomorphic records and understanding the local controls of glacial retreat from the Baspa Valley,  
853 Himachal Pradesh, India, *Current Science*, 100, 1555–1563, 2011.
- 854 Dimri, A. P.: Interseasonal oscillation associated with the Indian winter monsoon, *Journal of geophysical*  
855 *research: Atmospheres*, 118, 1189-1198, <https://doi.org/10.1002/jgrd.50144>, 2013.
- 856 Dobhal, D. P., Mehta, M. and Srivastava, D.: Influence of debris cover on terminus retreat and mass changes of  
857 Chorabari Glacier, Garhwal region, central Himalaya, India, *Journal of Glaciology*, 59, 961–971,  
858 <https://doi.org/10.3189/2013jog12j180>, 2013.
- 859 Gardelle, J., Berthier, E., Arnaud, Y. and Kääb, A.: Region-wide glacier mass balances over the Pamir-  
860 Karakoram-Himalaya during 1999–2011, *The Cryosphere*, 7, 1263–1286, 2013.
- 861 Garg, P. K., Shukla, A., Tiwari, R. K. and Jasrotia, A. S.: Assessing the status of glaciers in parts of the Chandra  
862 basin, Himachal Himalaya: A multiparametric approach, *Geomorphology*, 284,99-114,  
863 <https://doi.org/10.1016/j.geomorph.2016.10.022>, 2017a.
- 864 Garg, P. K., Shukla, A. and Jasrotia, A. S.: Influence of topography on glacier changes in the central Himalaya,  
865 India, *Global and Planetary change*, 155, 196-212, <https://doi.org/10.1016/j.gloplacha.2017.07.007>, 2017b.
- 867 Garg, S., Shukla, A., Mehta, M., Kumar, V., Samuel, S. A., Bartarya, S. and Shukla, U. K.: Field evidences  
868 showing rapid frontal degeneration of the Kangriz glacier, Suru basin, Jammu and Kashmir. *Journal of*  
869 *mountain science*, 15, 1199–1208, <https://doi.org/10.1007/s11629-017-4809-x>, 2018.
- 870 Garg, S., Shukla, A., Mehta, M., Kumar, V. and Shukla, U. K.: On geomorphic manifestations and glaciation  
871 history of the Kangriz glacier, western Himalaya. *Himalayan Geology*, 40, 115–127, 2019.
- 872 Granshaw, F. D. and Fountain, A. G.: Glacier change (1958– 1998) in the North Cascades National Park  
873 Complex, Washington, USA, *Journal of Glaciology*, 52, 251–256  
874 <https://doi.org/10.3189/172756506781828782>, 2006.
- 875 Guo, Z., Wanga, N., Kehrwald, N. M., Mao, R., Wua, H., Wu, Y. and Jiang, X.: Temporal and spatial changes  
876 in western Himalayan firn line altitudes from 1998 to 2009, *Global and Planetary Change*, 118, 97–  
877 105, <https://doi.org/10.1016/j.gloplacha.2014.03.012>, 2014.

- 878 Hall, D. K., Bayr, K. J., Schöner, W., Bindschadler, R. A. and Chiene, J. Y. L.: Consideration of the Errors  
879 Inherent in Mapping Historical Glacier Positions in Austria from the Ground and Space (1893–2001),  
880 Remote Sensing of Environment, 86, 566–577, [https://doi.org/10.1016/S0034-4257\(03\)00134-2](https://doi.org/10.1016/S0034-4257(03)00134-2), 2003.
- 881 Hanshaw, M. N., and Bookhagen, B.: Glacial Areas, Lake Areas, and Snow Lines from 1975 to 2012:  
882 Status of the Cordillera Vilcanota, Including the Quelccaya Ice Cap, Northern Central Andes, Peru,  
883 The Cryosphere, 8, 359–376, <https://doi.org/10.5194/tc-8-359> 2014, 2014.
- 884 Harris, I.C. and Jones, P.D.: CRU TS 4.02: Climatic Research Unit (CRU) year-by-year variation of selected  
885 climate variables by country (CY) version 4.02 (Jan. 1901 - Dec. 2017). Centre for Environmental  
886 Data Analysis, <http://dx.doi.org/10.5285/d4e823f0172947c5ae6e6b265656c273>, 2018.
- 887 India Meteorological Department (IMD), Climatological table: Available online:  
888 [http://www.imd.gov.in/pages/city\\_weather\\_show.php](http://www.imd.gov.in/pages/city_weather_show.php), 2015.
- 889 Immerzeel, W. W., Beek, L. P. H. and Bierkens M. F. P.: Climate change will affect the Asian water towers,  
890 Science, 328, 1382–1385, <https://doi.org/10.1126/science.1183188>, 2010.
- 891 IPCC. Summary for policymakers. In: Stocker, T. F. et al. (Eds), Climate Change 2013: The Physical Science  
892 Basis. Contribution of Working Group III to the Fifth Assessment Report of Intergovernmental Panel  
893 on Climate Change. Cambridge University Press, Cambridge and New York, 2013.
- 894 Kääh, A., Berthier, E., Nuth, C., Gardelle, J. and Arnaud, Y.: Contrasting patterns of early twenty first century  
895 glacier mass change in the Himalayas, Nature, 488, 495–498, <https://doi.org/10.1038/nature11324>,  
896 2012.
- 897 Kääh, A., Treichler, D., Nuth, C., and Berthier, E.: Brief Communication: Contending estimates of 2003–  
898 2008 glacier mass balance over the Pamir–Karakoram–Himalaya, The Cryosphere, 9, 557–564,  
899 <https://doi.org/10.5194/tc-9-557-2015>, 2015.
- 900 Kamp, U., Byrne, M. and Bolch, T.: Glacier Fluctuations between 1975 and 2008 in the Greater  
901 Himalaya Range of Zaskar, Southern Ladakh, Journal of Mountain Sciences, 8, 374–389,  
902 <https://doi.org/10.1007/s11629-011-2007-9>, 2011.
- 903 Kaser, G., Großhauser, M. and Marzeion, B: Contribution potential of glaciers to water availability in different  
904 climate regimes, Proceedings of National academy of Sciences of the United States of America, 107,  
905 20223–20227, <https://doi.org/10.1073/pnas.1008162107>, 2010.
- 906 Kulkarni, A. V., Bahuguna, I. M., Rathore, B. P., Singh, S. K., Randhawa, S. S., Sood, R. K. and Dhar, S.:  
907 Glacial retreat in Himalaya using remote sensing satellite data, Current Science, 92, 69–  
908 74, <https://doi.org/10.1117/12.694004>, 2007.
- 909 Kulkarni, A. V., Rathore, B. P., Singh, S. K. and Bahuguna, I. M.: Understanding changes in Himalayan  
910 Cryosphere using remote sensing technique, International Journal of Remote Sensing, 32,  
911 601–615, <https://doi.org/10.1080/01431161.2010.517802>, 2011.
- 912 Maurer, J. M., Schaefer, J. M., Rupper, S., Corley, A.: Acceleration of ice loss across the Himalayas over the  
913 past 40 years, Science Advances, 5, 1–12 <https://doi.org/10.1126/sciadv.aav7266>, 2019.
- 914 Mayewski, P. A., and Jeschke, P. A.: Himalayan and Trans-Himalayan Glacier Fluctuations Since A.D. 1812,  
915 Arctic and Alpine Research, 11, 267–287, <https://doi.org/>, 1980.
- 916 Miller, J. D., Immerzeel, W. W. and Rees, G.: Climate change impacts on glacier hydrology and river discharge  
917 in the Hindu Kush- Himalaya, Mountain research and development, 32, 461–467,  
918 <http://doi.org/10.1659/MRD-JOURNAL-D-12-00027.1>, 2012.
- 919 Mir, R. A., Jain, S. K., Jain, Thayyen, R. J. and Saraf, A. K.: Assessment of recent glacier changes and its  
920 controlling factors from 1976 to 2011 in Baspa Basin, western Himalaya, Arctic, Antarctic, and Alpine  
921 Research, 49, 621–647, <https://doi.org/10.1657/AAAR0015-070>, 2017.
- 922 Mölg, N., Bolch, T., Rastner, P., Strozzi, T. and Paul, F.: A consistent glacier inventory for Karakoram and  
923 Pamir derived from Landsat data: distribution of debris cover and mapping challenges. Earth  
924 System Science Data, 10, 1807–1827, <https://doi.org/10.5194/essd-10-1807-2018>, 2018.

- 925 Murtaza K. O. and Romshoo S. A.: Recent glacier changes in the Kashmir Alpine Himalayas, India, *Geocarto*  
 926 *International*, 32, 188-205, <https://doi.org/10.1080/10106049.2015.1132482>, 2015.
- 927 Nuimura, T., Sakai, A., Taniguchi, K., Nagai, H., Lamsal, D., Tsutaki, S., Kozawa, A.,  
 928 Hoshina, Y., Takenaka, S., Omiya, S., Tsunematsu, K., Tshering, P. and Fujita, K.: The GAMDAM  
 929 glacier inventory: a quality-controlled inventory of Asian glaciers, *The Cryosphere*, 9, 849-864,  
 930 <https://doi.org/10.5194/tc-9-849-2015>, 2015.
- 931 Pandey, A., Ghosh, S. and Nathawat, M. S.: Evaluating patterns of temporal glacier changes in Greater  
 932 Himalayan Range, Jammu & Kashmir, India, *Geocarto International*, 26, 321-338,  
 933 <https://doi.org/10.1080/10106049.2011.554611>, 2011.
- 934 Pandey, P. and Venkataraman, G.: Changes in the glaciers of Chandra–Bhaga basin, Himachal Himalaya, India,  
 935 between 1980 and 2010 measured using remote sensing, *International Journal of Remote Sensing*, 34,  
 936 5584-5597, <https://doi.org/10.1080/01431161.2013.793464>, 2013.
- 937 Patel, L. K., Sharma, P., Fathima, T. N. and Thamban, M.: Geospatial observations of topographical control  
 938 over the glacier retreat, Miyar basin, western Himalaya, India, *Environmental Earth Sciences*, 77, 190,  
 939 <https://doi.org/10.1007/s12665-018-7379-5>, 2018.
- 940 Paul, F., Barrand, N.E., Baumann, S., Berthier, E., Bolch, T., Casey, K., Frey, H., Joshi, S.P., Kononov, V.,  
 941 Bris, R.L. and Mölg, N.: On the accuracy of glacier outlines derived from remote-sensing data, *Annals*  
 942 *of Glaciology*, 54, 171–182, <https://doi.org/10.3189/2013AoG63A296>, 2013.
- 943 Paul, F., Bolch, T., Kääb, A., Nagler, T., Nuth, C., Scharrer, K.: The glaciers climate change initiative:  
 944 methods for creating glacier area, elevation change and velocity products *Remote Sensing*  
 945 *Environment*, 162, 408-426, <http://dx.doi.org/10.1016/j.rse.2013.07.043>, 2015.
- 946 Paul, F., Bolch, T., Briggs, K., Kääb, A., McMillan, M., McNabb, R., Nagler, T., Nuth, C., Rastner, P., Strozzi,  
 947 T. and Wuite, J.: Error sources and guidelines for quality assessment of glacier area, elevation change,  
 948 and velocity products derived from satellite data in the Glaciers\_cci project, *Remote sensing of*  
 949 *Environment*, 203, 256-275, <https://doi.org/10.1016/j.rse.2017.08.038>, 2017.
- 950 Pfeffer, W. T., Arendt, A., Bliss, A., Bolch, T., Cogley, J. G., Gardner, A. S., Hagen, J. O., Hock, R., Kaser, G.,  
 951 Kienholz, C., Miles, E. S., Moholdt, G., Molg, N., Paul, F., Radic, V., Rastner, P., Raup, B. H., Rich, J.  
 952 and Sharp, M.: The Randolph Glacier Inventory: A globally complete inventory of glaciers, *Journal of*  
 953 *Glaciology*, 60, 537-552. doi:10.3189/2014JoG13J176, 2014.
- 954 Pritchard, H. D.: Asia's glaciers are a regionally important buffer against drought, *Nature*, 545, 169-187,  
 955 doi:10.1038/nature22062, 2017.
- 956 Racoviteanu, A. E., Arnaud, Y., Williams, M. W. and Ordonez, J.: Decadal changes in glacier parameters in  
 957 the Cordillera Blanca, Peru, derived from remote sensing, *Journal of Glaciology*, 54, 499–510,  
 958 <https://doi.org/10.3189/002214308785836922.2008a>.
- 959 Racoviteanu, A., Paul, F., Raup, B., Khalsa, S. J. S. and Armstrong, R.: Challenges and recommendations in  
 960 mapping of glacier parameters from space: results of the 2008 Global Land Ice Measurements from  
 961 Space (GLIMS) workshop, Boulder, Colorado, USA, *Annals of Glaciology*, 50, 53–69,  
 962 <https://doi.org/10.3189/172756410790595804>, 2009.
- 963 Rai, P. K., Nathawat, M. S. and Mohan, K.: Glacier retreat in Doda valley, Zaskar basin, Jammu and Kashmir,  
 964 India, *Universal Journal of Geoscience*, 1, 139-149, <https://doi.org/10.13189/ujg.2013.010304>, 2013.
- 965 Raina, V. K.: Himalayan glaciers: a state-of-art review of glacial studies, glacial retreat and climate  
 966 change. *Himal. Glaciers State-Art Review*, *Glacial Stud. Glacial Retreat Climate Change*, 2009.
- 967 Raina, R. K. and Koul, M. N.: Impact of Climatic Change on Agro-Ecological Zones of the Suru-Zaskar  
 968 Valley, Ladakh (Jammu and Kashmir), India, *Journal of Ecology and the Natural Environment* 3,  
 969 424–440, 2011.
- 970 Rashid, I., Romshoo, S. A. and Abdullah, T.: The recent deglaciation of Kolahoi Valley in Kashmir Himalaya,  
 971 India in response to the changing climate, *Journal of Asian Earth Science*, 138, 38–50,  
 972 <https://doi.org/10.1016/j.jseas.2017.02.002>, 2017.

- 973 Raup, B., Racoviteanu, A., Khals, S. J. S., Helm, C., Armstrong, R., Arnaud, Y.: The GLIMS geospatial glacier  
974 database: a new tool for studying glacier change, *Global and Planetary Change* 56, 101–110,  
975 doi:10.1016/j.gloplacha.2006.07.018, 2007.
- 976 Rivera, A., Cawkwell, F., Rada, C. and Bravo, C.: Hypsometry. In: *Encyclopaedia of Snow, Ice and glaciers*,  
977 Springer, Netherlands, 551-554, 2011.
- 978 Space Application Centre (SAC): Report: Monitoring Snow and Glaciers of Himalayan Region. Space  
979 Application Centre, ISRO, Ahmedabad, India, 413 pages, ISBN: 978-93-82760-24-5, 2016.
- 980 Sakai, A.: Glacial lakes in the Himalayas: A review on formation and Expansion process, *Global environmental*  
981 *research*, 23-30, 2012.
- 982 Sakai A. and Fujita, K.: Contrasting glacier responses to recent climate change in high-mountain Asia, *Scientific*  
983 *reports*, 7, 1-18, <https://doi.org/10.1038/s41598-017-14256-5>, 2017.
- 984 Sangewar, C. V., and S. P. Shukla.: Inventory of the Himalayan Glaciers: A Contribution to the International  
985 Hydrological Programme, An Updated Edition. Kolkata: Geological Survey of India (Special  
986 Publication 34), IISN: 1:0254-0436, 2009.
- 987 Scherler, D., Bookhagen, B. and Strecker, M.R.: Spatially variable response of Himalayan glaciers to climate  
988 change affected by debris cover, *Nature Geoscience*, 4, 156–159, <https://doi.org/10.1038/ngeo1068>,  
989 2011.
- 990 Schmidt, S. and Nusser, M.: Changes of High Altitude Glaciers in the Trans-Himalaya of Ladakh over the Past  
991 Five Decades (1969–2016), *Geosciences*, 7, 27, <https://doi.org/10.3390/geosciences7020027>, 2017.
- 992 Sen, P. K.: Estimates of the regression coefficient based on Kendall's Tau, *American Statistics Journal*, 63,  
993 1379-1389, <https://doi.org/10.2307/2285891>, 1968.
- 994 Shekhar, M., Bhardwaj, A., Singh, S., Ranhotra1, P. S., Bhattacharyya, A., Pal, A. K., Roy, I., Martín-  
995 Torres, F. J. and Zorzano, M.P.: Himalayan glaciers experienced significant mass loss during later  
996 phases of little ice age, *Scientific Reports*, 7, 1-14, 2017.
- 997 Shiyin, L., Donghui, S., Junli, Xu., Xin, W., Xiaojun, Y., Zongli, J., Wanqin, G., Anxin, L., Shiqiang, Z.,  
998 Baisheng, Ye., Zhen, Li., Junfeng, W. and Lizong, W.: Glaciers in China and Their Variations, In:  
999 Kargel J., Leonard G., Bishop M., Käab A., Raup B. (eds) *Global Land Ice Measurements from Space*,  
1000 Springer Praxis Books, Springer, Berlin, Heidelberg, 2014
- 1001 Shukla, A., Gupta, R. P. and Arora, M. K.: Estimation of debris cover and its temporal variation using optical  
1002 satellite sensor data: a case study in Chenab basin, Himalaya, *Journal of Glaciology*, 55, 444-452,  
1003 <http://doi.org/10.3189/002214309788816632>, 2009.
- 1004 Shukla, A. and Qadir, J.: Differential response of glaciers with varying debris cover extent: evidence from  
1005 changing glacier parameters, *International Journal of Remote Sensing*, 37, 2453–2479,  
1006 <http://doi.org/10.1080/01431161.2016.1176272>, 2016.
- 1007 Shukla, A., Garg, P.K., Manish, M., Kumar, V.: Changes in dynamics of Pensilungpa glacier, western  
1008 Himalaya, over the past two decades, in: *Proceedings of the 38<sup>th</sup> Asian Conference on Remote*  
1009 *Sensing*, Delhi, India, 23-27 October 2017, 2017.
- 1010 Shukla, A., Garg, S., Manish, M., Kumar, V and Shukla, U. K.: Temporal inventory of glaciers in the Suru  
1011 sub-basin, western Himalaya, PANGAEA, <https://doi.pangaea.de/10.1594/PANGAEA.904131>, 2019.
- 1012 Singh, J. and Yadav, R. R.: Tree-ring indications of recent glacier fluctuations in Gangotri, western Himalaya,  
1013 India, *Current Science*, 79(11), 1598–1601, 2000.
- 1014 Vaughan, D. G., Comiso, J. C., Allison, I., Carrasco, J., Kaser, G., Kwok, R., Mote, P., Murray, T., Paul, F.,  
1015 Ren, J., Rignot, E., Solomina, O., Steffen, K. and Zhang, T.: Observations: Cryosphere. in *Climate*  
1016 *change 2013: The physical science basis. Contribution of working group I to the fifth assessment report*  
1017 *of the intergovernmental panel on climate change*, Stocker, T. F., Qin, D., Plattner, G. K., Tignor, M.,  
1018 Allen, S. K., Boschung, J., Nauels, A., Xia, Y., Bex, V. and Midgley, P. M. (Eds.), Cambridge  
1019 University Press, Cambridge, United Kingdom and New York, NY, USA, 2013.
- 1020 Venkatesh, T. N., Kulkarni, A. V. and Srinivasan, J.: Relative effect of slope and equilibrium line altitude on the  
1021 retreat of Himalayan glaciers, *The Cryosphere*, 6, 301-311, <http://doi.org/10.5194/tc-6-301-2012>, 2012.

- 1022 Vijay, S and Braun, M.: Early 21st century spatially detailed elevation changes of Jammu and Kashmir glaciers  
1023 (Karakoram–Himalaya), *Global and Planetary Change*, 165, 137-146,  
1024 <http://doi.org/10.1016/j.gloplacha.2018.03.014>, 2018.
- 1025 Vittoz, P.: *Ascent of the Nun in the Mountain World: 1954* (Marcel Kurz, ed.), George Allen & Unwin, Ltd.,  
1026 London, 1954.
- 1027 Zhou, Y., Li, Z., Li, J., Zhao, R. and Ding, X.: Geodetic glacier mass balance (1975-1999) in the central  
1028 Pamir using the SRTM DEM and KH-9 imagery, *Journal of Glaciology*, 65, 309-320, doi:  
1029 10.1017/jog.2019.8, 2018.



1 **Temporal inventory of glaciers in the Suru sub-basin, western**  
2 **Himalaya: Impacts of the regional climate variability**

3

4 Aparna Shukla<sup>1,2\*</sup>, Siddhi Garg<sup>1</sup>, Manish Mehta<sup>1</sup>, Vinit Kumar<sup>1</sup>, Uma Kant Shukla<sup>3</sup>

5

6 <sup>1</sup>Wadia Institute of Himalayan Geology, 33, GMS Road, Dehradun-248001, India7 <sup>2</sup>Ministry of Earth Sciences, New Delhi- 110003, India8 <sup>3</sup>Department of Geology, Banaras Hindu University, Varanasi -221005, India

9

10 \*Correspondence to: Aparna Shukla (aparna.shukla22@gmail.com)

11

12

13

14

15

16

17

18

19

20

21

22

23

24

25

26

27

28

29

30

31

32

33

34

35

36

37

38

39

40

41

## 42 Abstract

43 Updated knowledge about the glacier extent and characteristics in the Himalaya cannot be overemphasised.  
 44 Availability of precise glacier inventories in the latitudinally diverse western Himalayan region is particularly  
 45 crucial. In this study we have created an inventory of the Suru sub-basin, western Himalaya for year 2017 using  
 46 Landsat OLI data. Changes in glacier parameters have also been monitored from 1971 to 2017 using temporal  
 47 satellite remote sensing data and limited field observations. Inventory data show that the sub-basin has 252  
 48 glaciers covering 11% of the basin, having an average slope of  $25 \pm 6^\circ$  and dominantly north orientation. The  
 49 average snow line altitude (SLA) of the basin is  $5011 \pm 54$  masl with smaller (47%) and cleaner (43%) glaciers  
 50 occupying the bulk area. Longterm climate data (1901-2017) show an increase in the mean annual temperature  
 51 ( $T_{\max}$  &  $T_{\min}$ ) by  $0.77^\circ\text{C}$  ( $0.25^\circ\text{C}$  &  $1.3^\circ\text{C}$ ) in the sub-basin, driving the overall glacier variability in the region.  
 52 Temporal analysis reveals a glacier shrinkage of  $\sim 6 \pm 0.02\%$ , an average retreat rate of  $4.3 \pm 1.02 \text{ ma}^{-1}$ , debris  
 53 increase of 62% and  $22 \pm 60$  m SLA rise in past 46 years. This confirms their transitional response between the  
 54 Karakoram and the Greater Himalayan Range (GHR) glaciers. Besides, glaciers in the sub-basin occupy two  
 55 major ranges, i.e., GHR and Ladakh range (LR) and experience local climate variability, with the GHR glaciers  
 56 exhibiting a warmer and wetter climate as compared to the LR glaciers. This variability manifestes itself in the  
 57 varied response of GHR and LR glaciers. While the GHR glaciers exhibit an overall rise in SLA (GHR:  $49 \pm 69$   
 58 m; LR: decrease by  $18 \pm 50$  m), the LR glaciers have deglaciated more (LR: 7%; GHR: 6%) with an enhanced  
 59 accumulation of debris cover (LR: 73%; GHR: 59%). Inferences from this study reveal prevalence of glacier  
 60 disintegration and overall degeneration, transition of clean ice to partially debris covered glaciers, local climate  
 61 variability and non-climatic (topographic and morphometric) factor induced heterogeinty in glacier response as  
 62 the major processes operatives in this region. The dataset Shukla et al., (2019) is accessible at  
 63 <https://doi.pangaea.de/10.1594/PANGAEA.904131>

Deleted: s

Deleted: s

64  
 65 **Key words:** Suru sub basin, western Himalaya, glacier inventory, climate change

66  
 67 **Location of the dataset:** <https://doi.pangaea.de/10.1594/PANGAEA.904131>

## 69 1 Introduction

70 State of the Himalayan cryosphere has a bearing on multiple aspects of hydrology, climatology, environment  
 71 and sustenance of living organisms at large (Immerzeel et al., 2010; Miller et al., 2012). Being sensitive to the  
 72 ongoing climate fluctutations, glaciers keep adjusting themselves and these adaptations record the changing  
 73 patterns in the global climate (Bolch et al., 2012). Any alteration in the glacier parameters would ultimately  
 74 affect the hydrology of the region, thereby influencing the downstream communities (Kaser et al., 2010;  
 75 Pritchard, 2017). Owing to these reasons, quantifying the mass loss over different Himalayan regions in the past  
 76 years, ascertaining present status of the cryosphere and how these changes are likely to affect the freshwater  
 77 accessibility in the region are at the forefront of contemporary cryospheric research (Brun et al. 2017; Sakai and  
 78 Fujita, 2017). This aptly triggered several regional (Kaab et al., 2012; Gardelle et al., 2013; Brun et al. 2017;  
 79 Zhou et al., 2018; Maurer et al., 2019), local (Bhushan et al., 2018; Vijay and Braun, 2018) and glacier specific  
 80 studies (Dobhal et al., 2013; Bhattacharya et al., 2016; Azam et al., 2018) in the region. These studies at varying

83 scales contribute towards solving the jigsaw puzzle of the Himalayan cryosphere. The regional scale studies  
84 operate on small scale for bringing out more comprehensive, holistic and synoptic spatio-temporal patterns of  
85 glacier response, the local scale studies monitor glaciers at basin level or groups and offer more details on  
86 heterogenous behaviour and plausible reasons thereof. However, the glacier specific studies whether based on  
87 field or satellite or integrative information are magnified versions of the local scale studies and hold the  
88 potential to provide valuable insights into various morphological, topographic and local-climate induced  
89 controls on glacier evolution. Despite these efforts, data on the glacier variability and response remain  
90 incomplete, knowledge of the governing processes still preliminary and the future viability pathways of the  
91 Himalayan cryospheric components are uncertain.

Deleted: s

92 Though the literature suggests a generalised mass loss scenario (except for the Karakoram region) over the  
93 Himalayan glaciers, disparities in rates and pace of shrinkage remain. Maurer et al. (2019) report the average  
94 mass wastage of  $-0.32 \text{ m w.e.a}^{-1}$  for the Himalayan glaciers during 1975-2016. They suggest that the glaciers in  
95 the eastern Himalaya ( $-0.46 \text{ m w.e.a}^{-1}$ ) have experienced slightly higher mass loss as compared to the western ( $-$   
96  $0.45 \text{ m w.e.a}^{-1}$ ), followed by the central ( $-0.38 \text{ m w.e.a}^{-1}$ ). However, considerable variability in the glacier  
97 behaviour exists within the western Himalayas (Scherler et al., 2011; Kaab et al., 2012; Vijay and Braun, 2017;  
98 Bhushan et al., 2018; Mölg et al., 2018). Studies suggest that largely the glaciers in the Karakoram Himalayas  
99 have either remained stable or gained mass in the last few decades (Kääb et al., 2015; Cogley, 2016), while a  
100 contrasting behaviour is observed for the GHR glaciers experiencing large scale degeneration, with more than  
101 65% glaciers retreating during 2000-2008 (Scherler et al., 2011). However, there are two views pertaining to the  
102 glaciers in the Trans Himalayan range, with one suggesting their intermediate response between the Karakoram  
103 Himalaya and GHR (Chudley et al., 2017) and the other emphasizing upon their affinity either towards the GHR  
104 or the Karakoram Himalayan glaciers (Schmidt and Nusser, 2017). Therefore, in order to add more data and  
105 build a complete understanding of the glacier response, particularly in the western Himalaya, more local scale  
106 studies are necessary.

107 Complete and precise glacier inventories form the basic prerequisites not only for comprehensive glacier  
108 assessment but also for various hydrological and climate modelling related applications (Vaughan et al., 2013).  
109 Information on spatial coverage of glaciers in any region is a much valued dataset and holds paramount  
110 importance in the future assessment of glaciers. Errors in the glacier outlines may propagate and introduce  
111 higher uncertainties in the modelled outputs (Paul et al., 2017). Besides, results from modelling studies  
112 conducted over same region but using different sources of glacier boundaries are rendered uncomparable,  
113 constraining the evaluation of models and thus their future development. On the other hand, quality, accuracy  
114 and precision associated with glacier mapping and outline delineation requires dedicated efforts. Several past  
115 studies discuss the methods for, challenges in achieving an accurate glacier inventory and resolutions for the  
116 same (Paul et al., 2013; 2015; 2017). Thorough knowledge of glaciology and committed manual endeavour are  
117 two vital requirements in this regard. Realisation of above facts did result in several devoted attempts to prepare  
118 detailed glacier inventories at global scale, such as Randolph glacier inventory (RGI), Global land ice  
119 measurements from space (GLIMS) and recently Chinese glacier inventory (CGI) and Glacier area mapping for  
120 discharge from the Asian mountains (GAMDAM) (Raup et al., 2007; Pfeffer et al., 2014; Shiyin et al., 2014;  
121 Nuimura et al., 2015). However, several issues related to gap areas, differences in mapping methods and skills  
122 of the analysts involved act as limitations and need further attention.

124 Considering the above, present work studies the glaciers in the Suru Sub-basin (SSB), western Himalaya,  
 125 Jammu and Kashmir. Primary objectives of this study include: 1) presenting the inventory of recent glacier data  
 126 [area, length, debris cover, SLA, elevation (min & max), slope and aspect] in the SSB; 2) assessing the temporal  
 127 changes for four epochs in past 46 years; and 3) analysing the observed glacier response in relation to the  
 128 regional climate trends, local climate variability and other factors (regional hypsometry, topographic  
 129 characteristics, debris cover and geomorphic features). Several remote sensing and field based studies of  
 130 regional (Vijay and Braun, 2018) , local (Bhushan et al., 2018, Kamp et al., 2011; Pandey et al., 2011; Shukla  
 131 and Qadir, 2016, Rashid et al 2017, Murtaza and Romshoo, 2015) and glacier-specific nature (Garg et al., 2018;  
 132 2019; Shukla et al., 2018) have been conducted for monitoring the response of the glaciers to the climate  
 133 change. Glaciological studies carried out in or adjacent to the SSB suggest increased shrinkage, slowdown and  
 134 downwasting of the studied glaciers at variable rates (Kamp et al., 2011; Pandey et al., 2011; Shukla and Qadir,  
 135 2016; Bhushan et al., 2018). These studies also hint towards the possible role of topographic & morphometric  
 136 factors as well as debris cover in glacier evolution, though confined to their own specific regions. Previous  
 137 studies have also estimated the glacier statistics of SSB and reported the total number of glaciers and the  
 138 glacierized area to be 284 and 718.86 km<sup>2</sup> (Sangewar and Shukla, 2009) and 110 and 156.61 km<sup>2</sup> (SAC report,  
 139 2016), respectively. While the RGI reports varying results by two groups of analysts (number of glaciers: 514 &  
 140 304 covering an area of 550 & 606 km<sup>2</sup>, respectively) for 2000 itself.  
 141 Previous findings suggesting progressive degeneration of glaciers, apparent variation and discrepancies in  
 142 inventory estimates and also the fact that the currently available glacier details for the sub-basin are nearly 20  
 143 years old, mandate the recent and accurate assessment of the glaciers in the SSB and drive the present study.

Deleted: Prime

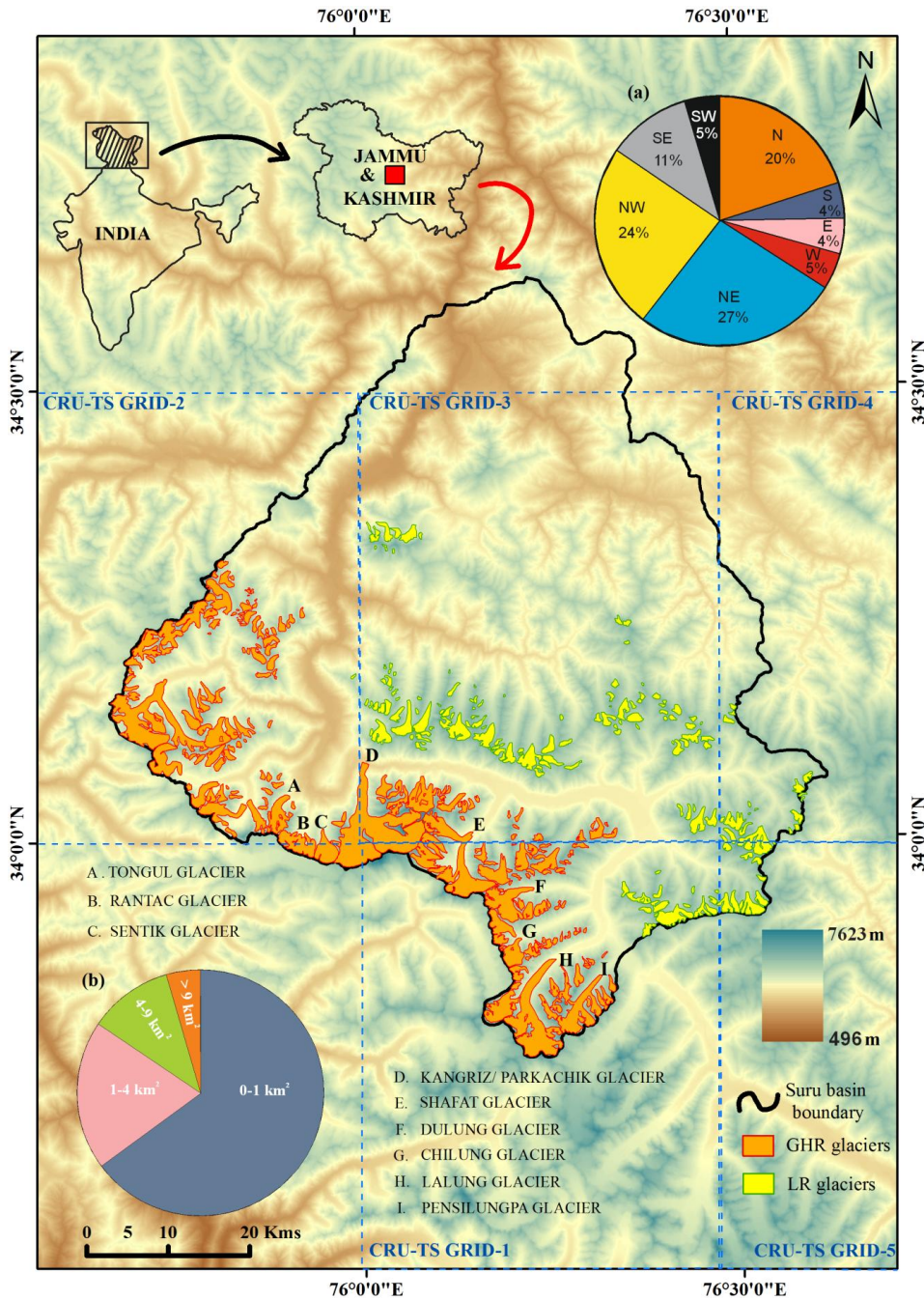
Deleted: ,

144

## 145 2 Study area

146 The present study focuses on the glaciers of the SSB situated in the state of Jammu and Kashmir, western  
 147 Himalaya (Fig. 1). The geographic extent of the study area lies within latitude and longitude of 33° 50' to 34°  
 148 40' N to 75° 40'to 76° 30' E.

149 Geographically, the sub-basin covers part of two major ranges, i.e., GHR and LR and shows the presence of the  
 150 highest peaks of Nun (7135 masl) and Kun (7077 masl) in the GHR (Vittoz, 1954). The glaciers in these ranges  
 151 have distinct morphology, with the larger ones located in the GHR and comparatively smaller towards the LR  
 152 (Fig. 1).



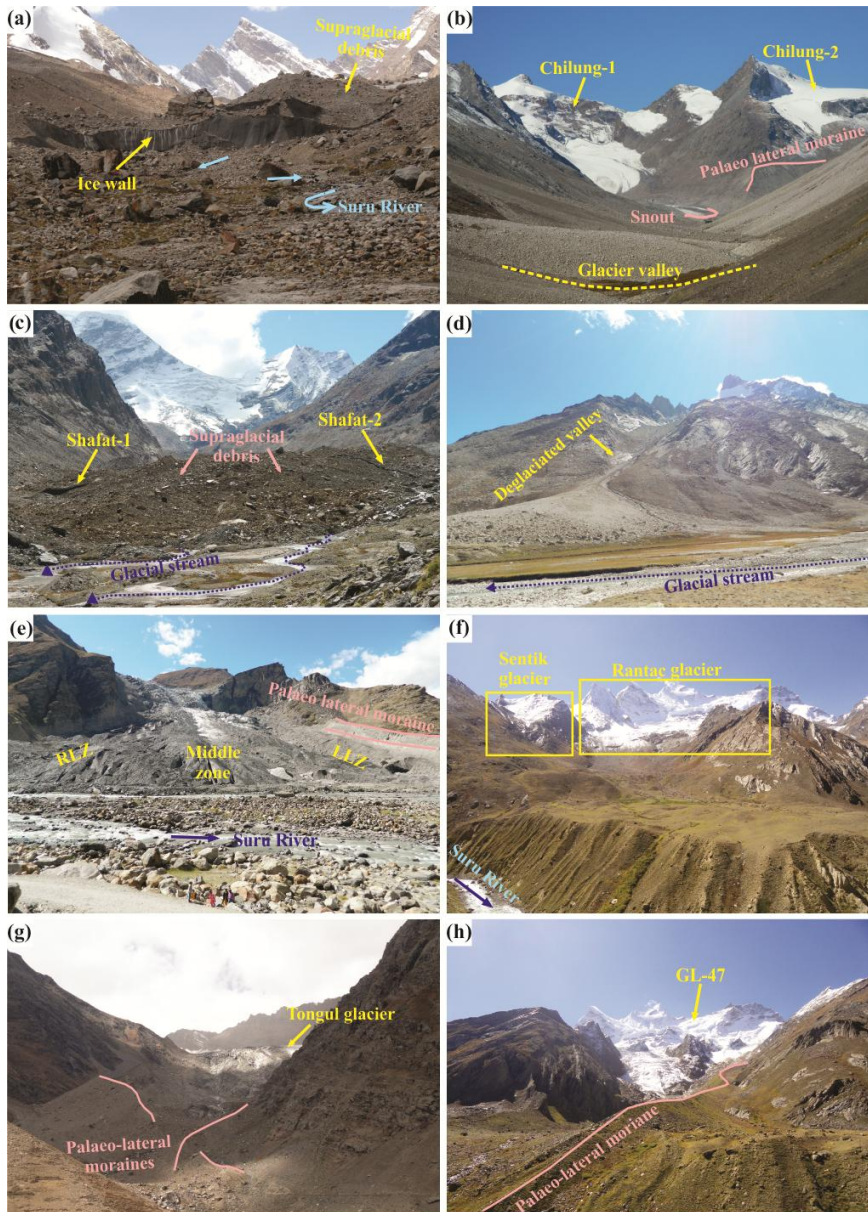
155  
 156 Figure 1: Location map of the study area. The glaciers in the Suru Sub-basin (black outline) are studied for their  
 157 response towards the climatic conditions during the period 1971-2017. Blue rectangles with dashed outlines  
 158 (GRID-1, 2, 3, 4 and 5) are the Climate Research Unit (CRU)-Time Series (TS) 4.02 grids of dimension  $0.5^\circ \times$   
 159  $0.5^\circ$ . (a) Pie-chart inset showing orientation-wise percentage distribution of glaciers in the sub-basin. North (N),  
 160 north-east (NE), north-west (NW), south (S), south-east (SE), south-west (SW), east (E) and west (W)

161 represents the direction of the glaciers. (b) Pie chart inset showing size-distribution of glaciers in the SSB. The  
162 glacier boundaries [GHR (orange) and LR (yellow)] are overlain on the Advanced Land Observing Satellite  
163 (ALOS) Digital Surface Model (DSM).

164

165 The meltwater from these glaciers feeds the Suru River (tributary of Indus River), which emerges from the  
166 Pensilungpa glacier (Fig. 2a) at an altitude of ~4675 m asl. The river further flows north for a distance of ~24  
167 kms and takes a westward turn from Rangdum (~4200 m asl). While flowing through this path, the Suru River is  
168 fed by some of the major glaciers of the GHR namely Lalung, Dulung (Fig. 1), Chilung (Fig. 2b), Shafat (Fig.  
169 2c; d), Kangriz/ Parkachik (Fig. 2e), Sentik, Rantac (Fig.2f), Tongul (Fig. 2g) and Glacier no.47 (Fig. 2h).  
170 Amongst these major glaciers, Kangriz forms the largest glacier in the SSB, covering an area of ~53 km<sup>2</sup> and  
171 descends down from the peaks of Nun and Kun (Garg et al., 2018). The Suru River continues to flow for a  
172 distance of nearly 54 kms and after crossing a mountain spur and the townships of Tongul, Panikhar and  
173 Sankoo, the river further flows north until it finally merges with River Indus at Nurla (~3028 m asl).





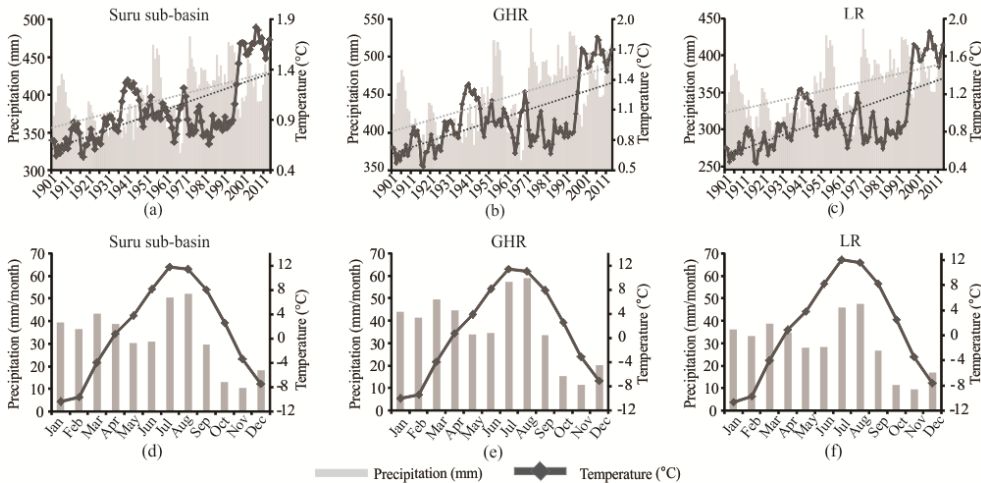
174  
 175 Figure 2: Field photographs of some of the investigated glaciers in the study area captured during the field visits  
 176 in September, 2016 and 2017. (a), (b), (c), (e), (f), (g), (h) Snouts of Pensilungpa, Chilung, Shafat, Kangriz,  
 177 Sentik & Rantac, Tongul glaciers and Glacier no.47, respectively. (d) Deglaciated valley near the Shafat glacier.  
 178

179 The westerlies are an important source of moisture in this region (Dimri, 2013) with wide range of fluctuations  
 180 in snowfall during winters. In the Padum valley, annual mean precipitation (Snowfall) and temperature amounts  
 181 to nearly 2050 to 6840 mm and 4.3 °C, respectively (Raina and Kaul, 2011; <http://en.climate-data.org>). The  
 182 longterm average annual temperature and precipitation have varied from 5.5 °C/ 588.77 mm (Kargil) to -2.04

Deleted: has



184 °C/ 278.65 mm in Leh during the period 1901-2002 (IMD, 2015). However, in order to understand the long term  
 185 variability of climatic conditions in the SSB, we have utilized the Climate Research Unit (CRU)-Time Series  
 186 (TS) 4.02 data during the period 1901-2017 (Fig. 3; Harris and Jones, 2018). Derived from this data, the annual  
 187 mean temperature and precipitation of the SSB for the period 1901-2017 has been  $0.99 \pm 0.45$  °C and  $393 \pm 76$   
 188 mm, respectively. (Standard deviations associated with the mean temperature and precipitation have been  
 189 italicized throughout the text).



190  
 191 Figure 3: Annual and seasonal variability in the climate data for the period 1901-2017. (a), (b) and (c) 5 year  
 192 moving average of the mean annual precipitation (mm) and temperature (°C) recorded for 5 grids covering the  
 193 glaciers in the entire SSB, GHR and LR (sub-regions), respectively during the period 1901-2017. The light and  
 194 dark grey colored dashed lines depict the respective trend lines for precipitation and temperature conditions  
 195 during the period 1901-2017. (d), (e) and (f) Monthly mean precipitation and temperature data for the entire  
 196 SSB, GHR and LR (sub-regions), respectively for the time period 1901-2017.

## 198 3 Datasets and Methods

### 199 3.1 Datasets used

200 The study uses multi-sensor and multi-temporal satellite remote sensing data for extracting the glacier  
 201 parameters for four time periods, i.e., 1971/1977, 1994, 2000 and 2017, details of which are mentioned in Table  
 202 1. It involves 6 Landsat level 1 terrain corrected (L1T), 3 strips of declassified Corona KH-4B and 1 Sentinel  
 203 multispectral scenes, downloaded from USGS Earth Explorer (<https://earthexplorer.usgs.gov/>). Besides, a global  
 204 digital surface model (DSM) dataset utilizing the data acquired by the Panchromatic remote-sensing Instrument  
 205 for Stereo Mapping (PRISM) onboard the Advanced Land Observing Satellite (ALOS) have also been  
 206 incorporated (<https://www.eorc.jaxa.jp/ALOS/en/aw3d30/>). ALOS World 3D comprises of a fine resolution  
 207 DSM (approx 5m vertical accuracy). It is primarily used for delineating the basin boundary, extraction of SLA,  
 208 elevation range, regional hypsometry and slope.

Deleted: has

209  
 210 Table 1: Detailed specifications of the satellite data utilised in the present study. GB= glacier boundaries,  
 211 DC=debris cover

S. no	Satellite sensors(Date of acquisition)	Remarks on quality	Scene Id	RMSE error	Registration accuracy (m)	Purpose
1.	Corona KH-4B (28 Sep 1971)	Cloud free	DS1115-2282DA056/ DS1115-2282DA055/ DS1115-2282DA054	0.1	0.3	Delineation of GB
2.	LandsatMSS (19 Aug 1977/ 1 Aug 1977)	Cloud free/ peak ablation (17 Aug)	LM02_L1TP_159036_19770819_20180422_01_T2/ LM02_L1TP_159036_19770801_20180422_01_T2	0.12	10	Delineation of GB, SLA&DC
3.	LandsatTM (27 Aug 1994)	Partially cloud covered/ peak ablation	LT05_L1TP_148036_19940827_20170113_01_T1/ LT05_L1GS_148037_19940827_20170113_01_T2	0.22	6	Delineation of GB, SLA&DC
4.	LandsatTM (26 July 1994)	Seasonal snow cover	LT05_L1TP_148036_19940726_20170113_01_T1	0.2	6	Delineation of GB
5.	LandsatET M <sup>+</sup> (4 Sep 2000)	Cloud free/ peak ablation	LE71480362000248S GS00	Base image		Delineation of GB, SLA& DC
6.	LandsatOLI (25 July 2017)	Partially cloud covered/ peak ablation	LC08_L1TP_148036_20170810_01_T1	0.15	4.5	Delineation of GB & DC, estimation of SLA
7.	Sentinel MSI (20 Sep 2017)	Cloud free	S2A_MSIL1C_20170920T053641_N0205_R005_T43SET_20170920T053854	0.12	1.2	Delineation of GB & DC
8.	LISS IV (27 Aug 2017)	Cloud free	183599611	0.2	1.16	Accuracy assessment

214 The aforementioned satellite images were acquired keeping into consideration certain necessary pre-requisites,  
 215 such as, peak ablation months (July/ August/ September), regional coverage, minimal snow and cloud cover for  
 216 the accurate identification and demarcation of the glaciers. Only three Corona KH-4B strips were available for  
 217 period 1971, which covered the SSB partially, i.e., 40% of the GHR and 57% of the LR glaciers. Therefore, rest  
 218 of the glaciers were delineated using the Landsat MSS image of the year 1977 (Table 1). Similarly, some of the  
 219 glaciers could not be mapped using the Landsat TM image of 27 Aug 1994 as the image was partially covered  
 220 with clouds. Therefore, 26 July 1994 image of the same sensor was used in order to delineate the boundaries of  
 221 the cloud covered glaciers.

222 Besides, long term climate data have been obtained from CRU-TS 4.02, which is a high resolution gridded  
 223 climate dataset obtained from the monthly meteorological observations collected at different weather stations of  
 224 the World. In order to generate this long term data, station anomalies from 1961-1990 are interpolated into 0.5°  
 225 latitude and longitude grid cells (Harris and Jones, 2018). This dataset includes six independent climate  
 226 variables (mean temperature, diurnal temperature range, precipitation, wet-day frequency, vapour pressure and  
 227 cloud cover). However, in this study monthly mean, minimum and maximum temperature and precipitation data  
 228 are taken into consideration.

Deleted: has

## 230 3.2 Methodology adopted

231 The following section mentions the methods adopted for data extraction, analysis and uncertainty estimation.

### 233 3.2.1 Glacier mapping and estimation of glacier parameters

234 Initially, the satellite images were co-registered by projective transformation at sub-pixel accuracy with the  
 235 Root Mean Square Error (RMSE) of less than 1m (Table 1), taking the Landsat ETM<sup>+</sup> image and ALOS DSM  
 236 as reference. However, the Corona image was co-registered following a two step approach: (1) projective  
 237 transformation was performed using nearly 160-250 GCPs (2) spline adjustment of the image strips (Bhambri et  
 238 al., 2012). The glaciers were mapped using a hybrid approach, i.e., normalized difference snow index (NDSI)  
 239 for delineating snow-ice boundaries and manual digitization of the debris cover. Considering that not many  
 240 changes would have occurred in the accumulation region, major modifications have been done in the boundaries  
 241 below the equilibrium line altitude (ELA) (Paul et al., 2017). The glacierets/ tributary glaciers contributing to  
 242 the main trunk are considered as single glacier entity. NDSI was applied on a reference image of Landsat ETM<sup>+</sup>  
 243 using an area threshold range of 0.55-0.6. A median filter of kernel size 3\*3 was used to remove the noise and  
 244 very small pixels. In this manner, glaciers covering a minimum area of 0.01 km<sup>2</sup> have been mapped. However,  
 245 some pixels of frozen water, shadowed regions were manually corrected. Thereafter, the debris covered part of  
 246 the glaciers was mapped manually by taking help from slope and thermal characteristics of the glaciers. Besides,  
 247 high resolution imageries from the Google Earth<sup>TM</sup> were also referred for the accurate demarcation of the  
 248 glaciers. Identification of the glacier terminus was done based on the presence of certain characteristic features  
 249 at the snout such as ice wall, proglacial lakes and emergence of streams. Length of the glacier was measured  
 250 along the central flow line (CFL) drawn from the bergschrund to the snout. Fluctuations in the snout position  
 251 (i.e., retreat) of an individual glacier was estimated using the parallel line method, in which parallel strips of 50  
 252 m spacing are taken on both sides of the CFL. Thereafter, the average values of these strips intersecting the  
 253 glacier boundaries were used to determine the frontal retreat of the glaciers (Shukla and Qadir, 2016; Garg et al.,

255 2017a;b). Mean SLA estimated at the end of the ablation season can be effectively used as a reliable proxy for  
 256 mass balance estimation for a hydrological year (Guo et al., 2014). The maximum spectral contrast between  
 257 snow and ice in the SWIR and NIR bands helps in delineation of the snow line separating the two facies. The  
 258 same principle was used in this study to yield the snow line. Further, a 15 m sized buffer was created on both  
 259 sides of the snow line to obtain the mean SLA. Other factors such as elevation (max & min), regional  
 260 hypsometry and slope were extracted utilising the ALOS DSM.

261

### 262 3.2.2 Analysis of climate variables

263 To ascertain the long term climate trends in the sub-basin, mean annual temperature (min & max) and  
 264 precipitation ~~are~~ derived by averaging the mean monthly data of the respective years. Besides, seasonal trends  
 265 ~~are~~ also analysed for winter (November-March) and summer (April-October) months. Moreover, the climate  
 266 variables ~~are~~ assessed separately for the ~46 year period (1971-2017), which is the study period of present  
 267 research.

Deleted: have been

Deleted: have

Deleted: been

Deleted: have also been

268 Further, the climate dataset was statistically analysed for five grids using Mann-Kendall test to obtain the  
 269 magnitude and significance of the trends (Supplementary table S2). The magnitude of trends in time series data  
 270 was determined using Sen's slope estimator (Sen, 1968). Quantitatively, the temperature and precipitation trends  
 271 have been assessed here in absolute terms (determined from Sen's slope). The change in climate parameters  
 272 (temperature and precipitation) was determined using following formula:

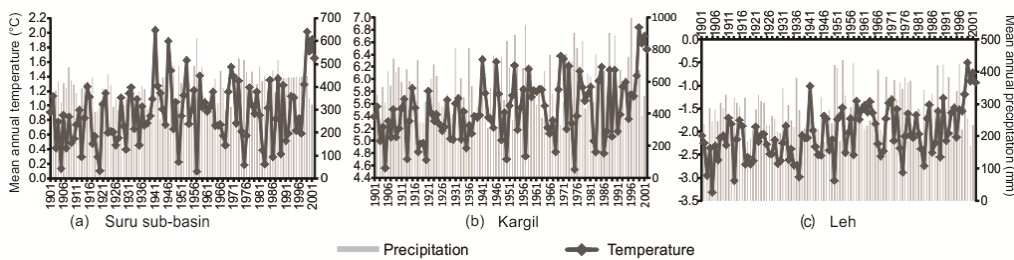
$$273 \text{Change} = (\beta * L) / M \quad (1)$$

274 where  $\beta$  is Sen's slope estimator,  $L$  is length of period and  $M$  is the long term mean.

275 These tests were performed at confidence level,  $S= 0.1(90\%)$ ,  $0.05(95\%)$  and  $0.01(99\%)$ , which differed for  
 276 both the variables (Supplementary table S2). Spatial interpolation of climate data was achieved using the Inverse  
 277 Distance Weighted (IDW) algorithm. For this purpose, a total number of 15 CRU TS grids (in vicinity of our  
 278 study area) were taken so as to have an ample number of data points in order to achieve the accurate results.

279 Further, in order to check data consistency, we have taken instrument data from nearest stations of Kargil and  
 280 Leh (due to the unavailability of meteorological stations in the Suru sub-basin) and compared with the CRU-TS  
 281 derived data for the entire Suru sub-basin during 1901-2002 period (Fig. 4).

Deleted: up

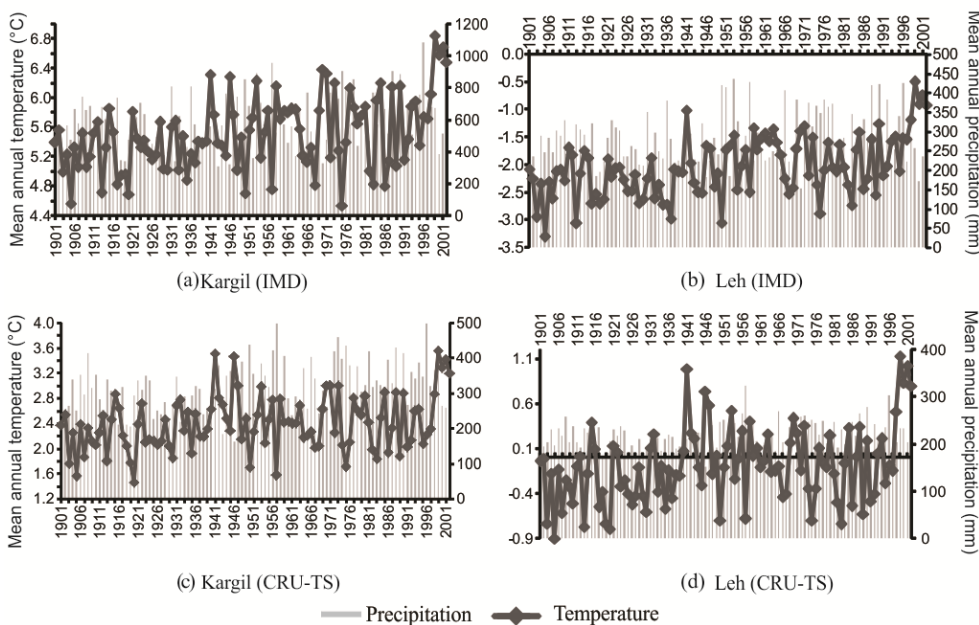


282

283 Figure 4: Mean annual temperature and precipitation patterns of CRU-TS derived gridded data in (a) Suru sub-  
 284 basin and IMD recorded station at (b) Kargil and (c) Leh.

290 The mean annual temperature pattern of Suru sub-basin shows a near negative trend till 1937, with an increase  
 291 thereafter. Similar trends have been observed for Kargil and Leh, despite their distant location from the Suru  
 292 sub-basin (areal distance of Kargil and Leh is ~63 and 126 km, respectively from the centre of Suru sub-basin).  
 293 However, it is noteworthy to mention that all the locations had attained maximum mean annual temperature in  
 294 1999 (Suru: 2.02°C; Kargil: 6.84°C; Leh: -0.5°C). We observe an almost similar trend in all the cases (Fig. 4),  
 295 with an accelerated warming post 1995/96. However, the magnitude varies, with longterm mean annual  
 296 temperature of 0.9, 5.5 and -2.04°C observed in Suru sub-basin, Kargil and Leh, respectively (Fig. 4). The  
 297 possible reason for this difference in their magnitudes could possibly be attributed to their distinct geographical  
 298 locations and difference in their nature, with former being point, while latter being the interpolated gridded data.

299 Also, we have used the station data, obtained from nearest available IMD sites, i.e., Kargil and Leh and  
 300 compared with their respective CRU-TS data (mean annual temperature and precipitation).



301  
 302 Figure 5: Analysis of meteorological (mean annual temperature and precipitation) datasets derived from Indian  
 303 Meteorological Department (IMD) stations at (a) Kargil & (b) Leh and the respective [(c) Kargil and (d) Leh]  
 304 gridded data obtained from climate research unit (CRU)-time series (TS).

305 Though varying in magnitude, the climate data obtained from IMD as well as CRU-TS suggest almost similar  
 306 trends of temperature and precipitation during the period 1901-2002 for both Kargil and Leh (Fig. 5). The  
 307 annual mean temperature/ precipitation amounted to 5.5°C/589 mm (IMD) and 2.4°C/315 mm (CRU-TS) in  
 308 Kargil, while -2.04/279 mm (IMD) and -0.09/ 216 mm (CRU-TS) in Leh during the period 1901-2002 (Fig.  
 309 5). We observed that climatic variables show lower magnitude in case of CRU-TS as compared to the station  
 310 data from IMD (except CRU-TS derived temperature data recorded for Leh). The possible reason for this  
 311 difference between CRU-TS and station data can primarily be attributed to the difference in their nature, with  
 312 former being point, while latter being a gridded data (0.5° latitude and longitude grid cells). This analysis aptly

Deleted: have

314 brings out the bias in the CRU TS gridded data. Majorly the comparison shows that though the gridded data  
 315 correctly bring out the temporal trends in meteorological data, but differ with station data in magnitude (being  
 316 on lower side than the station estimates). This helps us better appreciate the climate variations in the Suru sub-  
 317 basin as well, since we learn that the reported temperature and precipitation changes are probably on the lower  
 318 side of the actual variations.

### 319 3.2.3 Uncertainty assessment

320 This study involves extraction of various glacial parameters utilizing satellite data with variable characteristics,  
 321 hence, susceptible to uncertainties, which may arise from various sources. These sources may be locational  
 322 (LE), interpretational (IE), classification (CE) or processing (PE) errors (Racoviteanu et al., 2009; Shukla and  
 323 Qadir, 2016). In our study, the LE and PE may have resulted on account of miss-registration of the satellite  
 324 images and inaccurate mapping, respectively. While IE and CE would have introduced due to the miss-  
 325 interpretation of glacier features during mapping. The former can be rectified by co-registration of the images  
 326 and estimation of sub-pixel co-registration RMSE (Table 1) and using standard statistical measures. However,  
 327 the latter can be visually identified and corrected but difficult for exact quantification owing to lack of reliable  
 328 reference data (field data) in most cases. As a standard procedure for uncertainty estimation, glacier outlines are  
 329 compared directly with the ground truth data as acquired using a Differential Global Positioning System (DGPS)  
 330 (Racoviteanu et al., 2008a). In this study, DGPS survey was conducted on the Pensilungpa and Kangriz glaciers  
 331 at an error of less than 1cm. Therefore, by comparing the snout position of Pensilungpa (2017) and Kangriz  
 332 (2018) glaciers derived from DGPS and OLI image, an accuracy of  $\pm 23$  and  $\pm 1.4$  m, respectively was obtained.  
 333 Also, the frontal retreat estimated for the Kangriz glacier using DGPS and OLI image is found to be  $38.63 \pm 47.8$   
 334 and  $39.98 \pm 56.6$  m, respectively during the period 2017-18. In this study, high resolution Linear imaging self-  
 335 scanning system (LISS)-IV imagery (spatial resolution of 5.8 m) is also used for validating the glacier mapping  
 336 results for the year 2017 (Table 1). Glaciers of varying dimensions and distribution of debris cover were  
 337 selected for this purpose. The area and length mapping accuracy for these selected glacier boundaries (G-1, G-2,  
 338 G-3, G-13, G-41, G-209, G-215, G-216, G-220, G-233) was found to be 3% and 0.5%, respectively.  
 339 The multi-temporal datasets were assessed for glacier length and area change uncertainty as per the methods  
 340 given by Hall et al. (2003) and Granshaw and Fountain (2006). Following formulations (Hall et al., 2003) were  
 341 used for estimation of the said parameters:

$$342 \text{Terminus uncertainty } (U_T) = \sqrt{a^2 + b^2} + \sigma \quad (2)$$

343 where, 'a' and 'b' are the pixel resolution of image 1 and 2, respectively and ' $\sigma$ ' is the registration error. The  
 344 terminus and areal uncertainty estimated are given in Table 2.

$$345 \text{Area change uncertainty } (U_A) = 2 * U_T * x \quad (3)$$

347 where, 'x' is the spatial resolution of the sensor.

348 Table 2. Terminus and Area change uncertainty associated with satellite dataset as defined by Hall et al. (2003).  
 349  $U_T$  = terminus uncertainty,  $U_A$  = area change uncertainty,  $x$  = spatial resolution,  $\sigma$  = registration accuracy.  
 350

Serial no.	Satellite sensor	Terminus uncertainty $U_T$ $= \sqrt{a^2 + b^2} + \sigma$	Area change uncertainty $U_A = 2 U_T * x$
------------	------------------	---	--

Deleted: been

1.	Corona KH-4B	3.12 m	0.00007 km <sup>2</sup>
2.	Landsat MSS	123.13 m	0.03km <sup>2</sup>
3.	Landsat TM	41.42 m	0.003 km <sup>2</sup>
4.	Landsat ETM <sup>+</sup>	48.42 m	0.003km <sup>2</sup>
5.	Landsat OLI	46.92 m	0.003km <sup>2</sup>

352  
353  
354 Area mapping uncertainty ~~was~~ estimated using the buffer method, in which, a buffer size equal the registration  
355 error of the satellite image ~~was~~ taken into consideration (Bolch et al., 2012; Garg et al., 2017a,b). Error  
356 estimated using this method is found to be 0.48, 27.2, 9.6 and 3.41 km<sup>2</sup> for the 1971 (Corona), 1977 (MSS),  
357 1994 (TM) and 2017 (OLI) image, respectively. Since the debris extents were delineated within the respective  
358 glacier boundaries, the proportionate errors are likely to have propagated in debris cover estimations which were  
359 estimated accordingly (Garg et al., 2017b).

360 Uncertainty in SLA estimation needs to be reported in the X, Y and Z directions. In this context, error in X and  
361 Y directions should be equal to the distance taken for creating the buffer on either side of the snow line  
362 demarcating the snow and ice facies. Since, the buffer size taken in this study was 15 m, therefore, error in X  
363 and Y direction was considered as  $\pm 15$  m. However, uncertainty in Z direction would be similar to the ALOS  
364 DSM, i.e.,  $\pm 5$  m.

365

## 366 4 Results

367 The present study involved creation of glacier inventory for the year 2017 and estimation of glacier (area,  
368 length, debris cover and SLA) parameters for four different time periods. For detailed insight, the variability of  
369 the glacier parameters have also been evaluated on decadal scale, in which the total time period has been sub-  
370 divided into three time frames, i.e., 1971-1994 (23 years), 1994-2000 (6 years) and 2000-2017 (17 years).

371

### 372 4.1 Basin statistics

373 The SSB covers an area of  $\sim 4429$  km<sup>2</sup>. In 1971, the sub-basin had around 240 glaciers, with 126 glaciers located  
374 in the GHR and 114 in the LR, which remained the same till 2000. However, a major disintegration of glaciers  
375 took place during the period 2000-2017, which resulted into the breakdown of about 12 glaciers into smaller  
376 glacierets. The recent (2017) distribution of the glaciers in the GHR and LR is 130 and 122, respectively  
377 (Supplementary table S1). The overall glacierized area is  $\sim 11\%$ , with the size and length of the glaciers varying  
378 from 0.01 to 53.1 km<sup>2</sup> and 0.15 to 16.34 km, respectively.

379 Within the sub-basin, the size range of glaciers in the GHR and LR vary from 0.01 (G-115) to 53.1 km<sup>2</sup> (G-50)  
380 and 0.03 (G-155/165) to 6.73 km<sup>2</sup> (G-209), respectively. Considering this, glaciers have been categorized into  
381 small (0-7 km<sup>2</sup>/ 0-2 km), medium (7-15 km<sup>2</sup>/ 2-7 km) and large (>15 km<sup>2</sup>/ >7 km). Based on size distribution,  
382 small (comprising all the LR and some GHR glaciers), medium and large glaciers occupy 47%, 15% and 38% of  
383 the glacierized sub-basin. Depending upon the percentage area occupied by the supraglacial debris out of the  
384 total glacier area, the glaciers have been categorized into clean (CG: 0-25%), partially debris-covered (PDG: 25-  
385 50%) and heavily debris-covered (HDG: >50%). Categorization of the glaciers based on this criteria shows their  
386 proportion in the glacierized basin as: CG (43%), PDG (40%) and HDG (17%). Majority of the glaciers in the

Deleted: has also been

Deleted: is

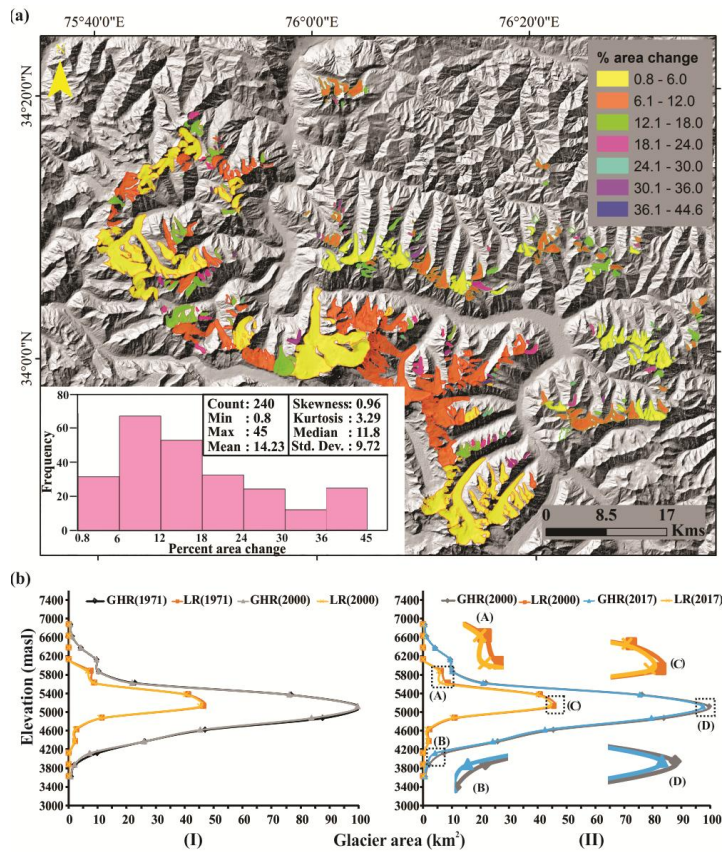


389 sub-basin are north facing (N/ NW/NE: 71%), followed by south (S/ SW/ SE: 20%), with very few oriented in  
 390 other (E/ W: 9%) directions (Fig. 1a). The mean elevation of the glaciers in the SSB is  $5134.8 \pm 225$  masl, with  
 391 an average elevation of  $5020 \pm 146$  and  $5260 \pm 117$  masl in the GHR and LR, respectively. Mean slope of the  
 392 glaciers is  $24.8 \pm 5.8^\circ$  and varies from  $24 \pm 6^\circ$  to  $25 \pm 6^\circ$  in the GHR and LR, respectively. While, percentage  
 393 distribution of glaciers shows that nearly 80% of the LR glaciers have steeper slope (20-40°) as compared to the  
 394 GHR glaciers (57%).

395

#### 396 4.2 Area changes

397 The glaciated area reduced from  $513 \pm 14$  km<sup>2</sup> (1971) to  $481 \pm 3.4$  km<sup>2</sup> (2017), exhibiting an overall deglaciation  
 398 of  $32 \pm 9$  km<sup>2</sup> ( $6 \pm 0.02\%$ ) during the period 1971-2017. Percentage area loss of the individual glaciers ranges  
 399 between 0.8 (G-50; Parkachik glacier) - 45 (G-81) %, with majority of the glaciers undergoing an area loss in  
 400 the range 6-12% during the period 1971-2017 (Fig.6a).



401

402 Figure 6: (a) Percent area loss of the glaciers in the SSB during the period 1971-2017. Frequency distribution  
 403 histogram depicting that majority of the glaciers have undergone an area loss in the range 6-12%. (b)  
 404 Hypsometric distribution of glacier area in the GHR and LR regions during the period (I) 1971-2000 and (II)  
 405 2000-2017. (A), (B), (C) and (D) insets in (II) shows the significant change in area at different elevation range  
 406 of the GHR and LR glaciers.

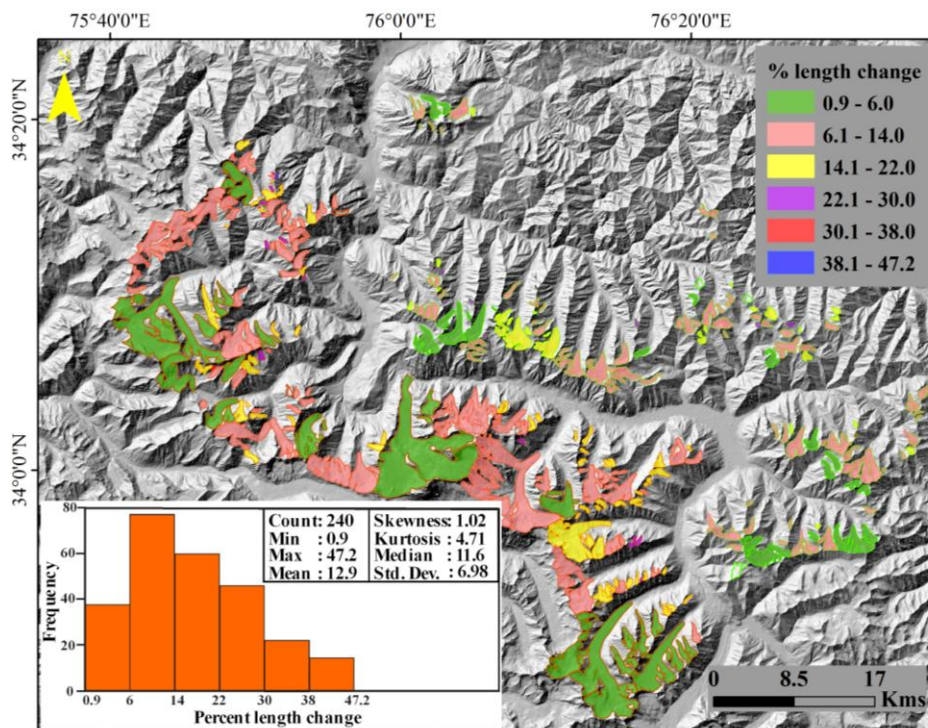
407

408 Results show that the highest pace of deglaciation is observed during 1994-2000 ( $0.95 \pm 0.005 \text{ km}^2\text{a}^{-1}$ ) and 2000-  
 409 2017 ( $0.86 \pm 0.0002 \text{ km}^2\text{a}^{-1}$ ) followed by 1971-1994 ( $0.5 \pm 0.001 \text{ km}^2\text{a}^{-1}$ ) (Supplementary figure S1a). Within the  
 410 SSB, glaciers in the LR exhibit higher deglaciation ( $7 \pm 7.2\%$ ) as compared to GHR ( $6 \pm 2\%$ ) during the period  
 411 1971-2017. Apart from deglaciation, G-50 also showed increment in glacier area during the period 1994-2000,  
 412 however, insignificantly.

413

### 414 4.3 Length changes

415 Fluctuations in the glacier snout have been estimated during the period 1971-2017 and it is observed that nearly  
 416 all the glaciers have retreated during the said period, however the retreat rates vary considerably. The overall  
 417 average retreat rate of the glaciers is observed to be  $4.3 \pm 1.02 \text{ ma}^{-1}$  during the period 1971-2017. Percentage  
 418 length change of the glaciers ranges between 0.9 to 47%, with majority of the glaciers retreating in the range 6-  
 419 14% during the period 1971-2017 (Fig.7).



420

421 Figure 7: Percent length change of the glaciers in the SSB during the period 1971-2017. Frequency distribution  
 422 histogram showing that majority of the glaciers have undergone length change of in the range 6-14%.

423

424 Decadal observations reveal the highest rate of retreat during 1994-2000 ( $7.37 \pm 8.6 \text{ ma}^{-1}$ ) followed by 2000-  
 425 2017 ( $4.66 \pm 1.04 \text{ ma}^{-1}$ ) and lowest during 1971-1994 ( $3.22 \pm 2.3 \text{ ma}^{-1}$ ) (Supplementary figure S 1b). Also, the  
 426 average retreat rate in the GHR and LR glaciers was observed to be  $5.4 \pm 1.04 \text{ ma}^{-1}$  and  $3.3 \pm 1.04 \text{ ma}^{-1}$ ,  
 427 respectively, during the period 1971-2017. The retreat rate of individual glaciers varied from  $0.72 \pm 1.02 \text{ ma}^{-1}$

428 (G-114) to  $28.92 \pm 1.02 \text{ ma}^{-1}$  (G-7, i.e., Dulung glacier) during the period 1971-2017. Besides, the Kangriz  
 429 glacier (G-50) also showed advancement during the period 1994-2000 by  $5.23 \pm 8.6 \text{ ma}^{-1}$ .

430

#### 431 **4.4 Debris-cover changes**

432 Results show an overall increase in debris-cover extent by 62% ( $\sim 37 \pm 0.002 \text{ km}^2$ ) in the SSB glaciers during the  
 433 period 1971-2017. Decadal variations exhibit the maximum increase in the debris-cover by approximately 19  
 434  $\pm 0.00004 \text{ km}^2$  (24%) during 2000-2017 followed by an increase of  $13 \pm 0.0001 \text{ km}^2$  (20%) and  $5 \pm 0.0001 \text{ km}^2$   
 435 (9%) during 1994-2000 and 1971-1994, respectively (Supplementary figure S1c). However, GHR and LR  
 436 glaciers show an overall increase of debris cover extent by 59% and 73%, respectively during the entire study  
 437 period, i.e., 1971-2017.

438

#### 439 **4.5 SLA variations**

440 The mean SLA shows an average increase of  $22 \pm 60 \text{ m}$  during the period 1977-2017. On the decadal scale, SLA  
 441 variations showed the highest increase ( $161 \pm 59 \text{ m}$ ) during 1994-2000 with a considerably lower increase ( $8 \pm 59$   
 442  $\text{ m}$ ) during 1977-1994 and decrease ( $150 \pm 60 \text{ m}$ ) during 2000-2017. Amongst the four time periods (1977, 1994,  
 443 2000 & 2017) used for mean SLA estimation, the highest SLA is noted during 2000 ( $5158 \pm 65 \text{ masl}$ ) and  
 444 minimum during 1977 ( $4988 \pm 65 \text{ masl}$ ) (Supplementary figure S1d).

445 During the period 1977-2017, the average SLA of the LR glaciers is observed to be relatively higher ( $5155 \pm 7$   
 446  $\text{ masl}$ ) as compared to the GHR glaciers ( $4962 \pm 9 \text{ masl}$ ). In contrast, an overall rise in mean SLA was noted in  
 447 GHR ( $49 \pm 69 \text{ m}$ ), while a decrease in LR glaciers ( $18 \pm 45 \text{ m}$ ) during the time frame of 1977-2017.

448

### 449 **5 Discussion**

450 The present study reports detailed temporal inventory data of the glaciers in the SSB considering multiple  
 451 glacier parameters, evaluates the ensuing changes for ascertaining the status of glaciers and relates them to  
 452 climate variability and other inherent terrain characteristics. The results suggest an overall degeneration of the  
 453 glaciers with pronounced spatial and temporal heterogeneity in response.

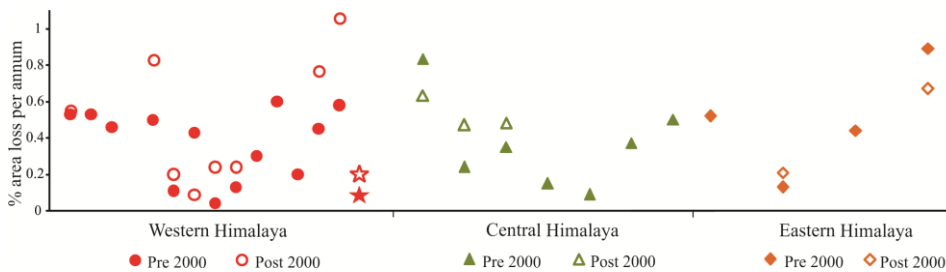
454

#### 455 **5.1 Glacier variability in Suru sub-basin: A comparative evaluation**

456 Basin statistics reveal that in the year 2000, the SSB comprised of 240 glaciers covering an area of  
 457 approximately  $496 \text{ km}^2$ . However, these figures differ considerably from the previously reported studies in this  
 458 particular sub-basin, with the total number of glaciers and the glacierized area varying from 284/  $718.86 \text{ km}^2$   
 459 (Sangewar and Shukla, 2009) to 110/  $156.61 \text{ km}^2$  (SAC report, 2016), respectively. In contrast, the glacierized  
 460 area is found to be less, however comparable with the RGI boundaries ( $550.88 \text{ km}^2$ ). Besides, debris cover  
 461 distribution of the glaciers during 2000 is observed to be  $\sim 16\%$  in the present study, which is almost half of that  
 462 reported in RGI (30%). Variability in these figures is possibly due to the differences in the mapping techniques,  
 463 thereby increasing the risk of systematic error. Moreover, due to the involvement of different analysts in the  
 464 latter, the results may more likely suffer with random errors.

465 Results from this study reveal an overall deglaciation of the glaciers in the SSB at an annual rate of  $\sim 0.1$   
 466  $\pm 0.0004\%$  during the period 1971-2017. This quantum of area loss is comparatively less to the average annual

467 rate of 0.4% reported in the western Himalaya (Supplementary table S3). However, our results are comparable  
 468 with Birajdar et al. (2014), Chand and Sharma (2015) and Patel et al. (2018) and differ considerably with other  
 469 studies in the western Himalayas (Supplementary table S3). Period wise deglaciation varied from  $0.1 \pm 0.0007$  to  
 470  $0.2 \pm 0.005\% \text{ a}^{-1}$  during 1971-2000 and 2000-2017, respectively. This result is in line with the recent findings by  
 471 Maurer et al. (2019), who suggest a higher average mass loss post 2000 ( $-0.43 \text{ m w.e.a}^{-1}$ ), which is almost  
 472 double the rate reported during 1975-2000 ( $-0.22 \text{ m w.e.a}^{-1}$ ) for the entire Himalaya.  
 473 Comparing the deglaciation rates of the glaciers within the western Himalayan region reveals considerable  
 474 heterogeneity therein (Supplementary table S3). It is observed that the Karakoram Himalayan glaciers, in  
 475 particular had been losing area till 2000 at an average rate of  $0.09\% \text{ a}^{-1}$ , with an increase in area thereafter by  
 476  $\sim 0.05\% \text{ a}^{-1}$  (Liu et al., 2006; Minora et al., 2013; Bhambri et al., 2013). However, glaciers in the GHR and Trans  
 477 Himalayan range have been deglaciating with higher average annual rate of 0.4 and  $0.6\% \text{ a}^{-1}$ , respectively during  
 478 the period 1962-2016 (Kulkarni et al., 2007; Kulkarni et al., 2011; Rai et al., 2013; Chand and Sharma, 2015;  
 479 Mir et al., 2017; Schmidt and Nusser, 2017; Chudley et al., 2017; Patel et al., 2018; Das and Sharma, 2018). In  
 480 contrast to these studies, deglaciation rates in SSB, which comprises of glaciers in GHR as well as LR have  
 481 varied from  $0.1\% \text{ a}^{-1}$  (GHR) to  $0.2\% \text{ a}^{-1}$  (LR) (present study). These results evidently depict that the response of  
 482 the SSB glaciers is transitional between the Karakoram Himalayan and GHR glaciers. Period wise area loss of  
 483 the glaciers in the Himalayan region suggest maximum average deglaciation of eastern ( $0.49\%/ \text{yr}$ ), followed by  
 484 central ( $0.36\%/ \text{yr}$ ) and western ( $0.35\%/ \text{yr}$ ) Himalayan glaciers before 2000. Contrarily, after 2000, the central  
 485 Himalayan glaciers deglaciated at the maximum rate ( $0.52\%/ \text{yr}$ ) followed by western ( $0.46\%/ \text{yr}$ ) and eastern  
 486 ( $0.44\%/ \text{yr}$ ) Himalayan glaciers (Fig.8). Though these rates reflect the possible trend of deglaciation in the  
 487 Himalayan terrain, however, any conclusion drawn would be biased due to insufficient data, particularly in  
 488 eastern and central Himalaya.



489  
 490 Figure 8: Annual rate of percentage area loss of glaciers in three major sections of Himalaya before and after  
 491 2000. Details of the same have been mentioned in Table S3 of Supplementary sheet. Results from the present  
 492 study have been star marked in the western Himalaya.  
 493

494 In this study, we found an overall average retreat rate of  $4.3 \pm 1.02 \text{ ma}^{-1}$  during the period 1971-2017. However,  
 495 the average retreat rates of seven glaciers in the SSB, reported by Kamp et al., (2011) is found to be nearly twice  
 496 ( $24 \text{ ma}^{-1}$ ) of that found in this study ( $10 \text{ ma}^{-1}$ ). The comparatively higher retreat rates in the former might be due  
 497 to the consideration of different time frames. The average retreat rates in other basins of the western Himalaya is  
 498 also found to be higher ( $7.8 \text{ ma}^{-1}$ ) in the Doda valley (Shukla and Qadir, 2016),  $8.4 \text{ ma}^{-1}$  in Liddar valley  
 499 (Murtaza and Romshoo, 2015),  $15.5 \text{ ma}^{-1}$  in the Chandra-Bhaga basin (Pandey and Venkataraman, 2013) and 19

500  $\text{ma}^{-1}$  in the Baspa basin (Mir et al., 2017). These results show lower average retreat rate of the glaciers in the  
 501 SSB as compared to the other studies in the western Himalaya.  
 502 The observed average retreat rates during 2000-2017 ( $4.6 \pm 1.02 \text{ ma}^{-1}$ ) is found to be nearly twice of that, noted  
 503 during 1971-2000 ( $2 \pm 1.7 \text{ ma}^{-1}$ ). Similar higher retreat rates post 2000 have been reported in the Tista basin  
 504 (Raina, 2009), Doda valley (Shukla and Qadir, 2016), Chandra Bhaga basin (Pandey and Venkataraman, 2013)  
 505 and Zaskar basin (Pandey et al., 2011). However, these studies may not sufficiently draw a generalized picture  
 506 of glacier recession in the Himalayan region.

507

## 508 5.2 Spatio-temporal variability in the climate data

509 Climatic fluctuations play a crucial role in understanding glacier variability. In this regard, CRU-TS 4.02 dataset  
 510 helped in delineating the long term fluctuations in the temperature and precipitation records.

### 511 5.2.1 Basin-wide climate variability

512 During an entire duration of 116 years, i.e. from 1901-2017, maximum mean annual temperature is observed in  
 513 2016 ( $3.23 \text{ }^\circ\text{C}$ ) and minimum during 1957 ( $-0.51 \text{ }^\circ\text{C}$ ). Mean annual temperature shows an almost uniform trend  
 514 till 1996, with a pronounced rise thereafter till 2005/06 period (Fig. 3a;b;c). The globally averaged combined  
 515 land and ocean surface temperature data of 1983-2012 period **are** considered as the warmest 30-year period in  
 516 the last 1400 years (IPCC, 2013). This unprecedented rate of warming **primarily** attributed to the rapid scale of  
 517 industrialization, increase in regional population and anthropogenic activities prevalent during this time period  
 518 (Bajracharya et al., 2008; IPCC, 2013). Thus, one of the probable reason for this sudden **increase** in temperature  
 519 pattern is possibly due to the greenhouse effect from enhanced emission of black carbon in this region (by 61%)  
 520 from 1991-2001. Evidences of incessant increase in temperature during 1990s **has** also been observed (through  
 521 chronology of Himalayan Pine) from the contemporaneous surge in tree growth rate (Singh and Yadav 2000). In  
 522 fact, 50% of the years since 1970 have experienced considerably high solar irradiance and warm phases of  
 523 ENSO, which is possibly one of the reasons for the considerable rise in temperature throughout the Himalaya  
 524 (Shekhar et al., 2017). Maximum mean annual precipitation is noted during 2015 (615 mm) and minimum  
 525 during 1946 (244 mm). However, the mean annual precipitation followed a similar trend till 1946 with an  
 526 increasing thereafter (Fig. 3a;b;c). Besides these general trends in temperature and precipitation, an overall  
 527 absolute increase in the mean annual temperature ( $T_{\text{max}}$  &  $T_{\text{min}}$ ) and precipitation data have been noted as  $0.77$   
 528  $^\circ\text{C}$  ( $0.25 \text{ }^\circ\text{C}$  &  $1.3 \text{ }^\circ\text{C}$ ) and 158 mm, respectively during the period 1901-2017. These observations suggest an  
 529 enhanced increase in  $T_{\text{min}}$  by nearly 5 times as compared to the  $T_{\text{max}}$  alongwith a simultaneous increase in the  
 530 precipitation during the period 1901-2017.

531 Seasonal variations reveal monthly mean temperature and precipitation of  $6.7 \text{ }^\circ\text{C}$  and 1071 mm during summer  
 532 (Apr-Oct) and  $-6.9 \text{ }^\circ\text{C}$  and 890 mm during winter (Nov-Mar) recorded during 1901-2017 period. Maximum  
 533 monthly mean temperature and precipitation have been observed in July ( $11.8 \text{ }^\circ\text{C}/ 50.4 \text{ mm}$ ) and August ( $11.4$   
 534  $^\circ\text{C}/ 52 \text{ mm}$ ) during the period 1901-2017, suggesting them to be the warmest and wettest months. While,  
 535 January is noted to be the coldest ( $-10.4 \text{ }^\circ\text{C}$ ) and November ( $10.3 \text{ mm}$ ) to be the driest months in the duration of  
 536 116 years (Fig. 3d;e;f). Summer/ winter mean annual temperature and precipitation have increased significantly  
 537 by an average  $0.74/ 1.28 \text{ }^\circ\text{C}$  and  $85/ 72 \text{ mm}$ , respectively during the period 1901-2017. These values reveal a  
 538 relatively higher rise in winter average temperature in contrast to the summer. However, enhanced increase in  
 539  $T_{\text{min}}$  ( $1.8^\circ\text{C}$ ) during winter and  $T_{\text{max}}$  ( $0.78^\circ\text{C}$ ) during summer have also been observed during the 1901-2017 time

Deleted: is

Deleted: has been

Deleted: increment

Deleted: have

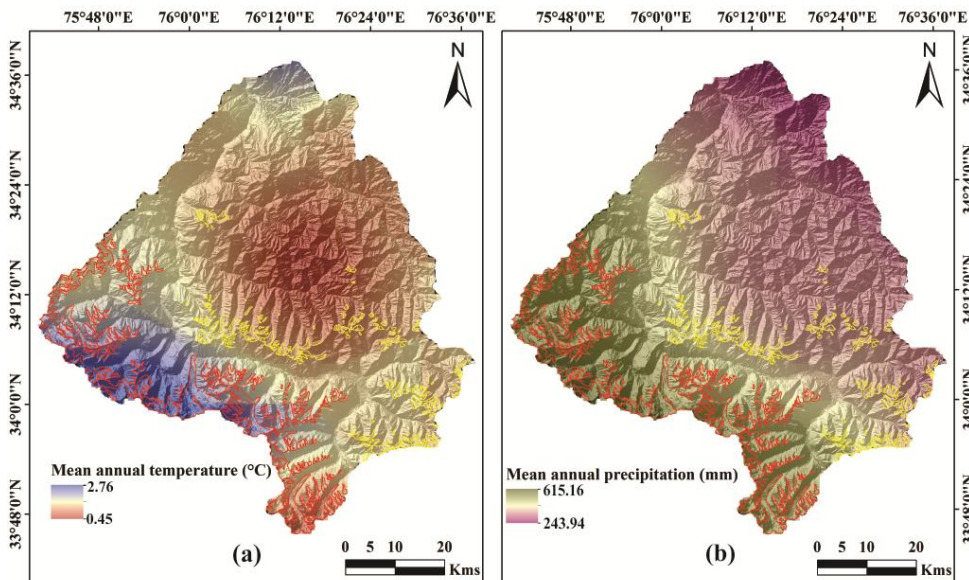


544 period. The relatively higher rise in the winter temperature (particularly  $T_{\min}$ ) and precipitation possibly suggest  
 545 that the form of precipitation might have changed from solid to liquid during this particular time span. Similar  
 546 increase in the winter temperature have also been reported from the NW Himalaya during the 20<sup>th</sup> century  
 547 (Bhutiyani et al., 2007).

548 In contrast to the long-term climate trends, we have also analyzed the climate data for the study period, i.e.,  
 549 1971-2017. An overall increase in the average temperature (0.3°C),  $T_{\max}$  (0.45°C)  $T_{\min}$  (1.02°C) and  
 550 precipitation by 213 mm is observed. Meanwhile, an enhanced increase in winter  $T_{\min}$  (1.7°C) and summer  $T_{\max}$   
 551 (0.45°C) are observed. These findings aptly indicate the important role of winter  $T_{\min}$  and summer  $T_{\max}$  in the  
 552 SSB.

### 553 5.2.2 Local climate variability

554 Apart from these generalized climatic variations, grid-wise analysis of the meteorological parameters reveal  
 555 existence of local climate variability within the sub-basin (Fig. 3; 9).



556  
 557 Figure 9: Spatial variation in meteorological data recorded for 15 grids in the SSB during the period 1901-2017.  
 558 Map showing the long term mean annual (a) temperature (°C) and (b) precipitation (mm) data within the sub-  
 559 basin suggesting the existence of significant local climate variability in the region. Glacier boundaries are shown  
 560 as: GHR (red) and LR (yellow).

561  
 562 Observations indicate that the glaciers covered in grid 4 have been experiencing a warmer climatic regimes with  
 563 the maximum annual mean temperature of 1.69 °C as compared to the other glaciers in the region (grid 2 = 1.4  
 564 °C, grid 5 = 0.74 °C, grid 1 = 0.65 °C and grid 3 = 0.45 °C). Spatial variability in annual mean precipitation data  
 565 reveal that grid 2 (448 mm) & grid 1 (442 mm) experienced wetter climate as compared to grid 4 (383 mm),  
 566 grid 3 (373 mm) and minimum in grid 5 (318 mm). These observations suggest that GHR glaciers have been  
 567 experiencing a warmer and wetter climate (1.03 °C/ 445 mm) as compared to the LR glaciers (0.96 °C/ 358 mm)

Deleted: s

Deleted: experiences

570 (Fig. 3e; f). These observations clearly show that local climate variability does exist in the basin for the entire  
 571 duration of 116 years (Fig. 9).

572

### 573 **5.3 Glacier changes: Impact of climatic and other plausible factors**

574 The alterations in the climatic conditions, discussed in Sect. 5.2, would in turn, influence the glacier parameters,  
 575 however varying with time. This section correlates the climatic and other factors (elevation range, regional  
 576 hypsometry, slope, aspect and proglacial lakes) with the variations in the glacier parameters.

577

#### 578 **5.3.1 Impact of climatic factors**

579 An overall degenerating pattern of the glaciers in the SSB is observed during the period 1971-2017, with  
 580 deglaciation of  $32 \pm 9 \text{ km}^2$  ( $6 \pm 0.02\%$ ). In the same duration, the glaciers have also retreated by an average  $199$   
 581  $\pm 46.9 \text{ m}$  (retreat rate:  $4.3 \pm 1.02 \text{ ma}^{-1}$ ) alongwith an increase in the debris cover by  $\sim 62\%$ . The observed overall  
 582 degeneration of the glaciers have possibly resulted due to the warming of climatic conditions during this  
 583 particular time frame. The conspicuous degeneration of these glaciers might have led to an increased melting of  
 584 the glacier surface, which in turn would have unveiled the englacial debris cover and increased its coverage in  
 585 the ablation zone (Shukla et al., 2009; Scherler et al., 2011). An enhanced degeneration of the glaciers have been  
 586 noted during 2000-2017 ( $0.85 \pm 0.005 \text{ km}^2\text{a}^{-1}$ ) than 1971-2000 ( $0.59 \pm 0.005 \text{ km}^2\text{a}^{-1}$ ). Also, nearly 12 glaciers  
 587 have shown disintegration into glacierets after 2000. These observations may be attributed to the relatively  
 588 higher annual mean temperature ( $1.68 \text{ }^\circ\text{C}$ ) during the former as compared to the period 1971-2000 ( $0.89 \text{ }^\circ\text{C}$ ).  
 589 Concomitant to the maximum glacier degeneration during the period 2000-2017, debris cover extent has also  
 590 increased more (24%) as compared to 1971-2000 (16%). The enhanced degeneration of the glaciers during  
 591 2000-2017 might have facilitated an increase in the distribution of supraglacial debris cover. A transition from  
 592 CGs to PDGs has also been noticed which resulted due to increase in the debris cover percentage over nearly 99  
 593 glaciers. The conversion from PDGs to HDGs (39) and from CGs to HDGs (2) has also occurred. Also, most of  
 594 these transitions have occurred during 2000-2017, which confirms the maximum degeneration of the glaciers  
 595 during this particular period.

596 It is observed in our study that smaller glaciers have deglaciated more (4.13%) than the medium (1.08%) and  
 597 larger (1.03%) sized glaciers during the period 1971-2017 (Supplementary figure S2). This result depicts an  
 598 enhanced sensitivity of the smaller glaciers towards the climate change (Bhambri et al., 2011; Basnett et al.,  
 599 2013; Ali et al., 2017). A similar pattern of glacier degeneration is noted during 1971-2000, with smaller  
 600 glaciers deglaciating more (5%) as compared to the medium sized (3%) and larger (1%) ones. However during  
 601 2000-2017, medium glaciers showed slightly greater degeneration (3.9%) as compared to the smaller (3.7%)  
 602 followed by larger ones (1.5%). We have also observed maximum length change for smaller glaciers (8%) in  
 603 comparison to medium (5%) and large glaciers (3%). These results indicate that the snout retreats are commonly  
 604 associated with small and medium sized glaciers (Mayewski et al., 1980).

605 Temporal and spatial variations in SLAs are an indicator of ELAs, which in turn provide direct evidences  
 606 related to the change in climatic conditions (Hanshaw and Bookhagen, 2014). SLAs are amongst the dynamic  
 607 glacier parameters that alters seasonally and annually, indicating their direct dependency towards the climatic  
 608 factors such as temperature and precipitation. In the present study, the mean SLA has gone up by an average  $22$   
 609  $\pm 60 \text{ m}$  during the period 1977-2017. This rise in SLA is synchronous with the increase in mean annual

610 temperature by 0.43°C. Moreover, the maximum rise in SLA during 1994-2000 is contemporaneous with the  
 611 rise of temperature by 0.64 °C during this time period.  
 612 Further, in order to understand the regional heterogeneity in glacier response within the sub-basin, parameters of  
 613 the GHR and LR glaciers are analyzed separately at four different time periods and correlated with the climatic  
 614 variables. It is found that the LR glaciers have deglaciated more (7.2%) as compared to the GHR glaciers  
 615 (5.9%). Similarly, more debris cover is found to have accumulated over the LR (73%) glaciers as compared to  
 616 the GHR (59%) glaciers during 1971-2017. This result shows that the relatively cleaner (LR) glaciers tend to  
 617 deglacierate more alongwith accumulation of more debris as compared to the debris and partially debris covered  
 618 glaciers (GHR glaciers) (Bolch et al., 2008; Scherler et al., 2011). Moreover, increase in mean annual  
 619 temperature in the LR (0.3°C) is slightly greater than in GHR (0.25°C) during the period 1971-2017, thus  
 620 exhibiting a positive correlation with deglaciation and debris cover distribution in these regions. We also  
 621 observed that the glacier area, length and debris cover extent of the LR glaciers show a good correlation with  
 622 winter  $T_{min}$  and average precipitation as compared to the GHR glaciers (Table 3). This shows that both  
 623 temperature as well as precipitation influence the degeneration of the glaciers and in turn affects the supraglacial  
 624 debris cover. It is believed that winter precipitation has a prime control on accumulation of snow on the glaciers,  
 625 hence acts as an essential determinant of glacier health (Mir et al., 2017). Also, the negative correlation of  
 626 glacier area with precipitation in this study possibly indicate the major role of increased winter temperature and  
 627 precipitation, which might have decreased the accumulation of snow, thereby decreasing the overall glacier area.  
 628 The average SLA for LR glaciers is observed to be higher as compared to the GHR glaciers. However, a  
 629 relatively higher rise in SLA is observed for GHR in contrast to the LR glaciers. Also, the mean SLA of the  
 630 GHR glaciers shows a good positive correlation with summer  $T_{max}$  as compared to the LR glaciers, while a  
 631 negative correlation with precipitation in the respective year (Table 3). Considering these observations, it  
 632 appears that a general rise in SLA can be attributed to regional climatic warming while that of individual SLA  
 633 variation in glaciers may be related to their unique topography (Shukla and Qadir, 2016).

634 From this analysis, it is quite evident that climatic factors directly influence the glacier response. Also, summer  
 635  $T_{max}$  have a stronger control over SLA, while glacier area,length and debris cover are predominantly controlled  
 636 by the winter  $T_{min}$  in the sub-basin.

637  
 638 Table 3: Coefficients of determination (r) between respective meteorological (temperature and precipitation)  
 639 data and observed glacier parameters in the Greater Himalayan Range (GHR) and Ladakh Range (LR) at 90%  
 640 confidence.  $T_{avg}$ ,  $T_{min}$  and  $T_{max}$  are montly mean, monthly mean minimum, monthly mean maximum  
 641 temperatures and Ppt is montly mean precipitation during different point in time (1971,1994, 2000 and 2017)

Major Mountain Ranges	Glacier Parameters	Climate Variables			
		$T_{avg}$	$T_{min}$	$T_{max}$	Ppt
GHR	Area	-0.826	<b>-0.897</b>	-0.347	-0.670
	Length	-0.908	<b>-0.926</b>	-0.345	-0.719
	Debris cover	0.842	<b>0.847</b>	0.434	0.593
	SLA	0.725	0.209	<b>0.725</b>	-0.315
LR	Area	-0.900	<b>-0.942</b>	-0.568	-0.779
	Length	-0.909	<b>-0.939</b>	-0.569	-0.778
	Debris cover	0.929	<b>0.907</b>	0.595	0.719
	SLA	0.658	0.395	<b>0.658</b>	-0.505



642

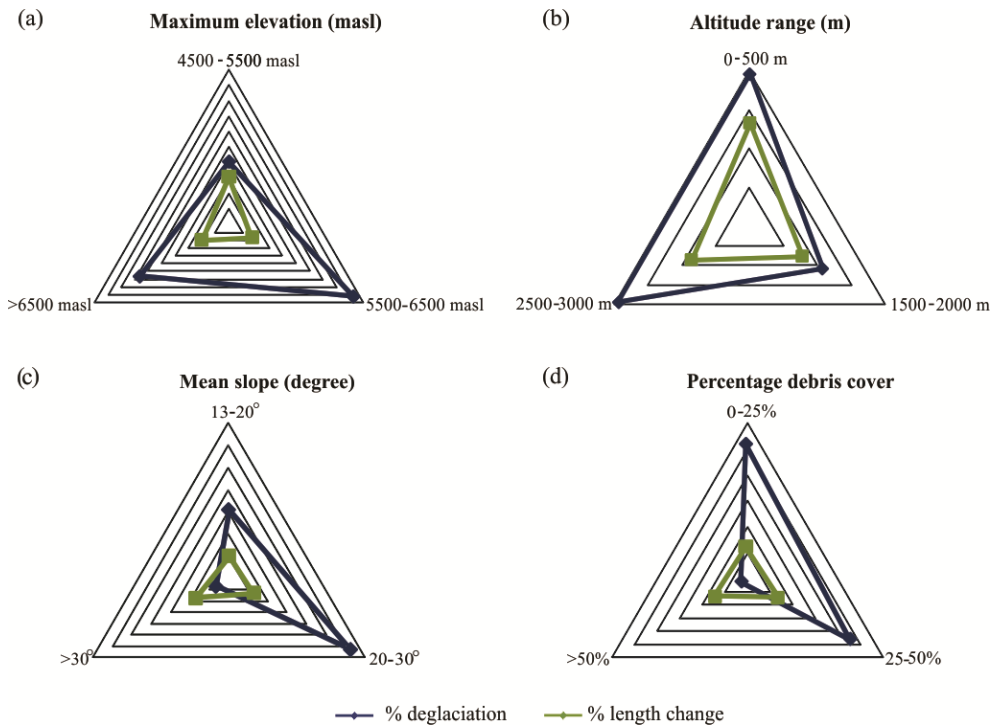
643 **5.3.2 Impact of other factors**

644 In addition to the climate variables, other factors such as hypsometry, maximum elevation, altitude range, slope,  
645 aspect and proglacial lakes also influence the response of individual glacier.

646 Glacier hypsometry is a measure of mass distribution over varying altitudes. It is affected by the mean SLA of  
647 the glaciers to a greater extent, as it is considered that if a large portion of the glacier has elevation equivalent to  
648 SLA, then even a slight alteration in SLA might significantly change the ablation and accumulation zones  
649 (Rivera et al., 2011; Garg et al., 2017b).

650 In this study, we observed that GHR and LR glaciers have nearly 45% and 10% of their area at an elevation  
651 similar to SLA. This suggests that GHR glaciers are more susceptible to retreat as compared to the LR glaciers,  
652 as a larger portion of the former belongs to the SLA. Moreover, the hypsometric distribution of glacier area in  
653 the GHR and LR of the SSB reveals maximum area change post 2000 (Fig.6b). In this regard, while GHR  
654 glaciers have undergone relatively higher area loss (21%) at lower elevation (3800-4200 masl), the LR glaciers  
655 lost maximum area (30%) at much higher elevation (5600-5900 masl) ranges (Fig.6b). Besides, a significant  
656 area loss has also been observed for both GHR (6%) and LR (7%) glaciers at their mean elevations post 2000  
657 (Fig.6b).

658 Elevation plays an important role in understanding the accumulation pattern at higher and ablation in the lower  
659 altitudes. The general perception is that the glaciers situated at relatively higher elevation are subjected to  
660 greater amount of precipitation and hence are susceptible to less deglaciation or even mass gain (Pandey and  
661 Venkataraman, 2013). Similarly, we have also noticed that the glaciers extending to comparatively higher  
662 maximum elevation experience minimum retreat (10%) and exhibit higher percentagedeglaciation (33%) as  
663 compared to the glaciers having lower maximum elevation (retreat:15% & deglaciation: 20%) (Fig.10a).



664  
 665 Figure 10: Differential degeneration of the glaciers during the period 1971-2017 with variability in non-climatic  
 666 factors. (a) Percentage deglaciation and length change of the glaciers at different ranges of maximum elevation,  
 667 (b) altitude range, (c) mean slope and (d) percentage debris cover.  
 668

669 Moreover, our study shows that the glaciers having lower altitude range have retreated and deglaciated more  
 670 (13% & 20%, respectively) as compared to the counterparts (Fig.10b). These observations indicate that glaciers  
 671 which possess higher maximum elevation and altitudinal range are subjected to less retreat and undergo greater  
 672 deglaciation.

673 Slope is another important factor which has a major role in the sustenance of the glacier as accumulation of ice  
 674 is facilitated by a gentler bedrock topography (DeBeer and Sharp, 2009; Patel et al., 2018). It is observed that  
 675 glaciers having steep slopes (30-40°) have retreated more (17%), however with minimum deglaciation (7%)  
 676 during the period 1971-2017 (Fig.10c). Similar results with steeper glaciers exhibiting minimum deglaciation  
 677 have been reported in the Parbati, Chandra and Miyar basins (Venkatesh et al., 2012; Patel et al., 2018).  
 678 However, it differs with Pandey and Venkataraman (2013) and Garg et al., (2017b), likely due to the differing  
 679 average size:  $25 \pm 33.78$  and  $17 \pm 33.2$  km<sup>2</sup> (present study:  $2 \pm 5.7$  km<sup>2</sup>) and slope: 5-20° and 12-26° (present  
 680 study: 13-41°), respectively, of glaciers used in these studies.

681 Presence of supraglacial debris cover influences the glacier processes. Depending on thickness, debris cover  
 682 may either enhance or retard the ablation process (Scherler et al., 2011). In this study, we observed that clean  
 683 glaciers have undergone maximum deglaciation (52%) as compared to the partially (46%) and heavily debris  
 684 covered glaciers (2%). However, they all have retreated almost similarly (12 to 14%), with slightly higher  
 685 retreat of partially debris covered glaciers (Fig.10d). Aspect/ orientation of glaciers provide information

686 regarding the duration for which they are exposed to the incoming solar radiation. Since, the south facing  
 687 glaciers are subjected to longer duration of exposure to the solar radiations as compared to the north facing  
 688 glaciers, therefore, are prone to greater deglaciation and retreat (Deota et al., 2011). Here, it is observed that the  
 689 glaciers having northerly aspect (north, north-east, north-west) have undergone maximum deglaciation as  
 690 compared to the counterparts. However, majority (71%) of the glaciers have northerly aspect, so any inferences  
 691 drawn in this respect would be biased. It is worthwhile to state that most of the south facing slopes in the basin  
 692 are devoid of glaciers but show presence of relict glacier valleys which would have been glaciated in the past.  
 693 At present only 48 south facing glaciers (south, south-east, south-west) with an average size of  $1 \pm 1.9 \text{ km}^2$  exist  
 694 in the SSB.

695 Similarly, the glacier changes are also influenced by the presence of certain features such as glacial (proglacial  
 696 or supraglacial) lakes or differential distribution of supraglacial debris cover. The presence of a proglacial or  
 697 supraglacial lakes significantly enhances the rate of glacier degeneration by increasing the melting processes  
 698 (Sakai, 2012; Basnett et al., 2013). As per our results, highest average retreat rate ( $\sim 31 \text{ ma}^{-1}$ ) is observed for  
 699 glaciers G-4 (Dulung glacier). Although, it is a debris free glacier, shows the highest retreat rates. Also, a  
 700 moraine-dammed lake is observed at the snout of this glacier and has continuously increased its size from  $0.15$   
 701  $\text{km}^2$  in 1977 to  $0.56 \text{ km}^2$  in 2017. This significant increase in the size of moraine-dammed lake has possibly  
 702 influenced the enhanced retreat rate of the glacier.

## 703 **6 Dataset availability**

704 Temporal inventory data for glaciers of Suru sub-basin, western Himalaya is available at  
 705 <https://doi.pangaea.de/10.1594/PANGAEA.904131> (Shukla et al., 2019).

706

## 707 **7 Conclusions**

708 The major inferences drawn from the study include:

709 1. The sub-basin comprised of 252 glaciers, covering an area of  $481.32 \pm 3.41 \text{ km}^2$  (11% of the glacierized area)  
 710 in 2017. Major disintegration of the glaciers occurred after 2000, with breakdown of 12 glaciers into glacierets.  
 711 Small (47%) and clean (43%) glaciers cover maximum glacierized area of the sub-basin. Topographic  
 712 parameters reveal that majority of the glaciers are north facing and the mean elevation and slope of the glaciers  
 713 are  $5134.8 \pm 225 \text{ masl}$  and  $24.8 \pm 5.8^\circ$ , respectively.

714

715 2. Variability in glacier parameters reveal an overall degeneration of the glaciers during the period 1971-2017,  
 716 with deglaciation of approximately  $0.13 \pm 0.0004\% \text{ a}^{-1}$  alongwith an increase in the debris cover by  $37 \pm 0.002$   
 717  $\text{km}^2$  ( $\sim 62\%$ ). Meanwhile, the glaciers have shown an average retreat rate of nearly  $4.3 \pm 1.02 \text{ ma}^{-1}$  with SLA  
 718 exhibiting an overall rise by an average  $22 \pm 60 \text{ m}$ .

719 3. Long-term meteorological records during the period 1901-2017 exhibit an overall increase in the temperature  
 720 ( $T_{\min}$ :  $1.3^\circ\text{C}$ ,  $T_{\max}$ :  $0.25^\circ\text{C}$ ,  $T_{\text{avg}}$ :  $0.77^\circ\text{C}$ ) and precipitation (158 mm) trends. Both temperature and precipitation  
 721 gradients influence the changes in glacier parameters, however, winter  $T_{\min}$  strongly influencing the glacier area,  
 722 length and debris cover while summer  $T_{\max}$  controlling the SLA. Spatial patterns in change of climate

723 parameters reveal existence of local climate variability in the sub-basin, with progressively warmer (1.03°C) and  
724 wetter (445 mm) climatic regime for glaciers hosted in the GHR as compared to the LR (0.96°C/ 358 mm).

725 4. The inherent local climate variability in the sub-basin has influenced the behavior of the glaciers in the GHR  
726 and LR. It has been observed that LR glaciers have been shrinking faster (area loss: 7%) and accumulating more  
727 debris cover (debris increase: 73%) as compared to the GHR glaciers (6% and 59%) during the period 1971-  
728 2017. The GHR glaciers have, however, experienced greater rise in SLA ( $220 \pm 121$  m) in comparison to the LR  
729 ones ( $91 \pm 56$  m) during the period 1977-2000, with a decrease thereafter.

730  
731 Results presented here show the transitional response of the glaciers in the SSB between the Karakoram  
732 Himalayan and GHR glaciers. The study also confirm the possible influence of factors other than climate such  
733 as glacier size, regional hypsometry, elevation range, slope, aspect and presence of proglacial lakes in the  
734 observed heterogenous response of the glaciers. Therefore, these factors need to be accounted for in more details  
735 in future for complete understanding of the observed glacier changes and response.

### 736 737 **Team list**

- 738 1. Aparna Shukla
- 739 2. Siddhi Garg
- 740 3. Manish Mehta
- 741 4. Vinit Kumar
- 742 5. Uma Kant Shukla

### 743 744 **Author contribution**

745 A.S. and S.G. conceived the idea and led the writing of manuscript. A.S. structured the study. S.G. performed  
746 the temporal analysis of the data. M.M. and V.K. helped in the field investigation of the glaciers. All the authors  
747 helped in interpretation of results and contributed towards the final form of the manuscript.

### 748 749 **Competing interests**

750 The authors declare that they have no conflict of interest.

### 751 752 **Acknowledgements**

753 Authors are grateful to the Director, Wadia Institute of Himalayan Geology, Dehradun for providing all the  
754 research facilities and support for successful completion of this work. We wish to convey our sincere thanks to  
755 the anonymous reviewers for detailed reviews and constructive comments, which greatly helped to improve the  
756 previous version of the manuscript. We are thankful to Prasad Gogineni (Handling Topical Editor) and Jens  
757 Klump (Handling Chief Editor) for their thoughtful suggestions on the manuscript. Also, we appreciate the  
758 efforts of the entire Editorial team of Earth System Science Data (ESSD) for timely processing of the article.  
759 Aparna Shukla acknowledges the Secretary, Ministry of Earth Science (MoES), New Delhi, India, for providing  
760 requisite support.

### 761 762 **References**

- 763 Ali, I., Shukla, A. and Romshoo, S. A.: Assessing linkages between spatial facies changes and dimensional  
764 variations of glaciers in the upper Indus Basin, western Himalaya, *Geomorphology*, 284, 115-129,  
765 <https://doi.org/10.1016/j.geomorph.2017.01.005>, 2017.
- 766 ALOS Global Digital Surface Model "ALOS World 3D - 30m" (AW3D30).  
767 <http://www.eorc.jaxa.jp/ALOS/en/aw3d30/> (accessed on 1 August 2017).
- 768 Azam, M. F., Wagnon, P., Berthier, E., Vincent, C., Fujita, K. and Kargel, J. F.: Review of the status and mass  
769 changes of Himalayan-Karakoram glaciers, *Journal of Glaciology*, 64, 61-74,  
770 <https://doi.org/10.1017/jog.2017.86>, 2018.
- 771 Bajracharya, S. R., Maharjan, S. B., and Shrestha, F.: The status and decadal change of glaciers in Bhutan from  
772 1980's to 2010 based on the satellite data, *Annals of Glaciology*, 55, 159-166,  
773 <https://doi.org/10.3189/2014AoG66A125>, 2014.
- 774 Bajracharya, S. R., Mool, P. K., Shrestha, B. R.: Global climate change and melting of Himalayan glaciers.  
775 Melting glaciers and rising sea levels: Impacts and implications, Prabha Shastri Ranade (ed), The  
776 Icfai's University Press, India, 28-46, 2008.
- 777 Basnett, S., Kulkarni, A.V. and Bolch, T.: The influence of debris cover and glacial lakes on the recession of  
778 glaciers in Sikkim Himalaya, India, *Journal of Glaciology*, 59, 1035-1046,  
779 <https://doi.org/10.3189/2013JoG12J184>, 2013.
- 780 Bhambri, R., Bolch, T., Chaujar, R. K., and Kulshreshtha, S. C.: Glacier changes in the Garhwal Himalaya,  
781 India, from 1968 to 2006 based on remote sensing, *Journal of Glaciology*, 57, 543-556,  
782 <https://doi.org/10.3189/002214311796905604>, 2011.
- 783 Bhambri, R., Bolch, T. and Chaujar, R. K.: Frontal recession of Gangotri Glacier, Garhwal Himalayas, from  
784 1965 to 2006, measured through high-resolution remote sensing data, *Current Science*, 102, 489-494,  
785 2012.
- 786 Bhambri, R., Bolch, T., Kawishwar, P., Dobhal, D. P., Srivastava, D. and Pratap, B.: Heterogeneity in Glacier  
787 Response in the Upper Shyok Valley, Northeast Karakoram, *The Cryosphere*, 7, 1385-1398.  
788 <https://doi.org/10.5194/tc-7-1385-2013>, 2013.
- 789 Bhattacharya, A., Bolch, Mukherjee, K., Pieczonka, T., Kropacek, J. and Buchroithner, M.: Overall recession  
790 and mass budget of Gangotri Glacier, Garhwal Himalayas, from 1965 to 2015 using remote sensing  
791 data, *Journal of Glaciology*, 62, 1115-1133, <https://doi.org/10.1017/jog.2016.96>, 2016.
- 792 Bhushan, S., Syed, T. H., Arendt, A. A., Kulkarni, A. V. and Sinha, D.: Assessing controls on mass budget and  
793 surface velocity variations of glaciers in Western Himalaya, *Scientific Reports*, 8, 8885,  
794 <https://doi.org/10.1038/s41598-018-27014-y>, 2018.
- 795 Bhutiyan, M. R., Kale, V. S. and Pawar, N. J.: Long term trends in maximum, minimum and mean annual air  
796 temperature across the Northwestern Himalaya during the twentieth century, *Climate change*, 85, 159-  
797 177, <https://doi.org/10.1007/s10584-006-9196-1>, 2007.
- 798 Birajdar, F., Venkataraman, G., Bahuguna, I. and Samant, H.: A revised glacier inventory of Bhaga Basin  
799 Himachal Pradesh, India: current status and recent glacier variations, *ISPRS Annals of*  
800 *Photogrammetry, Remote Sensing and Spatial Information Sciences*, II-8, 37-43, <https://doi.org/10.5194/isprannals-s-ii-8-37-2014>, 2014.
- 802 Bolch, T., Buchroithner, M., Pieczonka, T. and Kunert, A.: Planimetric and Volumetric Glacier Changes in the  
803 Khumbu Himal, Nepal, Since 1962 Using Corona, Landsat TM and ASTER Data, *Journal of*  
804 *Glaciology*, 54, 592-600, <https://doi.org/10.3189/002214308786570782>, 2008.
- 805 Bolch, T., Kulkarni, A., Käab, A., Huggel, C., Paul, F., Cogley, J. G., Frey, H., Kargel, J. S., Fujita, K., Scheel,  
806 M., Bajracharya, S., and Stoffel, M.: The State and Fate of Himalayan Glaciers, *Science*, 336, 310-314,  
807 <https://doi.org/10.1126/science.1215828>, 2012.
- 808 Brun, F., Berthier, E., Wagnon, P., Käab, A. and Treichler, D.: A spatially resolved estimate of High Mountain  
809 Asia glacier mass balances from 2000 to 2006, *Nature Geoscience*, 10, 668-673, [10.1038/NGEO2999](https://doi.org/10.1038/NGEO2999),  
810 2017.

- 811 Chand, P. and Sharma, M. C.: Glacier changes in Ravi basin, North-Western Himalaya (India) during the last  
812 four decades (1971-2010/13), *Global and Planetary change*, 135, 133-  
813 147, <https://doi.org/10.1016/j.gloplacha.2015.10.013>, 2015.
- 814 Chevuturi, A., Dimri, A. P. and Thayyen, R. J.: Climate change over Leh, Ladakh (India), *Theoretical and*  
815 *Applied Climatology*, 131, 531-545, <https://doi.org/10.1007/s0070401619891>, 2018.
- 816 Chudley, T. R., Miles, E. S. and Willis, I. C.: Glacier characteristics and retreat between 1991 and 2014 in the  
817 Ladakh Range, Jammu and Kashmir, *Remote Sensing Letters*, 8, 518-527,  
818 <https://doi.org/10.1080/2150704X.2017.1295480>, 2017.
- 819 Cogley, J. G.: Glacier shrinkage across High Mountain Asia, *Annals of Glaciology*, 57, 41-49,  
820 <https://doi.org/10.3189/2016AoG71A040>, 2016.
- 821 Das, S. and Sharma, M. C.: Glacier changes between 1971 and 2016 in the Jankar Chhu Watershed, Lahaul  
822 Himalaya, India, *Journal of glaciology*, 1-16, <https://doi.org/10.1017/jog.2018.77>, 2018.
- 823 DeBeer, C. M. and Sharp, M. J.: Topographic influences on recent changes of very small glaciers in the  
824 Monashee mountains, British Columbia, Canada, *Journal of Glaciology*, 55, 691-700,  
825 <https://doi.org/10.3189/002214309789470851>, 2009.
- 826 Deota, B. S., Trivedi, Y. N., Kulkarni, A. V., Bahuguna, I. M. and Rathore, B. P.: RS and GIS in mapping of  
827 geomorphic records and understanding the local controls of glacial retreat from the Baspa Valley,  
828 Himachal Pradesh, India, *Current Science*, 100, 1555–1563, 2011.
- 829 Dimri, A. P.: Interseasonal oscillation associated with the Indian winter monsoon, *Journal of geophysical*  
830 *research: Atmospheres*, 118, 1189-1198, <https://doi.org/10.1002/jgrd.50144>, 2013.
- 831 Dobhal, D. P., Mehta, M. and Srivastava, D.: Influence of debris cover on terminus retreat and mass changes of  
832 Chorabari Glacier, Garhwal region, central Himalaya, India, *Journal of Glaciology*, 59, 961–971,  
833 <https://doi.org/10.3189/2013jog12j180>, 2013.
- 834 Gardelle, J., Berthier, E., Arnaud, Y. and Kääb, A.: Region-wide glacier mass balances over the Pamir-  
835 Karakoram-Himalaya during 1999–2011, *The Cryosphere*, 7, 1263–1286, 2013.
- 836 Garg, P. K., Shukla, A., Tiwari, R. K. and Jasrotia, A. S.: Assessing the status of glaciers in parts of the Chandra  
837 basin, Himachal Himalaya: A multiparametric approach, *Geomorphology*, 284,99-114,  
838 <https://doi.org/10.1016/j.geomorph.2016.10.022>, 2017a.
- 839 Garg, P. K., Shukla, A. and Jasrotia, A. S.: Influence of topography on glacier changes in the central Himalaya,  
840 India, *Global and Planetary change*, 155, 196-212, <https://doi.org/10.1016/j.gloplacha.2017.07.007>, 2017b.
- 842 Garg, S., Shukla, A., Mehta, M., Kumar, V., Samuel, S. A., Bartarya, S. and Shukla, U. K.: Field evidences  
843 showing rapid frontal degeneration of the Kangriz glacier, Suru basin, Jammu and Kashmir. *Journal of*  
844 *mountain science*, 15, 1199–1208, <https://doi.org/10.1007/s11629-017-4809-x>, 2018.
- 845 Garg, S., Shukla, A., Mehta, M., Kumar, V. and Shukla, U. K.: On geomorphic manifestations and glaciation  
846 history of the Kangriz glacier, western Himalaya. *Himalayan Geology*, 40, 115–127, 2019.
- 847 Granshaw, F. D. and Fountain, A. G.: Glacier change (1958– 1998) in the North Cascades National Park  
848 Complex, Washington, USA, *Journal of Glaciology*, 52, 251–256  
849 <https://doi.org/10.3189/172756506781828782>, 2006.
- 850 Guo, Z., Wanga, N., Kehrwald, N. M., Mao, R., Wua, H., Wu, Y. and Jiang, X.: Temporal and spatial changes  
851 in western Himalayan firn line altitudes from 1998 to 2009, *Global and Planetary Change*, 118, 97–  
852 105, <https://doi.org/10.1016/j.gloplacha.2014.03.012>, 2014.

- 853 Hall, D. K., Bayr, K. J., Schöner, W., Bindschadler, R. A. and Chiene, J. Y. L.: Consideration of the Errors  
854 Inherent in Mapping Historical Glacier Positions in Austria from the Ground and Space (1893–2001),  
855 Remote Sensing of Environment, 86, 566–577, [https://doi.org/10.1016/S0034-4257\(03\)00134-2](https://doi.org/10.1016/S0034-4257(03)00134-2), 2003.
- 856 Hanshaw, M. N., and Bookhagen, B.: Glacial Areas, Lake Areas, and Snow Lines from 1975 to 2012:  
857 Status of the Cordillera Vilcanota, Including the Quelccaya Ice Cap, Northern Central Andes, Peru,  
858 The Cryosphere, 8, 359–376, <https://doi.org/10.5194/tc-8-359> 2014, 2014.
- 859 Harris, I.C. and Jones, P.D.: CRU TS 4.02: Climatic Research Unit (CRU) year-by-year variation of selected  
860 climate variables by country (CY) version 4.02 (Jan. 1901 - Dec. 2017). Centre for Environmental  
861 Data Analysis, <http://dx.doi.org/10.5285/d4e823f0172947c5ae6e6b265656c273>, 2018.
- 862 India Meteorological Department (IMD), Climatological table: Available online:  
863 [http://www.imd.gov.in/pages/city\\_weather\\_show.php](http://www.imd.gov.in/pages/city_weather_show.php), 2015.
- 864 Immerzeel, W. W., Beek, L. P. H. and Bierkens M. F. P.: Climate change will affect the Asian water towers,  
865 Science, 328, 1382–1385, <https://doi.org/10.1126/science.1183188>, 2010.
- 866 IPCC. Summary for policymakers. In: Stocker, T. F. et al. (Eds), Climate Change 2013: The Physical Science  
867 Basis. Contribution of Working Group III to the Fifth Assessment Report of Intergovernmental Panel  
868 on Climate Change. Cambridge University Press, Cambridge and New York, 2013.
- 869 Kääb, A., Berthier, E., Nuth, C., Gardelle, J. and Arnaud, Y.: Contrasting patterns of early twenty first century  
870 glacier mass change in the Himalayas, Nature, 488, 495–498, <https://doi.org/10.1038/nature11324>,  
871 2012.
- 872 Kääb, A., Treichler, D., Nuth, C., and Berthier, E.: Brief Communication: Contending estimates of 2003–  
873 2008 glacier mass balance over the Pamir–Karakoram–Himalaya, The Cryosphere, 9, 557–564,  
874 <https://doi.org/10.5194/tc-9-557-2015>, 2015.
- 875 Kamp, U., Byrne, M. and Bolch, T.: Glacier Fluctuations between 1975 and 2008 in the Greater  
876 Himalaya Range of Zaskar, Southern Ladakh, Journal of Mountain Sciences, 8, 374–389,  
877 <https://doi.org/10.1007/s11629-011-2007-9>, 2011.
- 878 Kaser, G., Großhauser, M. and Marzeion, B: Contribution potential of glaciers to water availability in different  
879 climate regimes, Proceedings of National academy of Sciences of the United States of America, 107,  
880 20223–20227, <https://doi.org/10.1073/pnas.1008162107>, 2010.
- 881 Kulkarni, A. V., Bahuguna, I. M., Rathore, B. P., Singh, S. K., Randhawa, S. S., Sood, R. K. and Dhar, S.:  
882 Glacial retreat in Himalaya using remote sensing satellite data, Current Science, 92, 69–  
883 74, <https://doi.org/10.1117/12.694004>, 2007.
- 884 Kulkarni, A. V., Rathore, B. P., Singh, S. K. and Bahuguna, I. M.: Understanding changes in Himalayan  
885 Cryosphere using remote sensing technique, International Journal of Remote Sensing, 32,  
886 601–615, <https://doi.org/10.1080/01431161.2010.517802>, 2011.
- 887 Maurer, J. M., Schaefer, J. M., Rupper, S., Corley, A.: Acceleration of ice loss across the Himalayas over the  
888 past 40 years, Science Advances, 5, 1–12 <https://doi.org/10.1126/sciadv.aav7266>, 2019.
- 889 Mayewski, P. A., and Jeschke, P. A.: Himalayan and Trans-Himalayan Glacier Fluctuations Since A.D. 1812,  
890 Arctic and Alpine Research, 11, 267–287, <https://doi.org/>, 1980.
- 891 Miller, J. D., Immerzeel, W. W. and Rees, G.: Climate change impacts on glacier hydrology and river discharge  
892 in the Hindu Kush- Himalaya, Mountain research and development, 32, 461–467,  
893 <http://doi.org/10.1659/MRD-JOURNAL-D-12-00027.1>, 2012.
- 894 Mir, R. A., Jain, S. K., Jain, Thayyen, R. J. and Saraf, A. K.: Assessment of recent glacier changes and its  
895 controlling factors from 1976 to 2011 in Baspa Basin, western Himalaya, Arctic, Antarctic, and Alpine  
896 Research, 49, 621–647, <https://doi.org/10.1657/AAAR0015-070>, 2017.
- 897 Mölg, N., Bolch, T., Rastner, P., Strozzi, T. and Paul, F.: A consistent glacier inventory for Karakoram and  
898 Pamir derived from Landsat data: distribution of debris cover and mapping challenges. Earth  
899 System Science Data, 10, 1807–1827, <https://doi.org/10.5194/essd-10-1807-2018>, 2018.

- 900 Murtaza K. O. and Romshoo S. A.: Recent glacier changes in the Kashmir Alpine Himalayas, India, *Geocarto*  
 901 *International*, 32, 188-205, <https://doi.org/10.1080/10106049.2015.1132482>, 2015.
- 902 Nuimura, T., Sakai, A., Taniguchi, K., Nagai, H., Lamsal, D., Tsutaki, S., Kozawa, A.,  
 903 Hoshina, Y., Takenaka, S., Omiya, S., Tsunematsu, K., Tshering, P. and Fujita, K.: The GAMDAM  
 904 glacier inventory: a quality-controlled inventory of Asian glaciers, *The Cryosphere*, 9, 849-864,  
 905 <https://doi.org/10.5194/tc-9-849-2015>, 2015.
- 906 Pandey, A., Ghosh, S. and Nathawat, M. S.: Evaluating patterns of temporal glacier changes in Greater  
 907 Himalayan Range, Jammu & Kashmir, India, *Geocarto International*, 26, 321-338,  
 908 <https://doi.org/10.1080/10106049.2011.554611>, 2011.
- 909 Pandey, P. and Venkataraman, G.: Changes in the glaciers of Chandra–Bhaga basin, Himachal Himalaya, India,  
 910 between 1980 and 2010 measured using remote sensing, *International Journal of Remote Sensing*, 34,  
 911 5584-5597, <https://doi.org/10.1080/01431161.2013.793464>, 2013.
- 912 Patel, L. K., Sharma, P., Fathima, T. N. and Thamban, M.: Geospatial observations of topographical control  
 913 over the glacier retreat, Miyar basin, western Himalaya, India, *Environmental Earth Sciences*, 77, 190,  
 914 <https://doi.org/10.1007/s12665-018-7379-5>, 2018.
- 915 Paul, F., Barrand, N.E., Baumann, S., Berthier, E., Bolch, T., Casey, K., Frey, H., Joshi, S.P., Kononov, V.,  
 916 Bris, R.L. and Mölg, N.: On the accuracy of glacier outlines derived from remote-sensing data, *Annals*  
 917 *of Glaciology*, 54, 171–182, <https://doi.org/10.3189/2013AoG63A296>, 2013.
- 918 Paul, F., Bolch, T., Kääb, A., Nagler, T., Nuth, C., Scharrer, K.: The glaciers climate change initiative:  
 919 methods for creating glacier area, elevation change and velocity products *Remote Sensing*  
 920 *Environment*, 162, 408-426, <http://dx.doi.org/10.1016/j.rse.2013.07.043>, 2015.
- 921 Paul, F., Bolch, T., Briggs, K., Kääb, A., McMillan, M., McNabb, R., Nagler, T., Nuth, C., Rastner, P., Strozzi,  
 922 T. and Wuite, J.: Error sources and guidelines for quality assessment of glacier area, elevation change,  
 923 and velocity products derived from satellite data in the *Glaciers\_cci* project, *Remote sensing of*  
 924 *Environment*, 203, 256-275, <https://doi.org/10.1016/j.rse.2017.08.038>, 2017.
- 925 Pfeffer, W. T., Arendt, A., Bliss, A., Bolch, T., Cogley, J. G., Gardner, A. S., Hagen, J. O., Hock, R., Kaser, G.,  
 926 Kienholz, C., Miles, E. S., Moholdt, G., Molg, N., Paul, F., Radic, V., Rastner, P., Raup, B. H., Rich, J.  
 927 and Sharp, M.: The Randolph Glacier Inventory: A globally complete inventory of glaciers, *Journal of*  
 928 *Glaciology*, 60, 537-552. doi:10.3189/2014JoG13J176, 2014.
- 929 Pritchard, H. D.: Asia's glaciers are a regionally important buffer against drought, *Nature*, 545, 169-187,  
 930 doi:10.1038/nature22062, 2017.
- 931 Racoviteanu, A. E., Arnaud, Y., Williams, M. W. and Ordonez, J.: Decadal changes in glacier parameters in  
 932 the Cordillera Blanca, Peru, derived from remote sensing, *Journal of Glaciology*, 54, 499–510,  
 933 <https://doi.org/10.3189/002214308785836922.2008a>.
- 934 Racoviteanu, A., Paul, F., Raup, B., Khalsa, S. J. S. and Armstrong, R.: Challenges and recommendations in  
 935 mapping of glacier parameters from space: results of the 2008 Global Land Ice Measurements from  
 936 Space (GLIMS) workshop, Boulder, Colorado, USA, *Annals of Glaciology*, 50, 53–69,  
 937 <https://doi.org/10.3189/172756410790595804>, 2009.
- 938 Rai, P. K., Nathawat, M. S. and Mohan, K.: Glacier retreat in Doda valley, Zaskar basin, Jammu and Kashmir,  
 939 India, *Universal Journal of Geoscience*, 1, 139-149, <https://doi.org/10.13189/ujg.2013.010304>, 2013.
- 940 Raina, V. K.: Himalayan glaciers: a state-of-art review of glacial studies, glacial retreat and climate  
 941 change. *Himal. Glaciers State-Art Review*, *Glacial Stud. Glacial Retreat Climate Change*, 2009.
- 942 Raina, R. K. and Koul, M. N.: Impact of Climatic Change on Agro-Ecological Zones of the Suru-Zaskar  
 943 Valley, Ladakh (Jammu and Kashmir), India, *Journal of Ecology and the Natural Environment* 3,  
 944 424–440, 2011.
- 945 Rashid, I., Romshoo, S. A. and Abdullah, T.: The recent deglaciation of Kolahoi Valley in Kashmir Himalaya,  
 946 India in response to the changing climate, *Journal of Asian Earth Science*, 138, 38–50,  
 947 <https://doi.org/10.1016/j.jseas.2017.02.002>, 2017.



- 948 Raup, B., Racoviteanu, A., Khals, S. J. S., Helm, C., Armstrong, R., Arnaud, Y.: The GLIMS geospatial glacier  
 949 database: a new tool for studying glacier change, *Global and Planetary Change* 56, 101–110,  
 950 doi:10.1016/j.gloplacha.2006.07.018, 2007.
- 951 Rivera, A., Cawkwell, F., Rada, C. and Bravo, C.: Hypsometry. In: *Encyclopaedia of Snow, Ice and glaciers*,  
 952 Springer, Netherlands, 551-554, 2011.
- 953 Space Application Centre (SAC): Report: Monitoring Snow and Glaciers of Himalayan Region. Space  
 954 Application Centre, ISRO, Ahmedabad, India, 413 pages, ISBN: 978-93-82760-24-5, 2016.
- 955 Sakai, A.: Glacial lakes in the Himalayas: A review on formation and Expansion process, *Global environmental*  
 956 *research*, 23-30, 2012.
- 957 Sakai A. and Fujita, K.: Contrasting glacier responses to recent climate change in high-mountain Asia, *Scientific*  
 958 *reports*, 7, 1-18, <https://doi.org/10.1038/s41598-017-14256-5>, 2017.
- 959 Sangewar, C. V., and S. P. Shukla.: Inventory of the Himalayan Glaciers: A Contribution to the International  
 960 Hydrological Programme, An Updated Edition. Kolkata: Geological Survey of India (Special  
 961 Publication 34), IISN: 1:0254-0436, 2009.
- 962 Scherler, D., Bookhagen, B. and Strecker, M.R.: Spatially variable response of Himalayan glaciers to climate  
 963 change affected by debris cover, *Nature Geoscience*, 4, 156–159, <https://doi.org/10.1038/ngeo1068>,  
 964 2011.
- 965 Schmidt, S. and Nusser, M.: Changes of High Altitude Glaciers in the Trans-Himalaya of Ladakh over the Past  
 966 Five Decades (1969–2016), *Geosciences*, 7, 27, <https://doi.org/10.3390/geosciences7020027>, 2017.
- 967 Sen, P. K.: Estimates of the regression coefficient based on Kendall's Tau, *American Statistics Journal*, 63,  
 968 1379-1389, <https://doi.org/10.2307/2285891>, 1968.
- 969 Shekhar, M., Bhardwaj, A., Singh, S., Ranhotra, P. S., Bhattacharyya, A., Pal, A. K., Roy, I., Martín-  
 970 Torres, F. J. and Zorzano, M.P.: Himalayan glaciers experienced significant mass loss during later  
 971 phases of little ice age, *Scientific Reports*, 7, 1-14, 2017.
- 972 Shiyin, L., Donghui, S., Junli, Xu., Xin, W., Xiaojun, Y., Zongli, J., Wanqin, G., Anxin, L., Shiqiang, Z.,  
 973 Baisheng, Ye., Zhen, Li., Junfeng, W. and Lizong, W.: Glaciers in China and Their Variations, In:  
 974 Kargel J., Leonard G., Bishop M., Käab A., Raup B. (eds) *Global Land Ice Measurements from Space*,  
 975 Springer Praxis Books, Springer, Berlin, Heidelberg, 2014
- 976 Shukla, A., Gupta, R. P. and Arora, M. K.: Estimation of debris cover and its temporal variation using optical  
 977 satellite sensor data: a case study in Chenab basin, Himalaya, *Journal of Glaciology*, 55, 444-452,  
 978 <http://doi.org/10.3189/002214309788816632>, 2009.
- 979 Shukla, A. and Qadir, J.: Differential response of glaciers with varying debris cover extent: evidence from  
 980 changing glacier parameters, *International Journal of Remote Sensing*, 37, 2453–2479,  
 981 <http://doi.org/10.1080/01431161.2016.1176272>, 2016.
- 982 Shukla, A., Garg, P.K., Manish, M., Kumar, V.: Changes in dynamics of Pensilungpa glacier, western  
 983 Himalaya, over the past two decades, in: *Proceedings of the 38<sup>th</sup> Asian Conference on Remote*  
 984 *Sensing*, Delhi, India, 23-27 October 2017, 2017.
- 985 Shukla, A., Garg, S., Manish, M., Kumar, V and Shukla, U. K.: Temporal inventory of glaciers in the Suru  
 986 sub-basin, western Himalaya, PANGAEA, <https://doi.pangaea.de/10.1594/PANGAEA.904131>, 2019.
- 987 Singh, J. and Yadav, R. R.: Tree-ring indications of recent glacier fluctuations in Gangotri, western Himalaya,  
 988 India, *Current Science*, 79(11), 1598–1601, 2000.
- 989 Vaughan, D. G., Comiso, J. C., Allison, I., Carrasco, J., Kaser, G., Kwok, R., Mote, P., Murray, T., Paul, F.,  
 990 Ren, J., Rignot, E., Solomina, O., Steffen, K. and Zhang, T.: Observations: Cryosphere. in *Climate*  
 991 *change 2013: The physical science basis. Contribution of working group I to the fifth assessment report*  
 992 *of the intergovernmental panel on climate change*, Stocker, T. F., Qin, D., Plattner, G. K., Tignor, M.,  
 993 Allen, S. K., Boschung, J., Nauels, A., Xia, Y., Bex, V. and Midgley, P. M. (Eds.), Cambridge  
 994 University Press, Cambridge, United Kingdom and New York, NY, USA, 2013.
- 995 Venkatesh, T. N., Kulkarni, A. V. and Srinivasan, J.: Relative effect of slope and equilibrium line altitude on the  
 996 retreat of Himalayan glaciers, *The Cryosphere*, 6, 301-311, <http://doi.org/10.5194/tc-6-301-2012>, 2012.

- 997 Vijay, S and Braun, M.: Early 21st century spatially detailed elevation changes of Jammu and Kashmir glaciers  
998 (Karakoram–Himalaya), *Global and Planetary Change*, 165, 137-146,  
999 <http://doi.org/10.1016/j.gloplacha.2018.03.014>, 2018.
- 1000 Vittoz, P.: *Ascent of the Nun in the Mountain World: 1954* (Marcel Kurz, ed.), George Allen & Unwin, Ltd.,  
1001 London, 1954.
- 1002 Zhou, Y., Li, Z., Li, J., Zhao, R. and Ding, X.: Geodetic glacier mass balance (1975-1999) in the central  
1003 Pamir using the SRTM DEM and KH-9 imagery, *Journal of Glaciology*, 65, 309-320, doi:  
1004 10.1017/jog.2019.8, 2018.